Alpha case removal from titanium alloys by machining with tungsten carbide cutting tools

by

Francois Willem Conradie

Thesis presented in partial fulfilment of the requirements for the degree of
Master of Industrial Engineering in the Faculty of Engineering at Stellenbosch University

Supervisor: Dr Gert Adriaan Oosthuizen

Department of Industrial Engineering, Faculty of Engineering,
Stellenbosch University

Co-supervisor: Prof Natasha Sacks

School of Chemical and Metallurgical Engineering, Faculty of
Engineering, University of the Witwatersrand

March 2016

Declaration

By submitting this thesis electronically, I declare that the entirety of the work contained therein is my own, original work, that I am the sole author thereof (save to the extent explicitly otherwise stated), that reproduction and publication thereof by Stellenbosch University will not infringe any third party rights and that I have not previously in its entirety or in part submitted it for obtaining any qualification.

March 2016

Abstract

The use of titanium is rising steadily. This surge is due to the metal's favourable biocompatibility, corrosion resistance and high specific strength. Despite the increasing demand, titanium production is currently limited by outdated manufacturing processes. New processing techniques are therefore under investigation so that raw material may be produced at lower cost. One of the manufacturing processes under review, is the use of chemical milling for the removal of the hard and brittle oxide layer (alpha case) which forms at production temperatures above T = 600°C. Chemical milling facilities currently used in alpha case removal demand high workplace and environmental safety standards which would incur high capital cost if constructed in South Africa.

Alternatively, the already established South African machining industry can be expanded to economically remove alpha case using existing infrastructure (milling machines). No machining guidelines are available and such a process is currently deemed uneconomical due to tooling cost. This study therefore investigated the performance of tungsten carbide indexable cutters in the removal of alpha case through machining, and developed guidelines for the economical removal of alpha case.

Background experiments determined the hardness-depth profile, composition and grain structure, which were used to aid in the experimental setup and design of primary experiments. The primary objective investigated the feasibility of replacing the acidic solutions of chemical milling, with tungsten carbide cutting tools in machining. The wear of the tungsten carbide cutters and the effect of alpha case on their performance were documented and used to measure the feasibility of machining.

At high cutting speeds the carbide cutting tools experienced excessive chipping and notching, which resulted in short tool life and low material removal. Alpha case removal was, however, readily achieved at low cutting speeds where traditional flank wear was experienced. At low cutting speeds, tool life also more closely resembled that which is observed with traditional titanium machining. Furthermore, feed rate had a negligible effect on tool wear and tool life at low cutting speeds. The most effective cutting strategy for alpha case removal with tungsten carbide indexable cutters, therefore involves the employment of low cutting speeds in combination with high feed rates. This will ensure long tool life while still realising reasonable material removal rates.

The secondary objective investigated is the scope of feasibility of alpha case machining removal in the context of the South African manufacturing industry. The already established machining industry in South Africa would profit from the expanded titanium machining industry, which could in turn hold further downstream manufacturing benefits. It is hypothesised that at low annual production volume, the tungsten carbide cutting tools used in machining removal of alpha case are the more economical option. Owing to the high cost of constructing new chemical milling facilities, only at high production volume would chemical milling become a viable option for long term manufacturing.

Opsomming

Titaanbenutting is besig om wêreldwyd te styg danksy die materiaal se gunstige eienskappe soos bioaanpasbaarheid, weerstand teen roes en hoë spesifieke sterkte. Ten spyte van die groeiende aanvraag, word titaanproduksie tans beperk deur verouderde produksieprosesse. Nuwe verwerkingstegnieke word dus ondersoek om rou materiaal te vervaardig teen laer koste. ’n Voorbeeld van so ’n produksieproses onder hersiening, is die gebruik van chemiese ets in die verwydering van die bros en harde oksiedlaag (alpha-laag) wat gevorm word by produksie-temperature bo T = 600°C.

As titaanbevoegdheid bereik wil word deur middel van programme soos die Titanium Centre of Competency, dan is die verwydering van die alpha-laag een van die kwessies wat aangespreek moet word. Chemiese ets fasiliteite vereis hoë werkplek- en omgewingsveiligheidstandaarde, wat op hoë kapitaalkoste sou uitloop indien dit in Suid-Afrika gebou sou word.

As alternatief kan die reeds-gevestigde Suid-Afrikaanse masjineringsbedryf uitgebrei word om ekonomiese verwydering van die alpha-laag te bewerkstellig. So ’n proses word tans beskou as onekonomies en geen riglyne is beskikbaar vir masjineringsverwydering nie. Hierdie studie ondersoek dus die vermoë van wolfram-karbied geïndekseerde beitels in the verwydering van die alpha-laag deur masjinering, en ontwikkel riglyne vir die ekonomiese verwydering van die alpha-laag.

Agtergrondeksperimente het die hardheid-diepte profiel, samestelling en greinstruktuur van die alpha-laag bepaal. Dit is gebruik om met verdere ontwerp van eksperimente te help. Die primêre doel, was die ondersoek van die lewensvatbaarheid om die suuroplossing van chemiese ets te vervang met wolfram karbied-geïndekseerde beitels in masjinering. Verskeie metingstegnieke is gebruik om die werksverrigtingvermoë, asook die effek wat die alpha-laag op die karbied-beitels hou, vas te stel.

Teen hoë snyspoed het die karbied-beitels oormatige afsplintering en slytasie ervaar. Dit het gelei tot kort beitel lewensverwagting en lae materiaalverwydering. In lae snyspoedgevalle is die alpha-laag effektief verwyder met min slytasie en snyleeftyd nader aan wat waargeneem word met tradisionele titaanmasjinering. Teen lae snysnelhede het die voerkoers ook ’n geringe uitwerking op die karbied-beitel se lewensduur. Die effektiefste snystrategie vir die verwydering van alpha-laag met wolfram-karbiedbeitels behels dus die gebruik van lae snysnelhede in kombinasie met hoë voertempo.

Die sekondêre doel was ’n ondersoek na die omvang van die lewensvatbaarheid van alpha-laagmasjinering in die konteks van die Suid-Afrikaanse vervaardigingsbedryf. Die reeds-gevestigde masjineringsbedryf sal voordeel trek uit die uitgebreide titaan masjineringsbedryf, wat verdere voordele vir die vervaardigingsbedryf kan hou. Daar word gepostuleer, dat masjinering met wolfram-karbied snybeitels vir die verwydering van die alpha-laag, die mees ekonomiese opsie is indien lae jaarlikse produksievolume gehandhaaf word. Weens die hoē konstruksiekostes, sal chemiese meulfasiliteite net op die langtermyn vatbaar wees indien hoë produksie-volumes bereik kan word.

Acknowledgements

I would like to acknowledge the financial and technical support received from the Department of Science and Technology and the National Research Foundation in South Africa. I furthermore wish to extend my gratitude to the following people who contributed in various different ways, both directly and indirectly, to the completion of this document.

My initial supervisor Mr N Treurnicht: For laying the groundwork which allowed me to complete my Master's degree.

My supervisor, Dr GA Oosthuizen of the Department of Industrial Engineering, Faculty of Engineering, and Stellenbosch University: For his guidance and support without which I would probably still have been working on this thesis.

My co-supervisor, Prof N Sacks of the School of Chemical and Metallurgical Engineering, University of the Witwatersrand: For her valuable financial support, guidance and patience.

Prof D Dimitrov of the Department of Industrial Engineering, Faculty of Engineering, Stellenbosch University: For his vision in establishing and leading the titanium research group at Stellenbosch University.

My colleagues, Mr PJT Conradie, Mr A Enever, Mr C van Staden, Mr R de Bruyn, Mr M Bezuidenhout and Mr L Delport: For their advice, support, friendship and collaborative procrastination.

My mother and father: For their continued love and support throughout my academic and non-academic life.

My brothers: For keeping me honest.

My friends: For providing the necessary excuses to allow for study breaks.

My r∞mz: For taking in stray students, making sure there was never a dull moment, and becoming best friends 2∞&β.

My Heavenly Father: For granting me the ability and grace to pursue my dreams.

Table of Contents

Declaration i

Abstract ii

Opsomming iii

Acknowledgements iv

Table of Contents v

List of Figures vii

List of Tables xii

Glossary xiii

Nomenclature xviii

1. Introduction 1

1.1. Problem statement 2

1.2. Objectives 4

1.3. Significance of study 5

1.4. Research methodology 6

1.5. Research roadmap 7

2. Literature Study 8

2.1. Challenges of alpha case 8

2.2. Alpha case removal methods 16

2.3. Materials and Geometries 19

2.4. Modes of tool wear 31

2.5. Economic benefits 38

3. Experimental Setup and Design 42

3.1. Background experiments 42

3.1.1. Initial alpha case formation 42

3.1.2. Alpha case evaluation 43

3.2. Feasibility testing of alpha case machining removal 45

3.2.1. Establishment of test conditions 45

3.2.2. Machining execution 49

3.2.3. Sampling plan 50
3.3. Scope of feasibility testing 52
4. Experimental Results and Discussion 54
4.1. Background experiments 54
4.1.1. Alpha case evaluation and weight gain 54
4.1.2. Hardness testing 55
4.1.3. Composition 57
4.1.4. Background experiments conclusion 58
4.2. Primary objective 59
4.3. Workpiece sample inspection 59
4.4. Confirmation of alpha case removal 60
4.5. Chip formation 62
4.6. Tool wear 63
4.6.1. Types of wear 64
4.6.2. Stair-formed wear pattern 71
4.6.3. Projected tool life 72
4.6.4. Statistical interpretation 76
4.6.5. The effect of repeated heat-treating 80
4.7. Deeper carbide insert analysis 82
4.8. Completion of primary objective 86
4.9. Cost model 87
4.9.1. Cost calculations of alpha case titanium machining removal 87
4.9.2. Break even analysis 89
5. Conclusion 92
References 94
Appendix A: Regression Analysis 103
Appendix B: Statistical Interpretation 115
Appendix C: Cost Calculation 117

List of Figures

Figure 1: (a) Damaged area of passenger cabin and No.1 Engine of Delta Airlines flight 1288 (b) Pratt & Whitney JT8D-200 series engine fan hub – adapted from (National Transportation Safety Board, 1996) 3

Figure 2: Appearance of titanium crystal structures at atomic level; (a) Hexagonal, close packed alpha phase (b) Cubic, body centred beta phase - adapted from (Donachie, 2000) 9

Figure 3: Phase diagram indicating the position of some titanium alloys depending on chemical composition and temperature – adapted from (Donachie, 2000) 9

Figure 4: 1000X enlarged scanning electron microscope image of typical Ti6Al4V sample where dark alpha grains portray alpha phase (α), and lighter surrounding areas portray beta phase (β) 10

Figure 5: Oxide scale formation and growth where (a) the initial TiO_2 layer is formed once exposed to oxygen (b) outwards diffusing aluminium reacts with open atmosphere forming Al_2O_3 surface layer(c) crack formation once the double layer reaches a certain thickness (d) the formation of multiple layers due to crack formation – adapted from (Du, et al., 1994) 12

Figure 6: Weight gain over time for Ti6Al4V alloy oxidised in air between T = 650 - 850°C – adapted from (Du, et al., 1994) 14

Figure 7: Optical micrograph of the Ti6Al4V sample exposed to T = 700°C for t = 500 hours – adapted from (Gaddam, et al., 2013) 14

Figure 8: Variation of hardness from surface to the bulk of the Ti6Al4V sample exposed to T = 700°C for t = 500 hours – adapted from (Gaddam, et al., 2013) 15

Figure 9: Chemical milling process (a) maskant is applied and the component is submerged into a heated acidic solution (b) solution etches unmasked surface for the duration of submergence 17

Figure 10: Milling modes for face milling (a) Conventional or up milling (b) Climb or down milling – adapted from (Davies, 1997) 21

Figure 11: Relationship between various tool materials in relation with hardness and toughness – adapted from (Oosthuizen, et al., 2010) 23

Figure 12: (a) Double negative cutter geometry with negative radial rake ($\angle_{RRA}$) insert angle and negative axial insert angle ($\angle_{ARA}$) (b) Positive/negative cutter geometry with positive radial rake insert angle ($\angle_{RRA}$) and negative axial insert angle ($\angle_{ARA}$)– adapted from (Winegard, 2012) 26

Figure 13: Effects on chip thickness due to the variation of corner angles (a) 90° or square angle, (b) 15° angle, (c) 45° angle – adapted from (Mitsubishi Carbide, 2015) 26

Figure 14: Schematic diagrams of the sequence of events, showing various stages involved in chip formation when machining titanium alloys – adapted from (Komanduri & Von Turkovich, 1981) 28

Figure 15: Chip, workpiece and tool relationship (1) Primary shear zone (2) Secondary shear zone (3) Secondary shear zone at rake face (4) Secondary shear zone at flank face (5) Deformation advance zone – adapted from (Grote & Antonsson, 2008) 29

Figure 16: Energy partition (heat generation and dissipation) in the machining of steel - adapted from (Komanduri, 1982)..... 30
Figure 17: Energy partition (heat generation and dissipation) in the machining of titanium alloys - adapted from (Komanduri, 1982) 30
Figure 18: Typical wear surfaces – adapted from (Kendall, 1997)..... 32
Figure 19: Types of flank wear (a) uniform flank wear across the flank face of the tool (b) localised flank wear or notch wear on the flank face in the region opposite the workpiece surface 32
Figure 20: Typical wear curve experienced in milling operations from accelerated initial wear, followed by gradual wear in intermediary stage of tool life and once more accelerated wear at the end of tool life – adapted from (Dimitrov, et al., 2013) 34
Figure 21: High pressure through spindle cooling, directly cooling the cutting edge and helping with chip evacuation – (Richt, 2011)..... 36
Figure 22: Minimum unit cost curve for milling operations where the minimum accumulated cost is dependent on the sum of the machining cost and the tooling cost – adapted from (Dimitrov, et al., 2013)..... 38
Figure 23: Computer-aided manufacturing (CAM) model of an Intercostal illustrating the total amount of material to be removed in the machining process 40
Figure 24: Heat-treatment profile of titanium samples to be followed for every heat-treatment cycle 43
Figure 24: Final workpiece material dimensions of the titanium sample blocks to be used in the primary machining experiments 45
Figure 25: (a) Photo of ISCAR cutter to be use in machining experiments, (b) dimensions of cutter, (c) dimensions of inserts to be used in machining experiments (d) sharp shape of insert edge, (e) 3D model of carbide insert to be used – adapted from (ISCAR, 2015)..... 47
Figure 26: Hermle C40U dynamic 5-axis CNC milling machine to be used in primary alpha case removal machining experiments..... 47
Figure 27: Titanium sample placed in Gallenkamp muffle furnace before heat-treatment begins..... 48
Figure 29: Rudimentary schematic of cutting strategy to be followed for the primary alpha case machining experiments..... 49
Figure 30: (a) Machining setup of workpiece and cutting tool for experimentation, (b) cutting tool setup for machining experiments..... 49
Figure 31: Experimentation flow chart to be used for all machining conditions from initial heat-treatment up until tool failure and end of experimentation..... 52
Figure 32: Weight gain representation for oxidised samples per square centimetre 54
Figure 33: Optical micrographs showing (a) white alpha case layer after etched with Weck's reagent (b) brittleness of alpha case when exposed to hardness tests..... 54
Figure 34: Optical micrograph illustrating hardness testing and measurement methodology..... 55

Figure 35: Variation in surface hardness of heat-treated samples, compared to untreated samples as measured from sample edge 56
Figure 36: Disparity of hardness indentation shape close to the harder sample edge, compared to the customary substrate indentation shape..... 56
Figure 37: Scanning electron micrograph of the edge of the heat-treated sample that shows large dark alpha grain structures overwhelming the smaller and lighter beta phase structures, and the substrate where lighter beta grain and darker alpha gain structures return to normal sizes 57
Figure 38: EDX analysis of heat-treated titanium sample at various sampling points 58
Figure 39: (a) Metallic appearance and colour of Ti6Al4V samples before heat-treatment (b) flaking of workpiece surface after heat-treatment (c) presence of alternating oxide layers with (i) the uppermost white representing titanium substrate (ii) dark TiO_2 layer is second from the top (iii) followed by the Al_2O_3 layer and (iv) the lowest layer representing the resin which is used to mount the sample 59
Figure 40: Oxidised surface is replaced by more common metallic surface after machining removal of alpha case 60
Figure 41: Surface roughness measurements of newly machined titanium in the X and Y direction .. 60
Figure 42: Surface hardness measurements before (0) and after (1-11) every experimental procedure 61
Figure 43: Various chip morphologies at (a) v_c = 40 m/min and f_z = 0.2 mm/z (b) v_c = 60 m/min and f_z = 0.15 mm/z and (c) v_c = 80 m/min and f_z = 0.1 mm/z 62
Figure 44: Rate of lamella formation on machining chips..... 63
Figure 45: Wear curves for different feed and speed combinations 64
Figure 46: Schematic representation of the metal cutting operation and the direction from which tool wear is measured from the flank face 65
Figure 47: Final tool wear observed on various cutting edges with the correlating cutting speed v_c, cutting feed f_z and total material removed MR (see Figure 46 for direction of measurement)..... 65
Figure 48: Collection of stereoscopic micrographs of carbide insert exposed to cutting parameters of v_c = 80 m/min at f_z = 0.1 mm/z. Shows the progression of tool wear in the removal of alpha case from (a) MR = 9 cm^3 – (i) MR = 81 cm^3 66
Figure 49: Collection of stereoscopic micrographs of carbide insert exposed to cutting parameters of v_c = 60 m/min at f_z = 0.15 mm/z. Shows the progression of tool wear in the removal of alpha case from (a) MR = 9 cm^3 – (h) MR = 72 cm^3 67
Figure 50: Schematic of the corner edge of the carbide inserts which shows the corner landing 68
Figure 51: Schematic of average tool wear as a function of depth on a carbide insert at cutting speed of v_c = 60 m/min and f_z = 0.15 mm/z feed rate..... 69

Figure 52: Collection of stereoscopic micrographs of carbide insert exposed to cutting parameters of v_c = 40 m/min at f_z = 0.2 mm/z. Shows the progression of tool wear in the removal of alpha case from (a) MR = 9 cm^3 – (k) MR = 100 cm^3 69
Figure 53: Programme a tool ramp into the workpiece in order to minimise notch wear on a localised point of the carbide insert 71
Figure 54: Visual representation of stair form notching (a) new tool engages in workpiece material (b) chip is formed in notch region adjacent to the workpiece surface (c) chip length is increased in order to expose material adjacent to the workpiece (d) chip depth is increased (e, f) process is repeated until tool failure 72
Figure 55: Tool life projection curve based on extrapolated data observed in experiments compared to benchmark data by (Jawaid, et al., 2000) 73
Figure 56: Collection of stereoscopic micrographs of carbide insert exposed to cutting parameters of v_c = 40 m/min at f_z = 0.15 mm/z. Shows the progression of tool wear in the removal of alpha case from (a) MR = 9 cm^3 – (k) MR = 81 cm^3, and (l) portrays the extent of chipping experienced by this particular insert edge after MR = 81 cm^3 74
Figure 57: Spread of tool wear as measured from (a) all the carbide inserts combined (b) individual carbide inserts that underwent machining at v_c = 40 m/min and f_z = 0.1 mm/z (c) individual carbide inserts that underwent machining at v_c = 40 m/min and f_z = 0.15 mm/z (d) individual carbide inserts that underwent machining at v_c = 40 m/min and f_z = 0.2 mm/z 75
Figure 58: Repricate plot of total material removed 77
Figure 59: Response distribution once data is placed in bins 77
Figure 61: Coefficient plot comparing the effect of the two indipendant variables Cutting speed, v_c [m/min] and feed rate, f_z [mm/z] 78
Figure 62: Observed data versus predicted regression plot as determined by the statistical model 79
Figure 63: 3D response contour plot for the predicted model (material removed) as a function of cutting speed, v_c [m/min] and cutting feed, f_z [mm/z] 80
Figure 64: Alpha case formation for repeated heat-treatment whereby (a) represents a yet untreated sample (b) after initial heat-treatment alpha case has formed (c) after a number of heat-treatment cycles the alpha case depth will reach its maximum 81
Figure 65: Hardness values measured from sample edge comparing a single heat-treatment cycle with multiple heat-treatment cycles 82
Figure 66: SEM of carbide edge flank wear at v_c = 40 m/min and f_z = 0.2 mm/z, showing five points of measure used the area composition analysis of Table 8, and 20 points in a linear line used in compositional analysis in Figure 67 83
Figure 67: Compositional analysis of array of data points represented by the red line in Figure 66 84
Figure 68: Scanning electron microscopy of carbide edge notch wear at v_c = 60 m/min and f_z = 0.15 mm/z, showing a near catastrophic chip in the notch region adjacent to the workpiece surface 85

Figure 69: SEM of a specific area above the notch wear at v_c = 60 m/min and f_z = 0.15 mm/z with the line indicating the 20 points of measure in a linear line for compositional analysis dipicted in Figure 70 85
Figure 70: Compositional analysis of array of data points represented by the red line in Figure 69.... 86
Figure 71: Basic estimation of the minimum cost curve for the removal of one cubic centimetre of material through milling. For illustration purposes only 88
Figure 72: Hypothesised cost comparison of (a) machining removal, (b) chemical milling and (c) combined comparison of machining removal and chemical milling for small, medium and large theoretical quantities. For illustrative purposes only 90

List of Tables

Table 1: Ti6Al4V composition - (Donachie, 2000) 10
Table 2: Number of samples in each heat-treatment 43
Table 3: Hermle milling machine technical data (Hermle, 2008) 48
Table 4: machining parameters to be used in experimental procedure 50
Table 5: Cutting feed and speed combinations for machining experiments 50
Table 6: Tool life criteria 51
Table 7: Experiment number 76
Table 8: Compositional analysis of numbered areas represented in Figure 66 83
Table 9: Machine time and total material removed for 10 inserts of 16 edges each 87
Table 10: Cost calculations for cutting tools displaying individual cost for the removal of MR = 1 cm^3 88

Glossary

Abrasion wear	A wear pattern that occurs due to the chips rubbing across the surface of the tool.
$(NH_4)_2S_2O_8$	Ammonium persulfate
$(NH_4)HF_2$	Ammonium hydrogen difluoride
Adhesiveness	A term describing the stickiness of a material.
Al_2O_3	Aluminium oxide
Allotropy	The property by which certain elements may exists in more than one crystal structure. An allotrope is a specific crystal structure of the metal.
Alloy system	A complete series of compositions produced by mixing in all proportions any group of two or more components, at least of which is metal.
Alpha	The low temperature allotrope of titanium with a hexagonal, close-packed crystal structure.
Alpha case	Oxygen-enriched phase that occurs when titanium and its alloys are exposed to heated air or oxygen
Alpha-beta structure	A microstructure containing alpha and beta as the principal phases at a specific temperature.
Bar	A metric (but not SI) unit of pressure exactly equal to 100 000 Pa
BEA	blue etch anodize
Beta	The high temperature allotrope of titanium with a body-centred cubic crystal structure that occurs above the β-transus temperature.
Binder	A substance added to the powder to increase the strength of the compact and cement together powder particles that alone would not sinter into a strong object.
Brinell hardness number (HB)	A number related to the applied load and to the surface area of the permanent impression made by a ball indenter.
Brittleness	The tendency of a material to fracture without first undergoing significant plastic deformation. Contrast with ductility.

Built-up edge	A condition where some of the work piece material welds to the cutting edge.
CAM	Computer-aided manufacturing
CBN	cubic boron nitride
Cemented carbide	Material manufactured by combining tungsten carbide (WC) powders and binder cobalt powders (Co).
Cermets	Sintered alloy comprised of titanium carbide (TiC), titanium nitride (TiN) and nickel (Ni) binder.
Corrosion	The deterioration of a metal through a chemical or electrochemical reaction with its environment.
Corrosive wear	Wear in which chemical or electrochemical reaction with the environment is significant.
CSIR	Council for Scientific and Industrial Research
$CuSO_4 \cdot 5H_2O$	copper sulphate pentahydrate
CVD	chemical vapour deposition
DACST	Department of Arts, Culture, Science and Technology
Depth of cut	Describes the thickness of the work piece material that is to be removed by the cutting edge when machining.
DST	Department of Science and Technology
Ductility	The ability of a material to deform plastically before fracturing. Measured by elongation or reduction of area in a tension test
EDM	electric discharge machining
EDX	energy dispersive X-ray spectroscopy
Fatigue	The phenomenon leading to fracture under repeated or fluctuating stresses having a maximum value less than the tensile strength of the material. Fatigue fractures are progressive, beginning as minute cracks that grow under the action of fluctuating stress.
FPI	fluorescent penetrant inspection
Fracture toughness	Term that is used as a measure of resistance of a material to failure from fracture from a pre-existing crack.

Hardness	A measure of the resistance of a material to surface indentation or abrasion. It could be reckoned as a function of the stress required to produce some specified type of surface deformation. There is no absolute scale for hardness.
HBF_4	fluoroboric acid
HF	hydrofluoric acid
HNO_3	nitric acid
HSM	high speed machining – more associated with finish operations
HSS	high speed steel
Impurities	Undesirable elements or compounds in the material.
Inclusion	A particle of foreign material in a metallic matrix. The particle is usually a compound (oxide, sulphide).
ISO	International Organisation for Standardisation
Machinability	The relative ease of machining a metal.
Melting point	The temperature at which a pure metal, compound, or eutectic changes from solid to liquid. The temperature at which the liquid and solid are in equilibrium.
Microstructure	Refers to the phases and grain structure present in a metallic component.
NaF	Sodium fluoride
NRF	National Research Foundation
NRTF	National Research and Technology Foresight
Optical microscopy	A type of microscope which uses visible light and a system of lenses to magnify images of small samples.
Oxidation	A reaction in which there is an increase in valence resulting from a loss of electrons. Contrast with reduction.
Passes	Term given to the number of times the cut needs to be carried out.
PCD	polycrystalline diamond
ppm	parts per million

Press	An object produced by compression of metal powder, generally while confined in a die, with or without the inclusion of non-metallic constituents.
PVD	physical vapour deposition
Residual stress	Stress remaining in a structure or member as a result of thermal or mechanical treatment or both. Stress arises in fusion welding primarily the weld metal contracts on cooling from the solidus to room temperature.
Rockwell hardness number (HR)	A number derived from the net increase in depth of impression as the load of the indenter is increased and decreased from a fixed load. The numbers are always quoted with a scale symbol.
RT	Room temperature (25°C)
SEM	scanning electron microscope
Shoulder milling	A machining process (milling) in which 90° walls can be achieved.
Sintering	A process of heating a material and bonding its powder particles or compressed powder particles.
Spindle	A rotation axis of a machine, on which a cutting tool is mounted.
Stereoscopic microscope	An optical microscope variant designed for low magnification observation of a sample.
Substrate	A solid substance or medium, to which another substance is applied and to which that second substance adheres.
Surface Hardening	A generic term covering several processes applicable to a suitable ferrous alloy that produces, by quench hardening only; a surface layer harder or more wear-resistant than the core.
Ti6Al4V	Titanium alloys containing 6 wt.% aluminium and 4 wt.% vanadium.
TiAlN	titanium aluminium nitride
TiN	titanium nitride
TiO_2	titanium dioxide

Vickers Hardness number	An indentation hardness test employing a 136° diamond pyramid indenter (Vickers) and variable loads, enabling the use of one hardness scale for all ranges of hardness.
WC	Tungsten carbide
WDX	wavelength dispersive X-ray spectroscopy
XRD	x-ray diffraction
Y_2O_3	yttrium oxide, also known as yttria
ZrO_2	zirconium dioxide

Nomenclature

f_z	Feed rate	[mm/z]
v_c	Cutting speed	[m/min]
a_p	Depth of cut	[mm]
a_p'	Chip thickness	[mm]
a_e	Of cut	[mm]
v_f	Feed speed	[mm/min]
v_a	Chemical milling speed	[mm/min]
N	Spindle speed	[revolutions per minute, rpm]
°C	Degrees Celsius	
R_a	Surface roughness	[µm]
R_c	Rockwell hardness number	
HV	Vickers hardness number	
N	Reaction index	
K_n	Titanium reaction constant	
t	Time	[minutes, hours]
λ	Thermal conductivity	[watt per mol kelvin, W/m^oK]
A	Surface area	[cm^2]
Z	Number of teeth/cutters on cutting tool	
V_B	Flank wear	[µm]
V_{max}	Maximum wear	[µm]
wt.%	Weight percentage	
R^2	Coefficient of determination	
Q^2	Predictive squared correlation coefficient	
MRR	Material removal rate	[cm^3/min]
MR	Material removal / Volume	[cm^3]
T	Temperature in degrees Celsius	[°C]

ΔT	Change in temperature in degrees Celsius	[°C]
$\angle_{ARA}$	Axial rake angle	
$\angle_{RRA}$	Radial rake angle	
$\angle_{RA}$	Rake angle	[°]
$\angle_{CA}$	Clearance angle	[°]
$\angle_{CH}$	Corner angle	[°]
$\emptyset$	Shear angle	
w	Weight	[mg, g]
Ptl	Projected tool life	
$\Delta W/A$	weight gain over area	[mg/cm^2]
p	Pressure in Pascal	[Pa]
F	Length of a side on a cutting insert	
S	Width of a cutting insert	
τ	Torque	[Nm]
P	Power	[Watt]
a	Acceleration	[m/s^2]

1. Introduction

Shortly after the establishment of the Department of Arts, Culture, Science and Technology (DACST) in the early 1990s, the then-minister Ben Ngubane announced his department's intention to carry out a nationwide foresight exercise. A number of studies were conducted as part of its mandate to review and reform the science and technology system of South Africa (Department of Science and Technology, 2000). The National Research and Technology Foresight (NRTF) Project, and the concept which would later become the National Research Foundation (NRF), came into being through a White Paper Science and Technology policy disclosure (Bawa, et al., 2013).

In the White Paper on Science and Technology, DACST committed itself to using the results of the foresight exercise as an important input into its investments in research and development within the science budget. The foresight results would also be used as input for the management of the proposed Innovation Fund, and guide research capacity-building programmes in the higher education sector (Department of Science and Technology, 2000). Specific initiatives formed as a result of the foresight studies are;

- The DST-NRF Centre of Excellence in Strong Materials
- The Titanium Centre of Competence

The goal of the DST-NRF Centre of Excellence in Strong Materials was to seek, to understand and improve the properties of advanced strong materials, to increase efficiency, and reduce cost (Bawa, et al., 2013). Within the Centre of Excellence in Strong Materials were a number of focus areas. The long term strategy of the carbides and cements focus area is two-fold. Firstly, to improve the performance of existing carbides and cermets by providing an enhanced understanding of the relationships between properties, microstructure, composition and production conditions. Secondly, to develop new carbides, cermets and hard coatings containing South African primary resources, in order to create new knowledge and new potential markets for the materials (University of the Witwatersrand, 2015).

The Titanium Centre of Competence was contracted under the CSIR (Counsel for Scientific and Industrial Research) to support research and development in the improvement of production processing technology (Barcza, 2000). Improvements include more cost-effective, environmentally friendly and wider exploitation of titanium and titanium oxide from local raw materials (The National Research and Technology Foresight Project, 1999).

Titanium was identified as a beneficiation material as South Africa has the second largest titanium reserves in the world and is one of the world's largest suppliers of raw titanium dioxide (TiO_2). However, South Africa does not contribute to, or benefit from any downstream beneficiation of the mineral in the production or value addition of titanium metal. According to Van Vuuren, the value of

introducing a world-class 20,000 ton per annum titanium metal plant would be innumerable for South Africa. The most important benefit being additional annual revenue of US$400 million from the milled production plant alone. Further downstream industrialisation and production of finished and semi-finished goods could increase annual revenue to up to US$1000 million. Once a plant has been properly established, up to 1,500 additional permanent jobs will be created (Van Vuuren, 2009).

1.1. Problem statement

The potential applications and markets for titanium are a direct consequence of its physical, chemical and mechanical properties. Corrosion resistance and a high strength to weight ratio makes titanium an ideal material for aerospace applications. Titanium is also highly biocompatible due to its resistance to corrosion from bodily fluids, bio-inertness, capacity for osseointegration, and high fatigue limit, making it highly used as a prosthetic implant in the medical industry (Van Noort, 1987). However, despite the attractive properties of titanium, current market capacity is limited to around 300,000 tons per annum, mostly in the aerospace and medical industries (Bedinger, 2015). This is a direct result of the difficult-to-process nature of the titanium metal, which requires costly measures to overcome. Tungsten carbide is a commonly used cutting tool in the machining industry. It offers high hardness and high toughness which is required for industrial machining. With the use of proper machining guidelines, high production rates and surface finish can be achieved with difficult to machine materials such as titanium.

Titanium is naturally highly reactive, and shares a high chemical affinity with oxygen. This natural affinity is amplified at temperatures above $T = 600^{\circ}C$. At these high temperatures, oxygen readily diffuses into the titanium substrate. The result is the formation of a thin, stable, oxygen-enriched surface layer known as alpha case. The formation of this layer occurs through interstitial diffusion whereby small elements such as carbon, nitrogen, hydrogen and most commonly oxygen, dissolve into the crystal lattice structure as interstitial solid solutions (Boyer, et al., 2007).

The alpha case layer, or alpha case for short, exhibits increased surface hardness and stiffness compared to the substrate. This variation in stiffness across the surface of titanium components causes localised micro failures to form. Micro failures are the origin of fatigue crack initiation zones, which compromises the integrity of the component, causing it to fail (Sung, et al., 2005). Moreover, the alpha case layer causes a significant loss in tensile strength in addition to limited fatigue performance (Yue, et al., 2012). As titanium is often used in dynamic and load-bearing applications in aerospace, the formation and presence of this layer must be restricted or removed.

The case of Delta Air Lines flight 1288 is an example of the damaging effect of the alpha case layer. On July 6, 1996, a McDonnell Douglas MD-88 experienced an uncontained engine failure during the initial part of its take-off roll. Departing from Pensacola Florida airport on route to Atlanta, Georgia with 142 passengers and crew, engine debris from the compressor front hub of the No.1 (left) engine

penetrated the passenger cabin. The damage depicted in Figure 1 (a) resulted in the deaths of two passengers, and the serious injury of another. Take-off was aborted and cabin crew initiated an evacuation which resulted in serious injury of another passenger (Flight Safety Foundation, 1998).

(a)

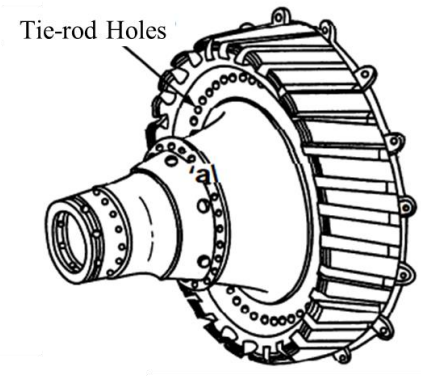

(b)

Figure 1: (a) Damaged area of passenger cabin and No.1 Engine of Delta Airlines flight 1288 (b) Pratt & Whitney JT8D-200 series engine fan hub – adapted from (National Transportation Safety Board, 1996)

The National Transportation Safety Board determined the fracture in one of the tie-rod holes in the fan hub assembly to be the probable cause of the accident. Examination of the hole wall surface revealed a darker surface finish at the fatigue origins than the surrounding area. In addition, a series of parallel surface cracks aligned with the longitudinal axis of the hole was observed. The accident board concluded that some form of drill breakdown, in combination with a loss of coolant and chip packing occurred in the machining process. This resulted in recrystallisation, increased hardness and elevated oxygen content, which could only be possible if a hard alpha case layer had been created during machining. Fatigue crack propagation had begun almost immediately after the hub was put into service in 1990 (National Transportation Safety Board, 1996).

If South Africa is to attain titanium beneficiation and produce titanium components on a larger scale, incidents such as the one above must be prevented during manufacturing. Oxidation can be restricted by performing specific manufacturing processes such as smelting, welding and additive manufacturing, under vacuum or inert atmosphere (Donachie, 2000). Oxidation at elevated temperatures can, however, not feasibly be restricted in certain manufacturing processes such as hot rolling. Subsequent manufacturing processes are therefore hampered by the presence of alpha case.

Machining is especially hampered by the increased hardness of the oxide surface layer on titanium workpiece material. Milling cutters, such as tungsten carbide, are ultra-hard and able to withstand the temperatures and forces experienced in titanium machining. The increased hardness of the alpha case layer, however, greatly increases tool wear and tooling cost if component roughing is performed with the alpha case layer still present. The alpha case layer therefore has to be removed in a pre-machining step before component roughing can commence.

Currently, the most common alpha case removal method is chemical milling. In this process the component is immersed in heated acidic solutions, such as hydrofluoric and nitric acids (Donachie, 2000). There are, however, a number of drawbacks for using chemical milling in the removal of alpha case. The acidic solutions used in alpha case removal are highly dangerous which compromises workplace safety. The disposal of used acids is also environmentally unfriendly. Therefore, the use, transport, processing and storage of these acids require highly stringent safety measures (Rossouw, 2015). Furthermore, the construction of new chemical milling facilities in South Africa requires high capital investment, which would need to be recuperated over the long term. Due to these and a number of other reasons, alternative removal methods are being pursued. One alternative is to use a dedicated machining removal step to remove the alpha case layer with the use of inexpensive, indexable tungsten carbide cutters.

Machining is a common mode of production for titanium components and is an already established industry in South Africa. Titanium machining competency can easily be achieved with limited capital spending, alleviating the need for high capital expenditure on the construction of new chemical milling facilities. Furthermore, developing guidelines for alpha case machining removal with tungsten carbide cutting tools will potentially reduce the environmental impact of chemical milling. Machining also lessens the workplace environmental hazards facing the operators tasked with handling highly acidic solutions. However, the increased hardness of the alpha case layer still hinders mechanical removal by increasing tool wear and lowering tool life (Sung, et al., 2005). An effective machining strategy for industrial machining removal of alpha case with inexpensive tungsten carbide cutting tools must therefore be identified.

1.2. Objectives

This study has two objectives. The primary objective is to determine whether tungsten carbide indexable cutters, can feasibly remove alpha case from hot rolled titanium through milling. Accelerated wear rates may render machining removal ineffective, owing to the hard oxygen enriched alpha case. Within the primary objective, the following sub-objectives are identified:

- Determine the effect that alpha case removal by method of machining has on indexable tungsten carbide cutting tools with respect to;
    - Tool life
    - Mode of tool wear
    - Machine surface-generated
    - Chip formation

In the event that tungsten carbide cutting tools can readily remove alpha case from heat-treated titanium samples, the secondary objective is to determine the scope of its feasibility. At first, the specific conditions for the most economical removal of alpha case from hot rolled titanium using

tungsten carbide cutters in machining removal will be identified. Thereafter, a cost comparison of machining removal will be made with chemical milling in order to determine the scope of feasibility.

The direct comparison will help to determine if machining removal is more suited for small batch production, large scale implementation, or not at all in an economic sense. However, other considerations should also be taken into account. These considerations include environmental impact, start-up cost, which removal method is the best suited, and which removal method will best benefit the South African manufacturing industry. If successful, tungsten carbide could replace the acidic solutions of chemical milling as the primary means of alpha case removal in a future South African titanium industry.

1.3. Significance of study

Few alternatives to chemical milling in the removal of alpha case are viewed as viable options. Those under investigation have thus far been found inferior either due to expense or applicability. Environmental regulations have, however, proliferated globally over the past several decades. The increasingly stringent environmental laws are making the disposal of used acidic solutions more difficult (Dechezleprêtre & Sato, 2014).

Developing a guideline to use tungsten carbide cutters in combination with existing machining infrastructure to remove alpha case will reduce the number of processes in the production of titanium components. Machining removal may result in components to be pre-machined closer to tolerance. This may reduce cycle time, increase productivity and remove unnecessary processing steps. Furthermore, the elimination of hazardous acids from the manufacturing process greatly increases the safety of operators tasked with the removal of alpha case, and eliminates the environmental impact of chemical milling. The confirmation that tungsten carbide cutting tools can remove alpha case from heat treated titanium will further expand its use in the machining industry. Specialised cutting tools can also be developed with the primary goal of alpha case removal. Lastly, in the event that machining removal is possible, doing a cost benefit analysis will help determine if the overall cost, and the underlying process of removing alpha case by means of mechanical milling, is a competitive alternative to chemical milling. Should machining removal not be economically viable, the information gained will lay the groundwork for future development. One deciding factor will, however, remain whether the safety and environmental dangers of chemical milling, outweigh the cost of removing the layer through mechanical means.

The removal of alpha case is a central issue to be addressed in order for South Africa to build a mature titanium industry. Currently, only small scale electrochemical etching is performed in South Africa. This leaves only two options: Constructing chemical milling facilities meeting international safety standards at great financial cost and endangerment of the environment, or finding an alternative.

1.4. Research methodology

Quantitative analysis will be conducted throughout this study, using numerous engineering principles ranging from manufacturing, material science, statistics to economics. Before any formal experimentation is to take place, literature and background studies need to be performed. A literature review will lay the foundation of the eventual experimentation by helping to understand the underlying problem. Literature with regards to titanium, alpha case, machining, carbides and wear, will summarise the work of previous researchers. The experimental setup and design will be based on the foundations laid by the literature study.

The background investigation focuses on the physical and chemical properties of alpha case that has been formed on heat-treated Ti6Al4V. Titanium samples will be heat-treated in a fashion similar to hot rolling in order to grow alpha case on the sample. Thereafter, microhardness testing of the sample cross section will be conducted to determine the extent of oxidation, and the depth of penetration into the substrate. Based on the alpha case depth, machining considerations such as depth of cut will be determined. Scanning electron microscopy (SEM) will also be performed on the heat-treated samples to view the microstructural changes as a result of heat-treatment, and to determine the composition of the samples.

Only once the alpha case layer has been investigated and its properties established will machining removal be attempted. Machining is to be performed based on the requirements of ISO 8688-1 (Tool life testing in milling – Part 1: Face milling), on a Hermle C40 U Dynamic 5-axis CNC milling machine. Titanium samples will be heat-treated in a similar fashion to the background experiments to instigate the formation of alpha case. Mechanical removal will then be attempted using tungsten carbide cutting tools at various cutting speeds and feeds. The samples will be heat-treated and machined a number of times until a satisfactory amount of material has been removed, or until tool failure criteria is met.

Tool wear analysis will be conducted throughout the machining process at regular intervals in order to determine the modes of wear, and total tool life. Furthermore, analysis of the machine chips will yield insight into the cutting process and surface roughness, and hardness testing will confirm the complete removal of alpha case from the newly-machined surface.

Statistical analysis of the cutting tool life will be conducted using Modde 10.1 Design of Experiments software by Umetrics, which would help to determine the reliability and repeatability of the experimental results. The tungsten carbide cutting tools will further undergo scanning electron microscopy in order to study adhesion wear and microstructural changes. Furthermore, a cost analysis will take place based on the tool life derived after experimentation. A cost analysis will determine the most economical machining parameters for machining removal of alpha case. Thereafter the processes for the two competing removal methods (chemical milling and machining) will be compared.

Recommendations will be made regarding the applicability of machining removal of alpha case with indexable carbide cutters, and the scope of its feasibility in a South African manufacturing industry.

1.5. Research roadmap

Chapter one comprise the introduction, including background, problem statement, objective, significance of study and methodology. The literature review in chapter two builds on chapter one, and provides the necessary background information on titanium, alpha case, machining, carbides and wear. Chapter one and two therefore sets the groundwork for the remainder of the thesis document.

Chapter three starts off with the experimental design of the background experiments. This will identify the physical and chemical characteristics, assisting certain aspects determination of primary experiments. Following the background experimental setup and design, are the setup and design of the primary alpha case removal experiments. It includes cutting strategy, machining parameters and methods for analysing the results.

The onset of chapter four reveals the results and discussion of the background experiments. Thereafter, the primary objective, determining the feasibility of machining removal of alpha case with indexable tungsten carbide cutters, will be determined by the results of the alpha case removal experiments. The secondary objective will be addressed by the cost comparison, which will determine if mechanical removal is economically feasible in a South African context.

Lastly, chapter five contains the final conclusions and future recommendations for further experimentation and analysis. The appendices which follow, elaborates on some of the statistical analysis and cost calculation conducted in chapter four.

2. Literature Study

This section yields a comprehensive overview of the literature needed to fully understand the background and objectives of the study. The literature study will review aspects including, but not limited to, titanium, the formation of alpha case, machinability, cutting considerations, cutting tool material, surface integrity and milling economics. In subsequent chapters the design of experiments, experimentation and discussion will follow.

2.1. Challenges of alpha case

Although a relatively new engineering material, titanium has quickly found wide application in various industries. Titanium alloys exhibit high specific strength, extreme lightness and corrosion resistance below $T = 500^{\circ}C$ (Nurul Amin, 2012). Exhibiting strength equivalent to many high-alloyed steels at half the weight, titanium has the highest strength-to-weight ratio of all metals. This makes it ideal for aerospace components in airframe applications and low to medium temperature sections of aero gas turbine engines (Kalpakjian & Schmid, 2013). Other than aerospace, titanium is used in industries such as automotive, shipbuilding, sporting, chemical and food processing. Moreover, its biocompatibility makes it a primary material to be used in the medical industry as prosthetic devices such as load-bearing hip and knee replacements, and heart-valve parts (Nurul Amin, 2012).

Adverse properties to the detriment of its processing, machinability and long-time use in an open and corrosive environment are, however, also present. The chemical reactivity of titanium is high at elevated (processing) temperatures. It therefore necessitates the use of unconventional processing techniques to perform melting, refining and casting. Unconventional processing techniques also add to its eventual cost. Consequently, countless research institutions are focussed on addressing the issues resulting from the physical and chemical characteristics of titanium in production (Nurul Amin, 2012).

One reason for the inherently difficult nature of titanium manufacturing lies with its atomic structure. Titanium exhibits a chemical phenomenon called allotropy, meaning that the material has the ability to exhibit multiple crystal structures while in the same phase (Haynes, et al., 2012).

Figure 2 depicts the two crystal structures into which titanium can arrange into. The first is Figure 2 (a), which shows titanium arranged in a hexagonal closed pack structure, also known as alpha phase (α). In Figure 2 (b) titanium is arranged in a body-centred cubic structure, commonly referred to as beta phase (β). At room temperature, commercially pure titanium is found in an alpha structure, and phase shift to beta structure is only possible at temperatures above the β-transus temperature of $T = 882.5^{\circ}C$ (Boyer, et al., 2007). The exact transformation temperature is however strongly influenced by alloying commercially pure titanium with other elements. This allows a beta phase structure to exist at room temperature (RT = 25°C), and an alpha phase structure to exist at higher temperatures.

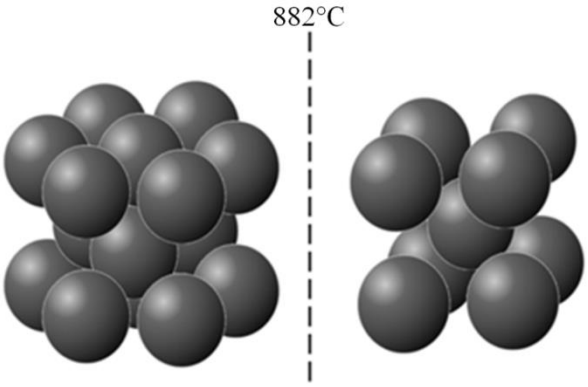

Figure 2: Appearance of titanium crystal structures at atomic level; (a) Hexagonal, close packed alpha phase (b) Cubic, body centred beta phase - adapted from (Donachie, 2000)

Elements that promote an alpha phase structure are called alpha stabilisers, and include aluminium, oxygen, carbon and nitrogen. On the other hand, elements promoting a beta structure are called beta stabilisers, and include molybdenum, vanadium and niobium (Boyer, et al., 2007). Alpha and beta stabilisers, such as aluminium, molybdenum and vanadium (commonly used in various titanium alloys), are known as substitutional alloying elements. The titanium atom is thereby substituted with a phase stabiliser, resulting in substitutional solid solution strengthening (Donachie, 2000). Solid solution strengthening is the event where metals are hardened and strengthened by elemental impurities. Alloying elements go into solid solutions, imposing lattice strains on the surrounding host atoms which allow alloys to exhibit higher ultimate tensile strength compared to pure metals (Soboyejo & Srivatsan, 2007). A range of different titanium alloys is illustrated in Figure 3.

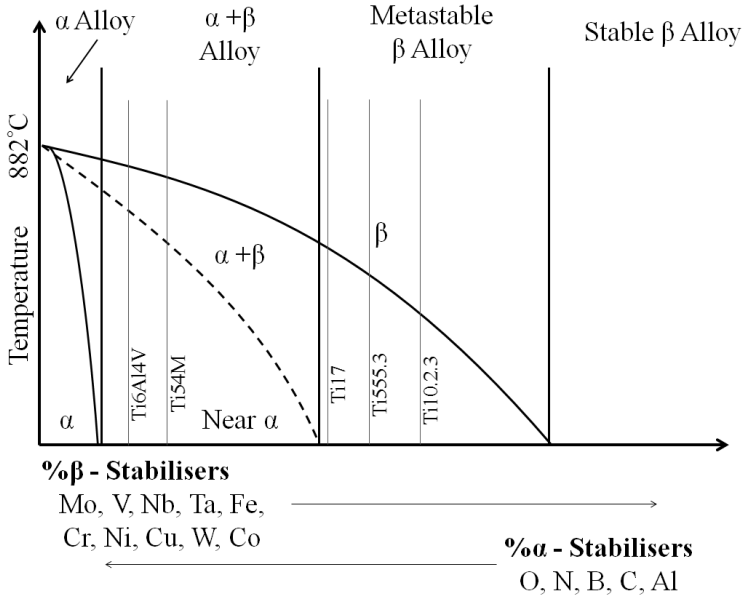

Figure 3: Phase diagram indicating the position of some titanium alloys depending on chemical composition and temperature – adapted from (Donachie, 2000)

As seen in Figure 3, alpha and beta stabilisers can be combined in such a way, to form four distinctive types of titanium alloys. Commercially pure titanium, as well as titanium alloys containing purely alpha stabilisers, is known as an alpha phase alloy, or alpha alloy. These alloys are arranged in a

hexagonal, close packed structure. Adding a small percentage beta stabiliser (1-2 wt.%) will result in a near alpha alloy. Adding roughly equal parts of alpha and beta stabilisers, results in an alpha-beta alloy. Alpha-beta alloys are the most common titanium alloys, accounting for more than half the total titanium usage in industry. The final alloy type, beta alloy, comprises predominantly of beta stabiliser, and maintains a body-centred cubic structure at low temperatures. Each of the four alloys exhibit a variety of properties, making it ideally suited for a wide variety of diversified applications (Donachie, 2000).

Commercially pure and alpha titanium alloys offer increased corrosion resistance, and beta alloys offer better mechanical properties and improved fatigue life. Alpha-beta alloys offer a combination of corrosion resistance, mechanical strength and inherent workability. It is this combination of attributes that makes alpha-beta alloys so desirable in titanium consuming industries (Arrazola, et al., 2012). The most commonly used titanium alloy is Ti6Al4V (6 wt.% aluminium, 4 wt.% vanadium), also considered the workhorse titanium alloy. It is an alpha-beta alloy and accounts for between 45-60% of all titanium used in industry (Arrazola, et al., 2012). Trace amounts of carbon, nitrogen, oxygen, iron and hydrogen are permitted, which may account for at most 1 wt.% of the total alloy weight. A full composition of Ti6Al4V is given in Table 1.

Table 1: Ti6Al4V composition - (Donachie, 2000)

Element	Ti	Al	V	C	Fe	H	N	O	Other
wt.%	Balance	5.5-6.75	3.5-4.5	0.1 max	0.4 max	0.015 max	0.05 max	0.02 max	0.4 max

Figure 4 displays a wrought Ti6Al4V alloy under scanning electron microscopy analysis. Alpha-beta alloys (such as the one depicted in Figure 4), exhibit a microstructure consisting of elongated alpha grains (dark grains), surrounded by a fine layer of beta grains (light grains). Analysis of the alpha grains would yield higher concentration aluminium as alpha stabiliser, and analysis of the beta grains would yield a higher concentration beta stabiliser in the form of vanadium (Che-Haron & Jawaid, 2005). Typical uses in the aerospace industry include gas turbine discs and compressor blades. Along with its corrosion resistance and mechanical properties, Ti6Al4V offer high biocompatibility which makes it an effective prosthesis in the medical industry (Boyer, et al., 2007).

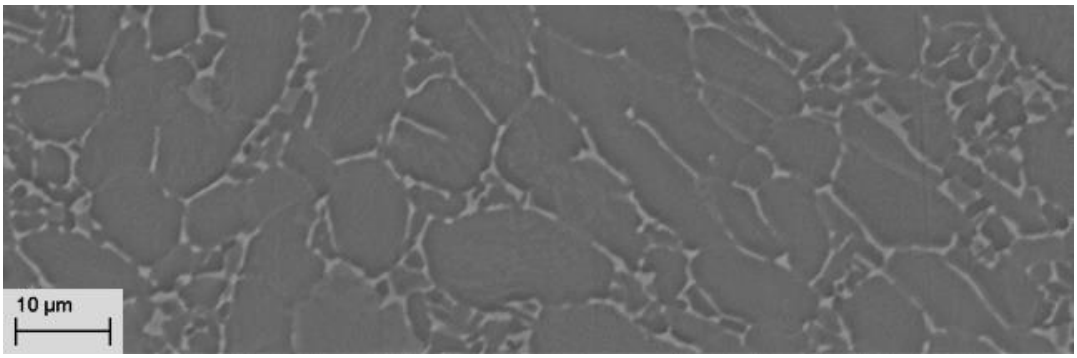

Figure 4: 1000X enlarged scanning electron microscope image of typical Ti6Al4V sample where dark alpha grains portray alpha phase (α), and lighter surrounding areas portray beta phase (β)

Apart from the voluntary addition of alloying elements to induce an alpha- or beta structure, titanium can also alloy with other elements inadvertently due to its highly reactive nature. Titanium shares a higher chemical affinity with oxygen than with any other element. The highly reactive nature, coupled with the high maximum solubility between titanium and oxygen of 14.3 wt.%, causes a thin, stable, continuous, highly adherent and protective oxide film to form when exposed to oxygen (Boyer, et al., 2007). The oxide layer, which is primarily TiO_2, is formed spontaneously when new metal is exposed to even low levels of oxygen, and is the origin of titanium's excellent corrosion resistance (Lütjering, et al., 2000). The formation of this layer is a result of interstitial diffusion, whereby small elements dissolve into the titanium phase crystal lattice as interstitial solid solutions, without substituting for titanium atoms. These elements are the opposite of substitutional elements such as aluminium and vanadium, and are known as interstitial elements. They include carbon, nitrogen, oxygen and hydrogen (Donachie, 2000). Interstitial elements are small enough to fit into spaces between the solvent atoms in the crystal lattice, and prevent it from moving further. A greater amount of stress or thermal energy is therefore required to initiate the same degree of movement.

Heat-treatment on titanium samples at high temperatures and for prolonged periods of time enables oxidation of the titanium surface on a whole different scale. At lower temperatures, the equilibrium spacing between the titanium atoms is less than the space required for the oxygen atoms to penetrate the crystal lattice structure. As the temperature rises, the distance between the Ti6Al4V atoms will increase. This leads to easier penetration of oxygen into Ti6Al4V (Sung, et al., 2005).

Du, Datta, Lewis and Burnell-Gray investigated the flanking exhibited by heat-treated titanium. Traditionally, the corrosion resistant TiO_2 layer forms and grows around titanium samples once it is exposed to oxygen. At higher temperatures, however, oxidation is increased and oxygen diffuses into the titanium sample, accelerating and expanding the formation of the TiO_2 surface layer.

Due to its reactivity at elevated temperatures, titanium and aluminium diffuse outwards towards the surface, and oxygen diffuses inwards toward the substrate. Titanium's high chemical affinity towards oxygen favours the formation of titanium oxide and dioxide as reaction products of the inwards-diffusing oxygen and outwards diffusing titanium. The lower chemical affinity that oxygen shares with aluminium causes the aluminium to continue to diffuse outwards past the titanium oxide layer, towards the surface of the titanium sample. The abundance of oxygen in the atmosphere and the abundance of aluminium available at the surface favour the formation of an Al_2O_3 surface layer at the gas/oxide interface.

Once this double-layered oxide scale has formed, the outer Al_2O_3 will continue to develop through aluminium outwards diffusion, whilst the TiO_2 layer will continue to grow through oxygen ingress. The alteration in composition brings a range of issues, including how to maintain contact between the alternating layers of oxide scale and the substrate.

Since the plasticity of this oxide scale is limited, cracks start to form between the oxide scale and the substrate once a critical thickness of the oxide scale is exceeded. The stresses caused by the mismatch in expansion coefficients between the oxide scale and the substrate can be released by cracking – initially at the edges of the specimen, and then expanding progressively through the entire specimen surface. The occurrence of the detachment at the oxide/substrate interface would make outward diffusion of aluminium and titanium difficult, and their transport rate would decrease. Due to the detachment, the inner surface of the TiO_2 layer would no longer be saturated with titanium specimen. In contrast, oxygen would still diffuse inward as a result of the partial pressure of oxygen in the newly formed crack. This would produce favourable conditions for the formation of a second TiO_2 layer. This layer would again separate the substrate from its environment in the crack where conditions might be similar to the bulk atmosphere. Aluminium from the substrate would again diffuse outward and form a second Al_2O_3 layer on top of the second TiO_2 layer in the crack (Du, et al., 1994). This process is depicted in Figure 5:

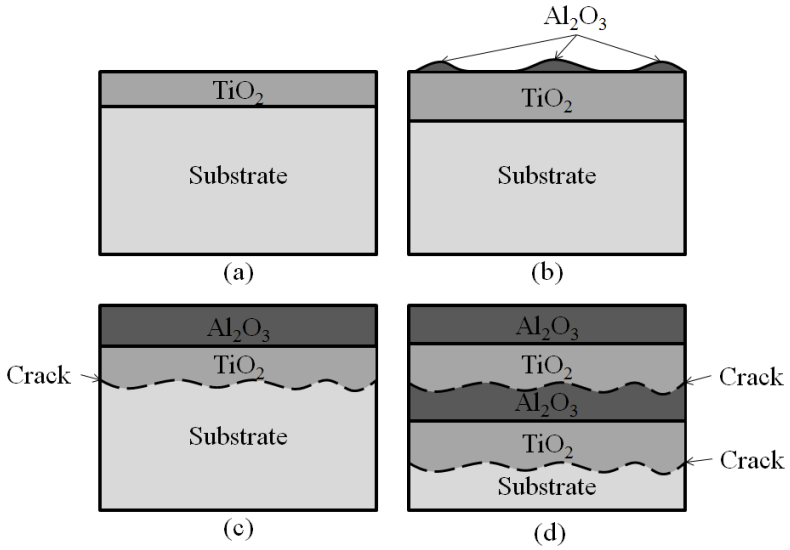

Figure 5: Oxide scale formation and growth where (a) the initial TiO_2 layer is formed once exposed to oxygen (b) outwards diffusing aluminium reacts with open atmosphere forming Al_2O_3 surface layer(c) crack formation once the double layer reaches a certain thickness (d) the formation of multiple layers due to crack formation – adapted from (Du, et al., 1994)

The formation of the multi-layered oxide scales is only one portion of the oxidation that titanium experiences at high temperatures. Oxygen ingress penetrates deep into the titanium substrate which further results in additional oxidation and growth of alpha grains at the expense of decaying beta grains under the abundance of oxygen (Patankar, et al., 2001). The oxygen pickup during heat-treatment results in a surface structure composed of a stable, oxygen-enriched predominantly alpha phase surface layer which is not caused by outwards diffusing titanium, but by inwards diffusing oxygen. The alpha case layer, or alpha case for short, is therefore formed in the substrate below the double layered oxide scales. The alpha case exhibits an increased Young's modulus (measure of stiffness) compared to the titanium substrate, and the variation in stiffness across the surface of the material causes localised micro failures to form. Fatigue crack initiation areas form as part of the

micro failures, compromising the integrity of the component, causing it to fail (Sung, et al., 2005). Additionally, alpha case causes a significant loss of tensile strength and a reduction in fatigue performance (Yue, et al., 2012).

At temperatures reaching close to T = 1000°C, the alpha structure can extend 0.2 to 0.3 mm below the surface and the hardness can reach over 1000 HV (Sung, et al., 2005). Alpha case therefore also makes machining of titanium difficult because of its extreme hardness and the removal has proven to be difficult (Boyer, et al., 2007). As a result, many kinds of titanium manufacturing processes are conducted either in inert gas atmosphere or in vacuum. However, some processes, such as hot rolling, are either too uneconomical, or completely unfeasible to be completed in controlled atmosphere. The alpha case layer consequently needs to be removed post-operation. Alternatively, an antioxidant spray coating may be applied to clean sheet metal in order to minimise oxidation. Such coatings effectively restrict oxygen pickup, but post-operation removal is not fully eliminated (Gurrappa & Gogia, 2001). In addition to oxygen pickup, nitrogen, carbon monoxide and carbon dioxide pickup is possible. Nitrogen pickup occurs at a much slower rate than oxygen pickup and therefore does not pose a serious threat. However, carbon gases readily decompose in the presence of hot titanium which results in surface oxidation (Boyer, et al., 2007).

Titanium castings are also not spared from alpha case formation. Titanium has a high melting point (T = 1700°C), and the inherent reactivity of molten titanium with the investment castings mould, results in an alpha case thickness ranging anywhere between 50-2000 μm. Moulds made of phosphate-bonded SiO_2 refractories varies in composition from the standard oxygen based layer, and include a mixture of oxygen, silicon, phosphor and titanium (Guilin, et al., 2007). More expensive, thermodynamically stable, refractories such as yttria-stabilized zirconia (Y_2O_3-ZrO_2) be used to minimise titanium oxidation. However, post-forming removal is only reduced and not eliminated (Choi & Kim, 2013). Alpha case generated thereby possibly includes both interstitially dissolved oxygen, and substitutionally dissolved yttrium and zirconium (Mutombo, et al., 2011).

Regardless of the alloying element, the formation of alpha case is generally well understood. As per Equation 1, heat acts as the instigating factor, allowing oxygen to react with the titanium surface. An increase in temperature accelerates the process by decreasing the reactive index (n). Coupled with the reaction constant of titanium (K_n), and time (t), the following equation can be developed (Du, et al., 1994).

$$\Delta W/A = K_n t^{1/n} \quad [1]$$

The rate of weight gain is greatly influenced by surface temperature as shown by Figure 6. It is also clear that the rate of weight gain varies throughout the course of heat-treatment as the thickness of alpha case increases. Oxidation is, as a result, restricted and slows down due to the greater distance that diffused oxygen needs to travel in order to bond with titanium (Du, et al., 1994). The lower

oxygen content deeper in the titanium substrate therefore lowers the formation of interstitial solid solutions. The extent of hardening caused by the interstitially diffused oxygen should therefore also decrease as distance from the heat-treated titanium edge is increased.

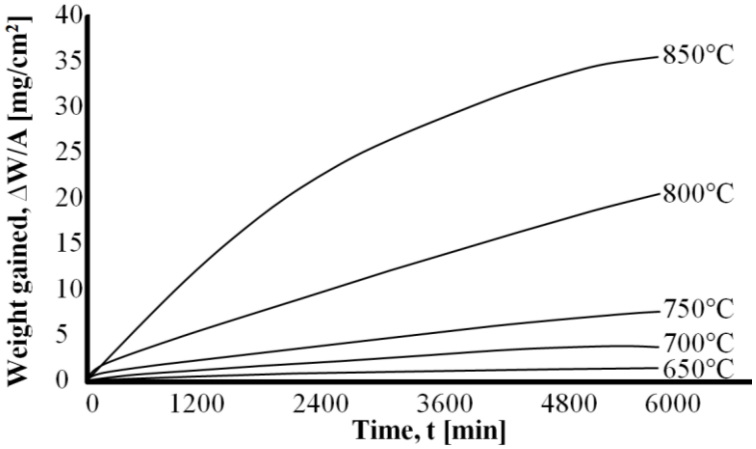

Figure 6: Weight gain over time for Ti6Al4V alloy oxidised in air between *T* = 650 - 850°C – adapted from (Du, et al., 1994)

Gaddam, Sefer, and Pederson studied the hardness depth penetration of alpha case formed after 500 hours of heat-treatment at $T = 700^{\circ}C$. Hardness measurements were taken by a micro-hardness tester applying a 100g load and a Vickers indenter (indent size: approximately 20 – 25 µm).

The micrograph in Figure 7 shows that alpha case formed on samples exposed to $T = 700^{\circ}C$ for 500 hours, as roughly 200 µm in thickness. Also, the distinction between alpha case and substrate is not a clearly-defined line. There is a gradual decrease in oxygen content as distance from the edge is increased, resulting in a gradual decrease in visibility of the alpha case displayed by etching.

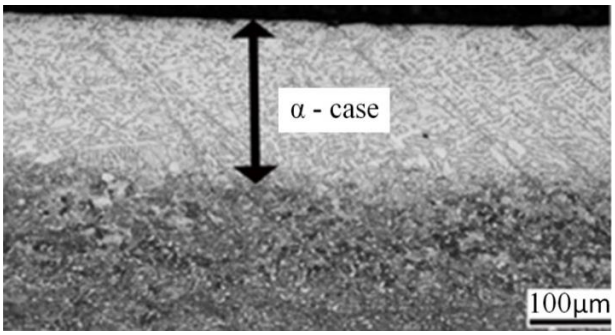

Figure 7: Optical micrograph of the Ti6Al4V sample exposed to *T* = 700°C for t = 500 hours – adapted from (Gaddam, et al., 2013)

The hardness measurements depicted in Figure 8 shows a significant increase in microhardness close to the edge compared to the rest of the substrate. The edge is therefore expected to yield the highest weight percentage concentration of oxygen. Hardness values, together with oxygen content, gradually decreases as distance from the edge is increased until it reaches equilibrium approximately 250 µm from the edge.

Comparing the alpha case depth as viewed optically in Figure 7, with what is measured through hardness testing in Figure 8, yields varying results. This suggests that there are uncertainties in

identifying the border between the alpha case layer, and the substrate bulk material in optical microscopy after etching (Gaddam, et al., 2013).

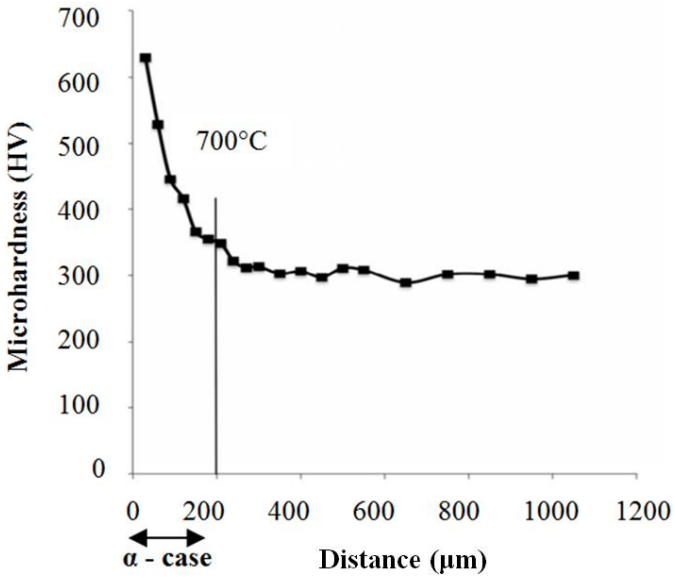

Figure 8: Variation of hardness from surface to the bulk of the Ti6Al4V sample exposed to *T* = 700°C for t = 500 hours – adapted from (Gaddam, et al., 2013)

The study shown above reflects a widely accepted academic approach of heat-treating the titanium samples to some arbitrary combination of time and temperature. This does not reflect conditions as expected in actual titanium processing facilities. Actual production facilities expose titanium to higher temperatures for shorter periods of time, resulting in accelerated alpha case formation, and a growing concern for fatigue cracks. There is therefore a degree of uncertainty attached to the study. Ideally, samples should be directly sourced containing alpha case as formed in hot processes, such as hot rolling. Failing that, the experimental conditions should be replicated to simulate that of industry practices. This would better consolidate the information obtained from the study.

Heat-treatment performed in a laboratory is different to industry manufacturing heat-treatment processes for a number of reasons. Firstly, rolling is defined as the reduction of the cross-sectional area of a component by compressive forces applied to the component through rolls. As the name suggests, hot rolling requires the material to be heated above its recrystallisation temperature, which is around $T = 900^{\circ}C$ for titanium. Minimising soaking time (the time required to preheat the entire titanium cross section) to prevent excessive oxidation and alpha case formation is an important factor. However post-process removal of the oxide layer is still performed (Boyer, et al., 2007).

Attempts have been made to carry out the rolling of titanium, and other reactive metals, in protective atmospheres such as vacuum or inert gas atmosphere. Only a vacuum better than $p = 10^{-2}$ Pa is sufficient to protect heated titanium from gas diffusion into the substrate. Solar manufacturing in Pennsylvania (USA), poses a 24-foot (7.32m) vacuum furnace capable of creating the high vacuum required for titanium heat-treatment in the aerospace industry (Solar Manufacturing, 2015). However, the incorporation of vacuum rolling mills has not been attempted. In principle, rolling vacuum mills

greatly hinder production due to the difficulties of maintaining a high vacuum in large spaces. Furthermore, the tendency of the metal to adhere to the rolling surfaces during vacuum rolling, and the difficulty in manipulating equipment under vacuum conditions remains an obstacle (Ray, 1996).

On the other hand, The Universal Cyclops Co. (USA) constructed an inert atmosphere chamber with a volume of MR = 2360 m^3, which was filled with 99.9% pure argon. Material handling was performed by an operator in a pressurised suit within the chamber. The amount of gas pick-up was studied for numerous metals including titanium. Titanium ingots heated to T = 1200°C prior to being rolled, produced negligent gas saturation. A slight increase in the weight of titanium at higher temperatures was however visible, indicating a certain oxidation of the metal (Ray, 1996).

When comparing production between hot rolled titanium under atmospheric conditions with production under inert gas or vacuum, it becomes clear that the oxide layer, in effect, eases production. Without the thin oxide layer the titanium tends to stick to the rollers making production difficult. Besides the oxide layer that eases production, the cost and overall production difficulties of maintaining a vacuum or pure inert gas atmosphere does not make it a viable alternative (Ray, 1996).

2.2. Alpha case removal methods

The removal of alpha case has been difficult because of its extreme hardness. When the need for removal first became apparent, cost saving was the primary goal as titanium manufacturing was, and still is, regarded as expensive. Inferior safety requirements and lower cost made chemical milling an attractive option, which soon became the norm in alpha case removal. Chemical milling can operate in one of two ways. Components can be submerged in a solution which offers uniform removal across the entire surface area of the part, or parts of the component can be coated with a maskant, which restricts the removal to areas that remain uncoated (Langworthy, 1989).

The chemical milling process is not complex, but if not executed properly, it can become hazardous, costly and time consuming. Simply up, it involves the part being submerged in an acidic solution heated to around T = 80°C. The steps used in chemical milling from masking to finishing are as follows (Langworthy, 1989):

a) The workpiece is cleaned and coated with a liquid maskant
b) The maskant is dried and cured
c) The pattern outline is scribed through the mask
d) The mask is peeled away in the areas to be etched
e) The desired reduction in thickness is made by immersion in the etchant for a controlled period
f) The preceding two steps are repeated if more than one removal step is required
g) The remainder of the mask is removed
h) The part is mechanically benched as required

Step number five (e) is the critical phase and also the phase that determines the cost effectiveness of the process. The desired reduction in thickness made by immersion in the etchant for a controlled

period is depicted in Figure 9. Underetching may lead to component failure due to the presence of unwanted alpha case, or increased tooling and machining cost as a result of the hard alpha case layer. Overetching the part dilutes the acidic solution which decreases the efficiency of subsequent etching processes and the acidic solution needs to be replaced sooner.

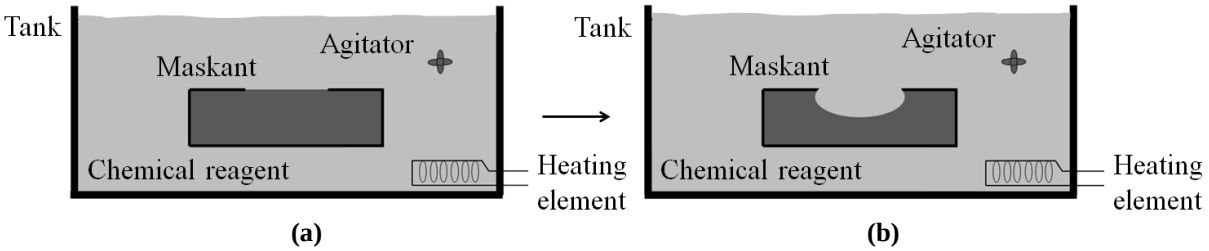

Figure 9: Chemical milling process (a) maskant is applied and the component is submerged into a heated acidic solution (b) solution etches unmasked surface for the duration of submergence

A mixture between hydrofluoric (HF) and nitric acids (HNO_3) are the most common titanium etchants because they form a highly acidic solution (Mutombo, et al., 2011). Other lesser acids such as copper sulphate pentahydrate ($CuSO_4 \bullet 5H_2O$), ammonium persulfate ($(NH_4)_2S_2O_8$), fluoroboric acid (HBF_4) and sodium fluoride (NaF) are also used. As a general rule, better material removal rates are achieved by more acidic solutions, but the disposal of the by-products are more expensive and difficult (Davies, 1997). The material removal rate for milling titanium forgings in hydrofluoric is between 0.015 and 0.03 mm/min (Donachie, 2000). Trials done by Pierre Rossouw at the Council for Scientific and Industrial Research (CSIR) was done by using a mixture of 5% HF and 20% HNO_3 which delivered acceptable results with little to no hydrogen retention (Rossouw, 2015).

Drawbacks associated with using chemical milling include high start-up cost of new facilities, stringent safety requirements, and extensive reprocessing and disposal cost of used acids (Langworthy, 1989). Safety requirements and equipment all contribute to the high facility cost and include special equipment such as extraction fans, scrubbers, specialised safety equipment, etc. (Rossouw, 2015). The South African Government defines a hazardous waste as:

An inorganic or organic element or compound that, because of its toxicological, physical, chemical or persistency properties, may exercise detrimental acute or chronic impacts on human health and the environment. It can be generated from a wide range of commercial, industrial, agricultural and domestic activities and may take the form of liquid, sludge or solid. These characteristics contribute not only to degree of hazard, but are also of great importance in the ultimate choice of a safe and environmentally acceptable method of disposal (Department of Water Affairs and Forestry, 1998).

The definition for waste is very broad since waste can vary substantially in nature, composition, size, volume, appearance and degree of harmfulness (Department of Water Affairs and Forestry, 1998). Hydrofluric acid is used due to its ability to dissolve metal oxides by removing oxide impurities from stainless steel and titanium in a process called picking (Richmond Sarpong, 2013). Hydrofluoric acid is specifically classified as a hazardous material due to the following (Tufts University, 2015):

- Hydrofluoric acid is dangerous to health and life in air concentration as little as 30 parts per million (ppm) = 0.003%
- It is an extremely corrosive material which attacks all body tissues
- Contact with the skin results in deep tissue burns that are slow to heal
- Skin contact with higher concentrations of HF causes immediate and painful burns as well as massive tissue and bone destruction
- Solutions as weak as 1% will still rapidly permeate the skin and severely damage underlying tissues
- Hydrofluoric acid vapour of as little as 10 to 15 ppm irritates the eyes, whereas higher concentrations burn the eyes, ultimately leading to blindness
- Brief exposure (five minutes) to concentrations greater than or equal to 50 ppm can be fatal

Due to the toxic nature of hydrofluoric acid extensive personal protective equipment must be worn at all times. Furthermore waste disposal guidelines, disaster spill measurements and emergency procedures must be in place for all cases of contact including skin, eye, ingestion and inhalation (The Institute for Molecular Engineering, 2014). Additionally, South Africa follows the 'polluter pays principle' whereby the person or organisation responsible for causing pollution is liable for any costs in cleaning it up or rehabilitating its effects (Department of Water Affairs and Forestry, 1998). Disposal of the acids has a safety and a financial implication and even if the acids are neutralised there is still a risk (Rossouw, 2015).

In recent years, however, alternative removal methods have been investigated to find new, safer and cost effective ways which can be employed to remove this layer. Machining and laser ablation are two of the methods under investigation, of which machining is the most common and widely used manufacturing process (Yue, et al., 2012).

Machining refers to all types of material removal and cutting processes, and traditionally includes turning, milling, drilling and grinding. Often used in small batch manufacturing, the global machining industry is worth over US$100 billion annually for metal part finishing processes (Ezugwu, 2005). Machining convert forgings, castings and preformed blocks of metal into desired shapes, with size and finish specified to fulfil design requirements (Ribeiro, et al., 2003).

The machinability of a material is defined as the ease or difficulty with which material is removed with respect to the tooling and machining processes involved. 'Good machinability' is a characteristic of a material that does not easily wear the cutting tool, results in low cutting forces, produce continuous chips which are readily removed, and results in an acceptable surface integrity (Kikuchi, et al., 2003). According to all these standards, titanium has been classified as a difficult-to-cut material with bad machinability (Choi & Kim, 2013).

The ease or difficulty in machining is a relative, not absolute, term (Watson, et al., 2007). In industry, machining cost per part is a rough estimate to determine the machinability of a material (Yang & Liu, 1999). Despite the superior properties of titanium alloys, its applications have been limited by cost

affordability because of expensive manufacturing processes as well as the high cost of raw materials. High reactivity at elevated temperatures, low production yield and limited shape in isothermal forgings also obstruct the expansion of their applications (Choi & Kim, 2013).

Siekmann in 1955 pointed out that titanium machining will always be difficult regardless of the machining techniques or cutting tools employed to transform metal into chips (Siekmann, 1955). This is still the case 60 years later. There are numerous studies that investigate the machinability of titanium alloys. These studies include the machinability, tool wear, heat exchange between chip and workpiece, chip formation and force measurements. All studies conclude that titanium is not an easy material to machine, and regardless of material and cutting tool advances, is likely to remain a difficult-to-machine material (Landers, et al., 2011).

In short, the properties that make titanium a desirable material are the same properties that limit its formability. Titanium machining has specifically been hampered by a relatively low modulus of elasticity which results in more springiness, high thermal strength (up to 400^{o}C for Ti6Al4V) and low thermal conductivity (Sun, et al., 2009). Irregular vibrations and chatter might also arise owing to the low modulus of elasticity which permits titanium greater deflection of the workpiece. This demands the use a rigid setup to properly hold the workpiece in place, and requires the use of sharp cutting tools (Kuljanic, et al., 2010). Despite all these complications, reasonable production rates and excellent surface finish can be obtained with conventional machining methods if the unique titanium characteristics are taken into account (Chandler, 1989).

2.3. Materials and Geometries

Of the different types of machining (turning, milling, drilling and grinding), milling is one of the most widely used processes. Milling makes use of rotary, multi-tooth cutters to remove material from a workpiece while advancing the cutter in the direction of the workpiece. A tooth is in contact with the workpiece for never more than half a spindle revolution, and removes a small amount of material during every revolution. Because the workpiece and cutter can both be moved in various directions at the same time, surfaces of almost any orientation can be machined (Davies, 1997). The three most common types of milling are referred to as peripheral, face, and end milling (Boyer, et al., 2007).

Face mill cutters (face milling) are used for milling plane, large, flat surfaces down to a specific height, a process which generally does not include any difficult contouring motions. The cutter is mounted on an axis positioned perpendicular with the workpiece. The face of the cutter is then used to produce the workpiece surface (Smid, 2003). Owing to the large size of face milling cutters, compared to end- and peripheral-cutters, power requirements are often higher (Boyer, et al., 2007). However, indexable tungsten carbide cutting tools are relatively inexpensive (compared to solid carbide end- and periphery mills) and the material removal rate of rough face milling is higher than

any other type of milling. This makes face milling the most viable milling technique to test the feasibility of alpha case removal by method of machining.

Face milling is fairly simple and is not often used in the manufacturing of highly complex and intricate parts. However the selection of the cutter diameter and the initial starting position of the tool in relation to the workpiece is a crucial factor (Smid, 2003).

Firstly, careful consideration should be given to the ratio between the cutter diameter and the width of cut. For a single face cut, the ideal face milling cutter diameter should be 1.3-1.6 times larger than the width of cut (a_e). This ratio will assure good chip formation and clear-out from the workpiece. It is not advised to use a full width face milling cut because face milling cutters are large and exert large amount of force on the workpiece. High forces on the cutting tool may result in chatter which further reduces surface finish and tool life. It is always advised to use the largest cutter diameter that is permitted by machining power, rigidity of setup and other related factors, while maintaining a cutter diameter 1.3 – 1.6 times larger than the width of cut (a_e) (Smid, 2003).

Furthermore, the relationship between the direction of feed and the rotation of the cutter determines how machine chips are formed and when the chip is at its thickest. There are three type of milling modes defined as conventional, climb or neutral milling (Smid, 2003). Milling strategies are chosen in such a way, that generated heat and chips are easily and continuously dissipated over a large and changing contact surface (Abele & Fröhlich, 2008).

A neutral milling mode is possible if the angle of entry is also neutral, meaning the centre line of the cutter passes over the centre line of the workpiece. This milling mode is not advisable as aligning the centre lines during milling may cause increased chatter which results in poor surface finish. It also leads to excessive wear and premature failure of the insert edge by causing the chip to weld itself on the insert.

Climb milling and conventional milling is enabled when the cutter centre line is offset from the workpiece centre line. The diagram in Figure 10 (a) depicts how the cutter pushes the workpiece away in conventional milling, and how with climb milling in Figure 10 (b), the cutter tries to *climb* over the workpiece (Davies, 1997).

With conventional milling, Figure 10 (a), chip formation starts at its thinnest, and exits the workpiece at the thickest. The initial contact is only a small area on the cutting edge and often the initial engagement is nothing more than rubbing between workpiece and cutting tool. The rubbing increases friction which results in higher temperatures and work hardening. This is especially problematic when machining heat resistant alloys such as titanium, as most of the heat will be absorbed by the cutting tool, resulting in faster wear. Conventional milling is more commonly used for high-speed steel and for machining forgings with very tough surfaces and removing scale (Davies, 1997).

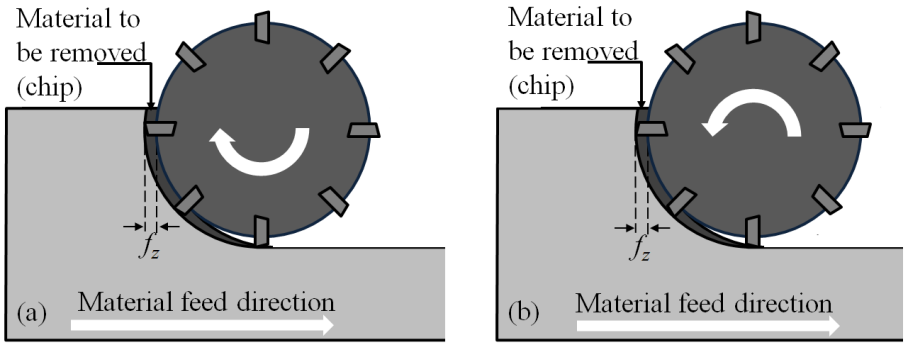

Figure 10: Milling modes for face milling (a) Conventional or up milling (b) Climb or down milling – adapted from (Davies, 1997)

Figure 10 (b) depicts climb milling, which is the primary technique used with carbide cutters when machining stainless steel and heat resistant alloys. It engages the full width of the workpiece at initial contact, and encourages the formation of thin chips upon exit. The potential for insert rubbing against the workpiece material before the cutting edge enters the workpiece material, which is common with conventional milling, is reduced with the use of a large engagement angle. Additionally, chips more easily exit the cutter as the cutting edge leaves the workpiece, and the generated heat is more easily dissipated between the cutting edge and the chip (Isakov & Ohlund, 2009). Climb milling is the preferred milling method over conventional milling for a variety of machining operations, provided that the proper equipment is available and a rigid machine and setup is achieved (Donachie, 2000).

Applying the correct milling techniques and strategies greatly increases milling effectiveness, productivity and profitability. However the ultimate success or failure of the machining operation is more dependent on whether the cutting tool and cutting tool material can withstand the harsh environment of the cutting operation.

Metal cutting involves extensive plastic deformation of the workpiece ahead of the tool tip, and at high cutting speeds the chemical and mechanical properties of Ti6Al4V cause complex wear mechanisms. High compressive and frictional contact stresses on the tool face result in substantial cutting forces which promotes deflections, chatter and movement of the cutting tool away from the workpiece (Oosthuizen, et al., 2011). Stress on the tool tip is high and most of the work (as a result of plastic deformation, frictional rubbing and compressive forces) is converted into heat, which further lowers the strength of the tool tip (Machado & Wallbank, 1990). In addition, the tool may experience repeated impact loads during interrupted cutting, whereby freshly produced chips chemically react with the tool material. The cutting tool is thus subjected to a variety of hostile conditions during industrial cutting. The actual values are dependent on the geometries, cutter type, cutting conditions and workpiece material (Santhanam & Tierney, 1997).

The service life of a cutting tool is hard, and is determined by its ability to resist the effects of a number of wear processes which includes flank, crater and abrasive wear (Santhanam & Tierney, 1997). The physical properties of the cutting edge must exhibit strength capable dealing with the

mechanical loads of the cutting operation, otherwise breakage and edge fracture may be common (Barry, et al., 2006) (Barnett-Ritcey, 2004). Furthermore, the harsh environment experienced by cutting tools at the tip results in a number of other requirements including, but limited to (Machado & Wallbank, 1990):

- High Transverse rupture strength
- Reduced tendency to react with titanium
- High hardness at elevated temperatures
- Toughness and fatigue resistance to withstand the chip segmentation process
- High thermal conductivity to minimize thermal shock on the tool

Transverse rupture strength (TRS) is the ability to withstand brittle fracture and the resistance to crack initiation. Chipping is a common wear mechanism in titanium machining and an important performance characteristic. The transverse rupture strength of a cutting tool should be greater than the applied load to avoid rake face chipping from the mechanical load. Cemented carbide has the highest transverse rupture strength of all commonly used titanium cutting tool material (Oosthuizen, 2010).

A final, equally important factor in the production management of titanium machining is low cost. Selecting the optimum cutting tool is a balance between requirements and cost. This is due to not one single cutting tool material exhibiting all the desired criteria. Carbide tools are widely used in industry to optimise titanium machining production rates. Other cutting tool material, not necessarily used in titanium machining, include high speed steel (HSS), polycrystalline diamond (PCD) and cubic boron nitride (CBN) (Oosthuizen, et al., 2010).

Figure 11 displays the various relationships that cutting tool material has with hardness and toughness. As emphasised by the arrow in the top right-hand corner, the ideal cutting tool material exhibits a combination of the highest degree of hardness with a high degree of toughness. Hardness is the ability of the material to resist deformation by surface indentation and resistance to wear which increases tool life (Oosthuizen, 2010). Toughness enhances resistance to chipping and catastrophic failure and is commonly exhibited by HSS. HSS is however limited in hardness (compared to PCD and CBN) which aids in wear resistance and hot hardness (Oosthuizen, et al., 2010).

The most widely used cutting tool material in titanium machining is cemented carbides. They belong to a class of hard and wear-resistant refractory material. The hard carbide particles, such as tungsten carbide (WC), are bound or cemented together by a soft and ductile metal binder, commonly cobalt. Carbide tools offer a balance between hardness and toughness required for titanium machining. The addition of wear and temperature resistant multi-coatings has made coated micro-grain cemented carbides comprehensive cutting tool material capable of almost any cutting operation.

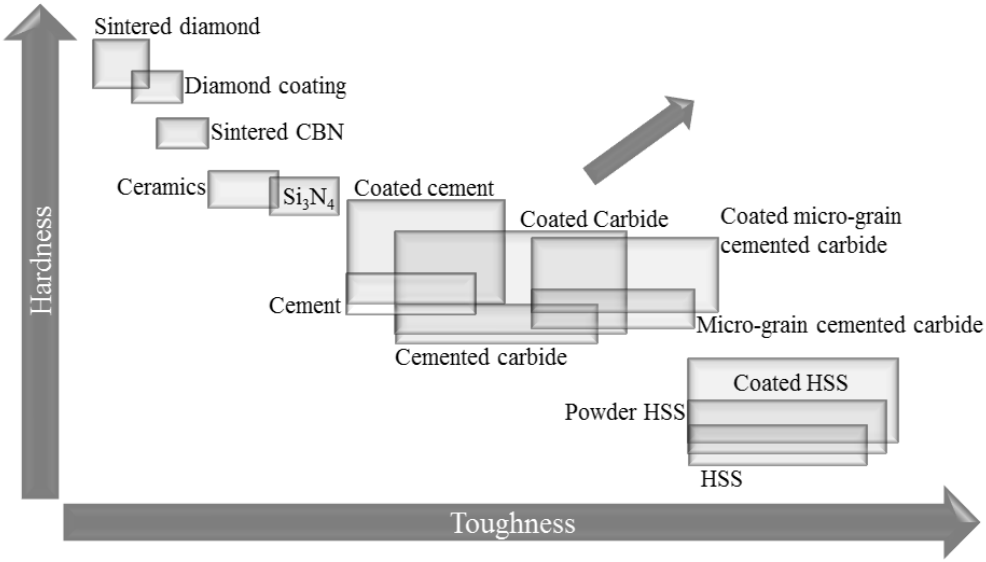

Figure 11: Relationship between various tool materials in relation with hardness and toughness – adapted from (Oosthuizen, et al., 2010)

The production of carbide cutters occurs by means of press and sinter from a mixture of a carbide compound, and a soft, ductile metal binder (Santhanam & Tierney, 1997). Tungsten carbide is used for its wear and temperature resistance which constitutes the majority of the cutting tool, and the binder adds fracture toughness. Although the highest possible carbide concentration greatly benefits wear resistance and hot hardness, sufficient binder is necessary to deter crack initiation, fracture and catastrophic failure. There is thus a direct relationship between the binder and carbide concentration, which results in cutting tool toughness and hardness respectively. The properties of cemented carbides not only depend on the type and amount of carbide, but also on the carbide grain size and binder amount (Santhanam & Tierney, 1997). Improvements in the composition and microstructure therefore greatly influence the performance of carbide cutters (Wang, et al., 2013).

More recently, new tool material such as ceramics, cubic boron nitride (CBN) and polycrystalline diamond (PCD) have become common. Studies have shown that PCD is a suitable cutting tool material in turning of titanium components and that it produced better surface integrity in finish turning operations (Sharman, et al., 2000). Studies have also proved that the same increase in tool life is experienced with milling. Uncoated tungsten carbide-cobalt inserts were compared with PCD inserts in machining Ti6Al4V by Nurul Amin et al. They reported that the PCD inserts were effective up to cutting speeds of v_c = 160 m/min with inserts exhibiting relatively low wear rates (Nurul Amin, et al., 2007). Oosthuizen et al. also concluded that at elevated cutting speeds the PCD insert outperformed the carbide alternative (Oosthuizen, et al., 2011).

These cutting tools offer increased material removal rates, wear resistance and better surface finish. However, the economic feasibility of these cutting tool materials is not evident in titanium machining (Nabhani, 2001). Wear resistance is a major concern regarding cutting tools in the machining industry as it affects the net shape and surface finish of the generated surface (Abdel-Aal, et al., 2008).

However economic feasibility is still the driving factor, which is why cemented carbides are more commonly used. The wear resistance of cemented carbide cutting tools can be enhanced by applying a coating to the cutting edge. Multi-layered tool coatings shield the substrate from the destructive influences of machining by enhancing the tribological properties of cutting tools (Donachie, 2000).

Rapid improvements in coating deposition techniques and the development of more advanced coating materials have resulted in coatings pervading numerous industry branches. This includes automotive, aerospace, cutting tool and precision machining (Grzesik & Nieslony, 2004). Typically, coating materials pose high mechano-chemical properties. Increased wear and chemical resistance is experienced until the hard coating is removed and the softer core material is exposed. Chemical resistance is highly beneficial in titanium machining as it enables the cutting tool to restrict diffusion wear (Abdel-Aal, et al., 2009). Coatings also allow for higher machining speeds when machining titanium which may increase productivity.

Coatings have shown to promote longer tool life by lowering friction at the tool-chip interface, which in turn reduces energy and contact temperature. Research has also shown coatings can help control the heat distribution by modifying the chip-tool contact area between the substrate or coating system and the chip material (Grzesik, 2003).

In practice, performance of coatings receives mixed approval with some studies finding that it improves tool life while others discourage the use of coatings. One study has found that the coating life is short and the protective properties are ineffective in prolonging metal cutting. Studies frequently observe that tool coatings fail at the initial moments of machining, rendering the tool substrate material exposed to the harsh environment exhibited by machining (Abdel-Aal, et al., 2009). Some research has attributed it to chemical reactions, whereas others have confirmed that it is due to crack propagation at the substrate interface. Nouari and Ginting also observed that the maximum cutting temperatures are higher for coated tools (T = 1180°C) compared to uncoated tools (T = 950°C). This is not conductive to prolonged tool life, crossing the temperature-threshold that sets off the diffusion process (T = 850°C), and increasing the pressure on the cutting edge. Consequently, the cutting tool loses its hardness and fails more rapidly (Nouari & Ginting, 2006).

Coatings are commonly applied by physical vapour deposition (PVD) or chemical vapour deposition (CVD) on both solid tools and indexable cutters of almost any geometry (Grzesik & Nieslony, 2004). This greatly aids in its wide application because cutting tools for metal cutting vary in shape and size, and the geometry is dictated by the operation to be executed.

The primary goal of cutter angles is the efficient separation of chips from the workpiece, and the disposal of newly cut chips. The type of workpiece material, machine power and cutting fluid all contribute to chip formation and evacuation (Davies, 1997). The tool angles are chosen to manage and counter the forces and high temperatures brought about the cutting operation. In titanium machining,

rounding or chamfering of the cutting edge should be avoided as it increases friction and rubbing. Instead, cutting tools should be kept sharp in order to restrict excessive heat build-up. Furthermore, tools and inserts should be replaced regularly as worn tools can also alter dimensional accuracy (Abele & Fröhlich, 2008).

Apart from the varying types of cutters (peripheral, end and face milling), a distinction is also made between the controlling angles of the cutting teeth. The axial rake angle ($\angle_{ARA}$), radial rake angle ($\angle_{RRA}$) and corner angles ($\angle_{CH}$) of the cutting teeth define the relationship between the cutting edge and the workpiece (Davies, 1997). Together they describe which part of the cutter makes first contact with the workpiece, what the power requirements are, they influence the shape of chips and decree how these chips are displaced. Each angle is the result of the angle measured with respect to a reference plane which passes through the axis of the cutter rotation, and the point of the tool (Boyer, et al., 2007).

The power efficiency of material removal and cutter life is largely determined by the radial rake angle which is determined with reference to the radius of the cutter face. A zero to positive radial rake angle is generally used when power is limited. Care must be taken as a positive radial rake cutter can potentially lift the workpiece if it is not properly clamped. The configuration produces good chip-breaking characteristics at the cost of insert strength and fragility (Smid, 2003). Negative radial rake angles offer higher strength to the cutting edge. The higher strength limits catastrophic shear failure as a result of chipping, but poorer chip formation, surface finish and tool life is observed compared to positive cutters. Negative radial rake angles also require higher machining power compared to positive cutters. However, negative inserts offer double the amount of cutting edges compared to positive cutters, potentially making negative inserts more economical than positive inserts.

The axial rake angle determines the strength of cutting edges and controls the flow of chips and thrust force of cut. Axial rake is the cutting insert's angle with respect to the central axis of the cutter/spindle assembly. High speed steel cutters as a rule employ positive axial angles except for end mill cutters that only cut on the periphery. Negative angles are used at times since negative cutters transfer cutter thrust back against the spindle bearings while simultaneously applying downward thrust to the workpiece. Carbide cutters alternate between positive and negative angles depending on the material and type of cutting operation (Davies, 1997).

Two combinations of axial and radial angles are commonly incorporated in titanium milling. They include the double negative setup depicted in Figure 12 (a), and the combined approach, or positive/negative setup (as it is more generally known), depicted in Figure 12 (b). Double positive cutters are also available however these cutters wear edges more rapidly by redirecting newly cut chips back into the cutter, causing chips to be re-cut. Double negative cutter geometry requires that both the cutting tool and workpiece material are securely fitted, and sufficient machining power to

penetrate the material. Double negative cutters use a combination of negative axial and negative radial rake angles. As a result, cutting forces are directed farther back from the cutting edge, allowing for greater insert strength compared to the alternatives. Hard-to-machine materials such as cast iron commonly benefit from the additional insert strength. However, jamming of the chips against the insert edge and workpiece material may be a problem owing to the machine chips not being evacuated effectively. To its benefit, the negative radial angle results in twice the number of available cutting edges due to the double sided nature of its design (Smid, 2003).

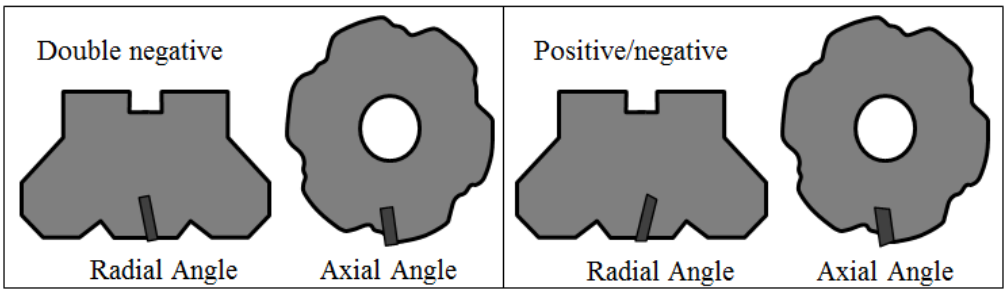

Figure 12: (a) Double negative cutter geometry with negative radial rake ($\angle_{RRA}$) insert angle and negative axial insert angle ($\angle_{ARA}$) (b) Positive/negative cutter geometry with positive radial rake insert angle ($\angle_{RRA}$) and negative axial insert angle ($\angle_{ARA}$)– adapted from (Winegard, 2012)

The alternative combination of axial and radial angles is greatly effective in face milling applications where chip-clogging is a problem. The positive/negative insert geometry offers the strength of a negative axial angle, with the capability of positive radial angle. This allows for lower cutting forces and for the chips to form a spiral shape (Smid, 2003).

There is one more controlling angle that directly influences the formation of chips and result in lower cutting forces experienced by the cutting edge. The use of corner angles ($\angle_{CH}$) and small nose radii on inserts provide for more efficient distribution of cutting forces over a greater area by evenly distributing cutting resistance and heat build-up (Boyer, et al., 2007). A number of variations of different corner angles are exhibited in Figure 13.

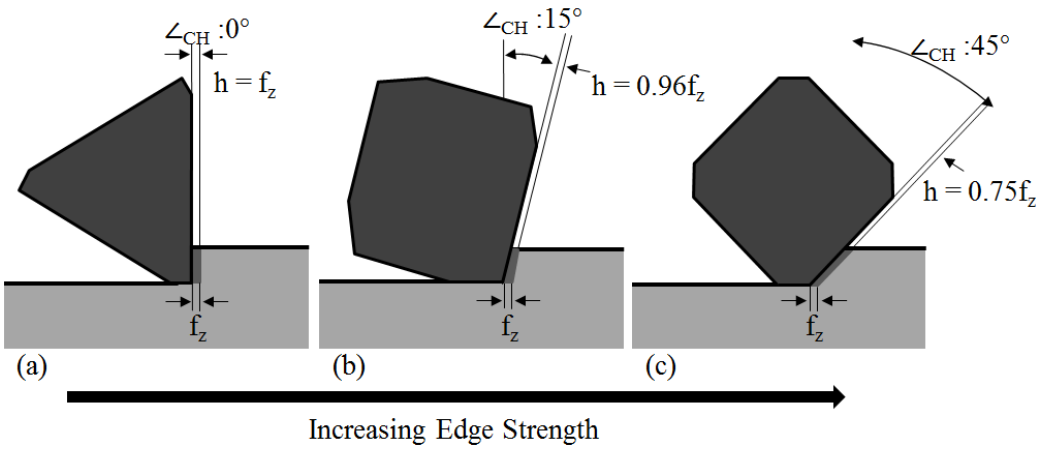

Figure 13: Effects on chip thickness due to the variation of corner angles (a) 90° or square angle, (b) 15° angle, (c) 45° angle – adapted from (Mitsubishi Carbide, 2015)

As exhibited in Figure 13, variations in shape- and lead angle, causes variation in the size and shape of the chips that cutting edges produce. These small changes effectively extend tool life without compromising material removal rate (Watson, et al., 2007). Cutters may exhibit corner angles of 90^{o} to machine a square shoulder, or range between 0 to 60° to reduce chip thickness and to ease the blade into the workpiece with less shock (Davies, 1997). The length of the contact area of a 45° corner angle is 75% longer than an insert with a 90°edge, whereas a round-cutting edge results in a contact area of 24% longer than an insert with a 45° edge. The distribution of cutting force increases tool life, allowing for more aggressing machining to be used during roughing, which increases productivity levels.

The formation of chips is therefore also different, depending on what type of corner angle is used. The differences in chip formation or chip segmentation play an important role in titanium machining and the phenomenon has been investigated extensively. Attempts have been made (dating back to work performed by Cook in 1953) to describe the chip morphology in titanium metal cutting. Cook investigated the chip morphology of titanium at different cutting speeds and proposed a thermodynamic theory for chip formation. Nakayama et al. in 1988 and Shaw and Vyas in 1993 proposed the periodic crack formation theory in machining hardened steel (Shaw & Vyas, 1993). Konmanduri et al. studied the chip formation process during high-speed machining of titanium alloys in 1981. They proposed the well-known ‘catastrophic shear’ theory which is consistent with the most practical evidence in titanium machining (Komanduri & Von Turkovich, 1981).

Titanium alloys are known for shear localisation which results in saw tooth (also termed, serrated, or segmented) chips. Komanduri and Von Turkovich observed the sequence of events leading to catastrophic shear-failed chip and determined that the event can be divided in two stages. The observations were made by studying video of high speed photography, in situ machining inside a scanning electron microscope. Figure 14 contains schematics based on the observations, showing the chip formation process at various moments involved in the catastrophic shear failed chip formation when machining titanium alloys.

Stage one involves plastic instability, which leads to strain localisation along a shear surface. Segment build-up starts with the gradual flattening of the wedge-shaped work material ahead of the tool. The initial contact on the tool face with the segment being formed is short, and the contact length increases as the flattening progresses (Komanduri & Reed, 1983). There is effectively no relative motion between the bottom surface of the chip segment being formed, and the tool face. That is until the end of the flattening stage of the chip formation process. Accelerated wear may be caused by the rapid and forced transfer of heat into the tool tip, which enables prompt chemical interaction between the chip and the tool.

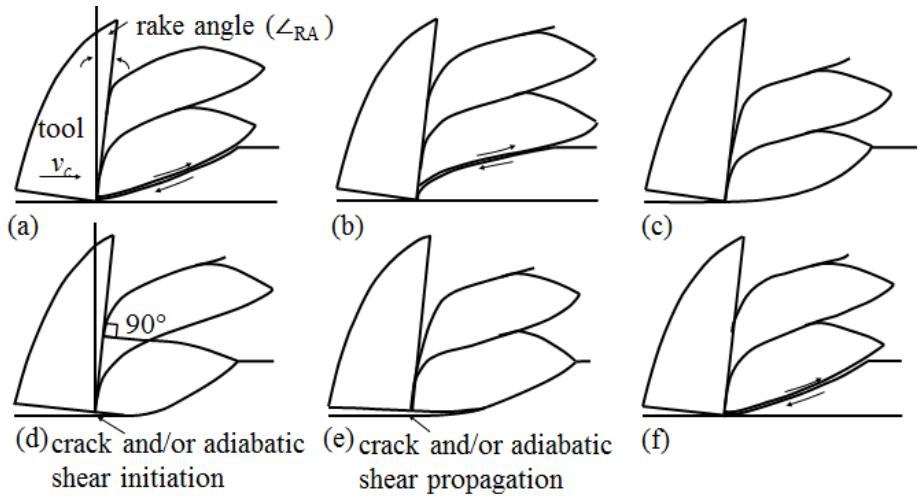

Figure 14: Schematic diagrams of the sequence of events, showing various stages involved in chip formation when machining titanium alloys – adapted from (Komanduri & Von Turkovich, 1981)

During the second stage, the previously-formed chip segment is slowly pushed upwards by the gradual bulging of the new chip. The contact between the previous segment and the segment being formed shifts gradually, starting close to the work surface and moving towards the tool face as flattening progresses. The velocity of the chip along the rake face is similar to the velocity of bulging of the chip segment. However, once shear is initiated and progresses rapidly, it will push the segment being formed faster parallel to the shear surface, which will in turn push the previously formed segment rapidly (Komanduri & Von Turkovich, 1981).

Figure 15 shows a schematic of a single point cutting operation of a tool rotating at a velocity v_c and a depth of cut a_p. The chip that forms has a thickness called a_p'. The chip is generated at a shear plane that is at an angle ∅ with the workpiece surface in the direction of cut. This rake angle ($\angle_{RA}$) is an important angle in the mechanics of chip formation and the relief, or clearance ($\angle_{CA}$), angle serves as a potential access point for cutting fluids to the cutting zone (Nachtman, 1997).

Considering Figure 15, zone 1 represents the commonly referred primary shear zone, indicating the area of strain hardening that forms in the metal being cut ahead of the tool. Microcracking and relatively high temperatures is often a possible consequence of deformation, which may result in the appearance of strain hardening. Secondary deformation due to the shearing and sliding of the chip against the tool is depicted in zone 2. The rubbing between the workpiece chip and cutting tool rake face generates more heat due to the friction between the two materials. As the tool traverses the freshly-cut surface, further rubbing of the tool against the workpiece material takes place in zone 3. Additional heat and deformation are caused through the frictional contact between the two materials. As chip formation proceeds, further plastic deformation and friction are caused by the formation of a built-up edge in zone 4. Below the area of primary material removal is zone 5, where additional plastic deformation and strain hardening takes place (Nachtman, 1997).

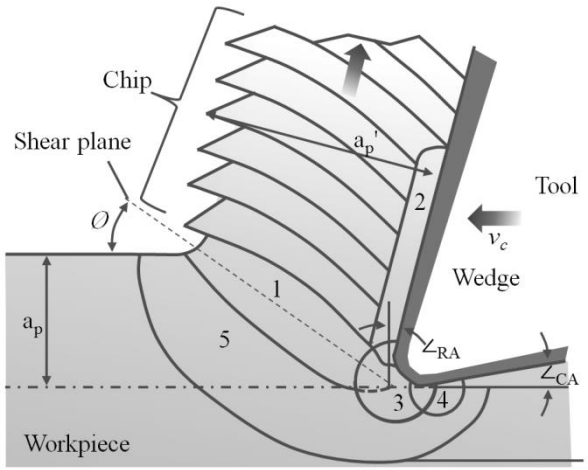

Figure 15: Chip, workpiece and tool relationship (1) Primary shear zone (2) Secondary shear zone (3) Secondary shear zone at rake face (4) Secondary shear zone at flank face (5) Deformation advance zone – adapted from (Grote & Antonsson, 2008)

It is well known that the continuous cycle of plastic deformation at the shear plane, followed by frictional rubbing between the cutting tool and the workpiece chip, are the two principle heat sources in metal cutting (Komanduri & Hou, 2001). The heat partition between the workpiece material and cutting tool depends on their thermal properties, cutting fluid, and cooling method (Yang & Liu, 1999). Temperature has an important effect on tool wear and it is generally known that progressive tool wear is produced by temperature-dependent mechanism (Grzesik & Nieslony, 2003). Furthermore, the notoriously poor thermal properties of titanium in combination with its high hot hardness further adds to tool wear and tool failure (Hong & Ding, 2001). It has also been reported that the temperature gradient is much steeper, and the heat affected zone much smaller and much closer to the cutting edge as a result of the shorter chip-tool contact length in titanium compared to machining steel (Nurul Amin, et al., 2007).

Figure 16 depicts the heat generation and heat dissipation when machining steel or most continuous chip forming materials. According to traditional continuous-chip theory, heat is generated in three zones: the primary shear zone, secondary shear zone, and the interface between the flank and the machined surface (Trent, 1988).

In Figure 16, the majority of heat generation takes place in the primary shear zone, but only a portion of the heat dissipation is through the cutting tool. The majority (80%) of the generated heat is dissipated through the chip. In titanium machining, however, owing to rapid flank wear and almost no secondary deformation on the rake face, the significance of zones 2 and 3 is virtually opposite to that for materials yielding continuous chips. Therefore, a significant portion of heat is generated at the clearance face as a result of rubbing between the flank and the machined surface, and an insignificant portion of heat is generated between the sliding chip and rake face. Additionally, the portion of heat getting into the tool and carried away by the chip will be different (Komanduri, 1982).

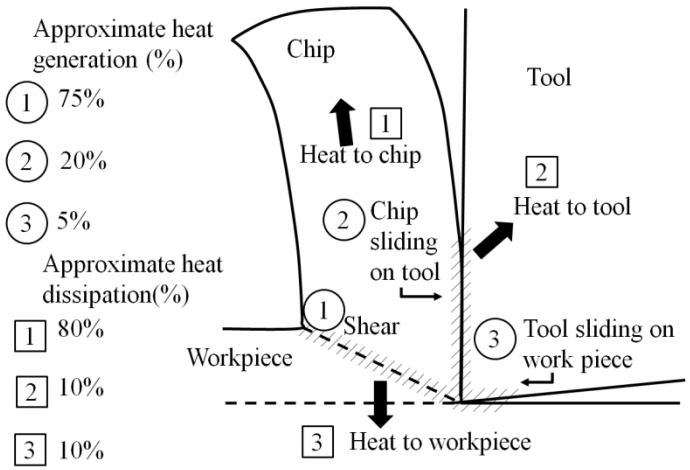

Figure 16: Energy partition (heat generation and dissipation) in the machining of steel - adapted from (Komanduri, 1982)

As a result of the thermal properties of titanium machining, the new energy partition is more likely to be similar to Figure 17. Other literature also suggests that the heat absorbed by the cutting edge in titanium metal cutting is up to 80% of the total heat that is generated. This is compared to the maximum estimation of 50% absorbed by the cutting edge when machining steel (Ezugwu & Wang, 1997). The poor thermal conductivity of titanium λ = 7.1 W/m^{o}K, compared to that of steel CK 45 at λ = 51.2 W/m^{o}K, is largely responsible for the additional heat absorption (Lopez de lacalle, et al., 2000). It has been shown that the location of the maximum temperature would be an area of high tool wear, which is due to the energy accumulated on the cutting edge over a period of time (Abdel-Aal, et al., 2008). The high temperatures generated during titanium machining also cause work hardening of the workpiece material. This affects the surface integrity of the titanium component, and could lead to geometrical inaccuracies and a reduction in fatigue strength (Nurul Amin, 2012).

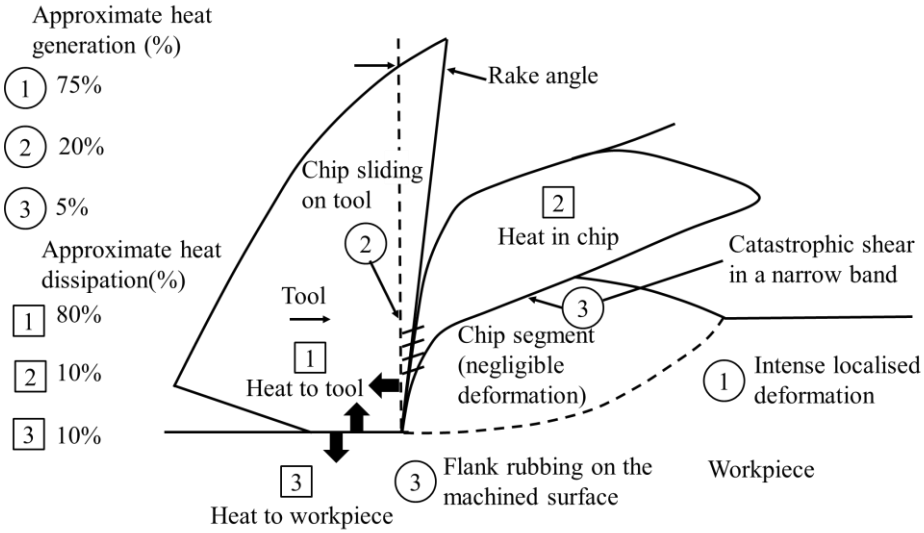

Figure 17: Energy partition (heat generation and dissipation) in the machining of titanium alloys - adapted from (Komanduri, 1982)

The thermal energy generated in titanium machining greatly influences the cutting tool and expedites tool deterioration. According to the International Organisation for Standardisation (ISO), tool

deterioration includes all changes in the cutting part of a tool caused by the cutting process. Three distinct classes of tool deterioration exist, namely tool wear, brittle fracture, and plastic deformation (International Organization for Standardization, 1989). Tool wear is related to the manner in which the thermal energy is transported and dissipated within the tool active region. Lower cutting speeds, at the cost of material removal rate, can be used to lower heat generation and tool wear, which in turn increases tool life (Abdel-Aal, et al., 2008). Feed rate and depth of cut can be increased to maintain high material removal rates, but may result in an increase in cutting forces, additional chatter, and loss of precision and surface integrity. It is therefore up to the machine operator to determine how best to weigh all the mechanisms of wear, and to determine the best machining strategy for each individual machining operation.

2.4. Modes of tool wear

Tool life is often depicted as the total machining time or volume of material removed before a tool fails either by excessive wear, chipping, or catastrophic failure. Any instance in which two material are in mechanical contact with the intention of material removal in the form of chips, forms a wearland (Yang & Liu, 1999). Wear is a constant factor and the many variants depend on the physical wear mechanisms of the mechanical contact (Odelros, 2012). The only form of tool degradation wholly accepted within the machining industry, is expected degradation (gradual wear). Being able to predict tool wear rates makes it possible to schedule tool replacement, and to find cutting parameters capable of optimising production rates (Henry, et al., 1995).

Catastrophic premature tool failure is an undesirable and unpredictable failure mode which can be damaging to the workpiece. A thorough understanding of the physical demands on the cutting tool and the effect of changing the operation conditions can minimise tool failure.

Cutting tools are subject to wear because normal loads on the wear surfaces are high, and the newly cut chips and the workpiece that apply these loads are moving rapidly over the wear surfaces. The cutting action and friction at these contact areas increase the temperature of the tool edge, which further accelerates the physical and chemical processes associated with tool wear. Tool wear is a natural result of chip formation and material removal, and is therefore a production management problem in manufacturing industries (Kendall, 1997).

Figure 18 shows how a typical sharp tool may wear. Along the rake surface a wear-scar called crater wear is formed due to the chip motion and high normal stresses. The clearance face experiences high normal stresses which increases the area of contact between the tool and workpiece which produces flank wear. Lastly, the cutting edge radius has increased due to plastic deformation under the extreme pressures of machining (Kendall, 1997). It therefore shows how the tool geometries are greatly altered by wear brought on by machining, as well as high temperature and high compressive forces.

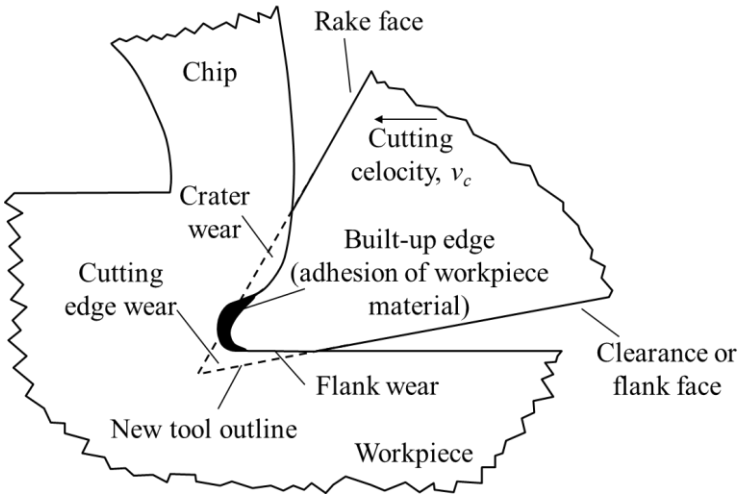

Figure 18: Typical wear surfaces – adapted from (Kendall, 1997)

Among the numerous types of wear, flank wear (V_B) as depicted in Figure 19, is the most common type of wear in titanium machining. Flank wear, forms with the unwanted rubbing of the clearance face (relief surface) against the workpiece material, and results in a loss of material in the tool flanks during cutting. A distinction is made between uniform and non-uniform flank wear. Wear of constant width, extending over the proportion of the tool flank active in the cutting operation, is generally deemed uniform flank wear. This is depicted by Figure 19 (a). Non-uniform flank wear has an irregular width, and the profile generated by the intersection of the wear land and the original flank varies at each position of measurement (International Organization for Standardization, 1989).Localised flank wear is an exaggerated form of non-uniform flank wear which develops at localised points on the flanks (ISO, 1989). Notch wear, as depicted in Figure 19 (b), is the most common type of localised flank wear and develops on the part of the major flank adjacent to the work surface during cutting. It is a common wear type when machining materials that work harden such as austenitic stainless steels and high temperature alloys (Santhanam & Tierney, 1997).

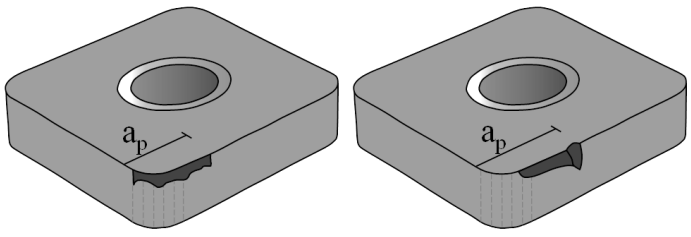

(a) **(b)**

Figure 19: Types of flank wear (a) uniform flank wear across the flank face of the tool (b) localised flank wear or notch wear on the flank face in the region opposite the workpiece surface

High performance metal cutting causes extreme cutting conditions at the tool-chip interface in the form of high temperature and high pressure. In material science, high temperatures facilitate particle flow from an area of high material concentration to low material concentration. In terms of machining, the flow of the chip over the contact surface of the cutting tool causes particles to diffuse from the tool into the newly machined chip. This process is called diffusion wear. The chip is then

evacuated along with the diffused particles, causing the formation of a crater on the tool rake surface which reduces the mechanical resistance of the tool. Diffusion wear typically only initiates at cutting speed greater than v_c = 150 m/min (Zhang, et al., 2009).

At low cutting speeds when the tool temperature is not high, diffusion wear is replaced with built-up edge (BUE) and adhesion wear (Santhanam & Tierney, 1997). The occurrence where work material is deposited on the rake face of the cutting tool is called built-up edge. It is the product of extreme localised high pressure at the tool-chip interface, which causes the workpiece material to adhere to the cutting tool edge. As this BUE becomes more prominent, it bonds chemically with the cutting tool material. When this BUE is eventually ripped from the cutting tool, a portion of the cutting tool is also removed, forming a crater (Donachie, 2000). As this process is repeated, the crater grows and wears the cutting tool. Should BUE not fracture and continue to accumulate on the cutting edge, the adhered workpiece material protects the cutting edge, but at the same time modifies the geometry of the tool. Built-up edge is not stable and its continual presence changes the shear angle, which leads to instabilities in the chip forming process and damage to the machined surface (Kendall, 1997).

Flank, diffusion and adhesion wear can result in a number of failure nodes ranging from chipping and cracks to brittle fracture. There are several classifications of chipping as described by the ISO. Uniform chipping is described as the loss of tool fragments of approximately equal size along the cutting edges, which significantly influences the uniformity of the flank wear land. Non-uniform chipping occurs mostly in connection with cracks at isolated positions along the active cutting edges with no consistency between one cutter or another. Isolated chipping occurs when chips are consistently formed along the active edge at certain positions. Chipping can also occur on the non-active part of the cutting edge. Brittle edge fracture is the disappearance of the major part of the active cutting edge which makes it impossible to continue cutting (International Organization for Standardization, 1989).

Cracks are defined as the fracturing of the cutting tool material which does not immediately cause loss of tool material. Comb cracks, parallel cracks and irregular cracks all appear on the tool face and tool flank face. Whereas comb cracks appear approximately perpendicular to the major cutting edge, parallel cracks appear parallel to the cutting edge and irregular cracks are irregularly orientated. A brittle fracture is the occurrence of cracks in the cutting part of a tool followed by the loss of small fragments of tool material which result from crack initiation during cutting (International Organization for Standardization, 1989).

The progression of wear typically occurs in a similar fashion to what is displayed in Figure 20 (Marinov, 2008). The wear curve depicts total tool wear of a cutting tool when using recommended cutting parameters over a period of time. Initially, accelerated wear is experienced in the tool ‘break in period’. Thereafter gradual wear is experienced and the rate of wear appears to be a linear line.

After the cutting tool life exceeds the scheduled replacement time (SRT), a tool change is forced even though the cutting tool is still within acceptable wear limits. The SRT is set to allow maximum utilisation of cutting tools, while minimising the possibility of cutting tool edge fracture which would result in workpiece surface damage. The SRT is therefore dependent on the type of machining, workpiece material and cutting parameters. In the final stages of the life of a cutting tool, accelerated wear is experienced until tool failure criteria are met. Further machining with the cutting tool may result in excessive chipping, increased cutting tool temperature and eventually, catastrophic failure.

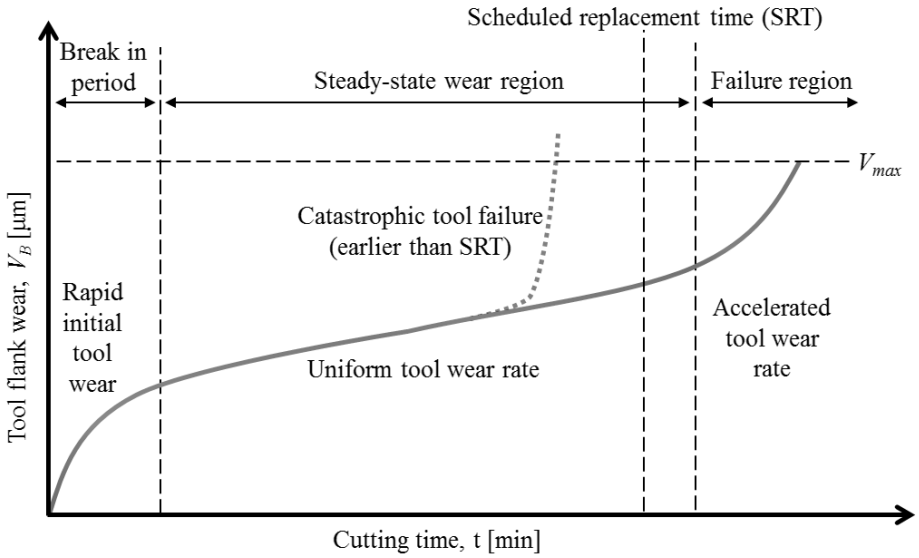

Figure 20: Typical wear curve experienced in milling operations from accelerated initial wear, followed by gradual wear in intermediary stage of tool life and once more accelerated wear at the end of tool life – adapted from (Dimitrov, et al., 2013)

Hard and wear-resistant cutting tools in combination with coatings offer some wear-resistance to prevent tool failure for a time. However, it is unavoidable in a metal cutting operation that the tool will fail. Wear can therefore not be completely prevented; however, it is possible to restrict heat build-up through the application of cutting fluids in the metal cutting operation.

Cutting fluids are critical to most titanium machining operations in that chip evacuation is performed more effectively and tool life is increased by lowering cutting temperature. Furthermore, cutting fluids reduces power consumption and cutting forces, which leads to improved dimensional accuracy, surface roughness and surface integrity. Further benefits include increased productivity and cost reduction by using higher cutting speeds, feeds and greater depth of cuts (Nachtman, 1997).

Depending on the machining operation being performed, cutting fluids have one of the following functions (Nachtman, 1997):

- Cooling the tool
- Lubricating (friction reduction and minimising erosion on the tool)
- Controlling the formation of built-up edge on the tool
- Removing chips
- Protecting the workpiece, tooling and machine from corrosion

Cutting fluids used in titanium machining commonly incorporate a number of these properties. Cutting fluid selection for any machining operation is influenced by the type of work material, cutting tool and the finish that is required for the tool (Nachtman, 1997). Distinction is made between coolants and lubricants. Coolants refer to the heat dissipation constituents where the primary function is to cool the tool at high cutting speeds. Lubricants become more important at lower cutting speeds where heat generation is less problematic. At lower speeds there is a greater tendency for the chip and workpiece material to adhere to surfaces of the tool (Donachie, 2000). Lubricants therefore reduce friction and the possibility of the chip to adhere to the tool (Nachtman, 1997). Nevertheless, in titanium machining lubricants are seldom used, and cooling liquids are the prevailing cutting fluid due to the high temperature nature of titanium machining.

A constant, uninterrupted flow of cooling fluid helps to minimise thermal shock and effectively removes chips from the cutting operation. It also prevents titanium chips from igniting. Most importantly, it reduces cutting temperature on the cutting edge by absorbing the heat that is generated by the frictional movement and plastic deformation experienced on the chip/tool interface (Ezugwu & Wang, 1997).

There are several methods used for applying cutting fluids to the cutting operation. These applications can vary between flood cooling, high pressure cooling and through spindle cooling. The most common cooling method used in the machining industry is flood cooling (Ezugwu & Wang, 1997). Flood cooling is primarily used at low cutting speed conditions with a significant sliding region and low cutting temperatures. Flood cooling is however inefficient for high cutting speeds titanium machining because the cutting fluid does not penetrate deep enough into the cutting operation to thoroughly cool the cutting edge. Furthermore, at high temperatures the coolant is vaporised before making contact with the cutting tool, rendering the coolant ineffective (Ezugwu, 2005).

As the cutting edge is the part which experiences the highest temperatures during the machining operation, it is important to ensure that it is cooled appropriately. At pressures of up to p = 200 bar, a high speed coolant jet traverses the cutting tool surface faster, and penetrates deeper into the chip-tool contact area. The coolant jet reduces the potential for adhesion and diffusion wear by removing machine chips from the tool-workpiece and tool-chip interface (Ezugwu, 2005). Recent advances have also allowed coolant to flow through the spindle as shown in Figure 21, known as ‘through spindle cooling’ (Davies, 1997).

The film (nucleate) boiling action exhibited by super-heated metals is somewhat mitigated under the action of high pressure cooling at the cutting area. Heat transfer to the cutting tool is consequently lowered, which increases tool life (Sobiyi, 2011). High pressure cooling also results in small, discontinuous and easily disposed chips, instead of the long continuous chips produced with flood

cooling. This method is proven to greatly improve tool life when machining at medium to high cutting speeds (Ezugwu, 2005).

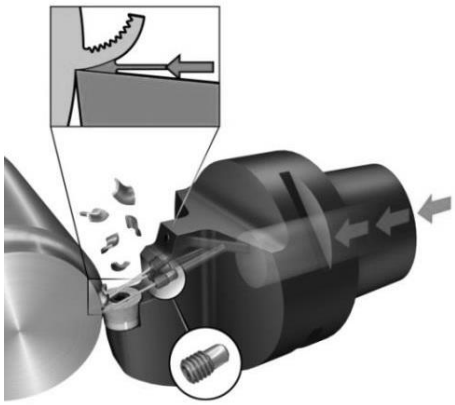

Figure 21: High pressure through spindle cooling, directly cooling the cutting edge and helping with chip evacuation – (Richt, 2011)

The latest development in indexable cutters is to allow coolant to flow through the insert itself (split tool cooling). Coolant is then applied directly to each cutting edge throughout the cutting procedure. This is the most cutting edge method devised to date, however little experimental data is available on the performance of this cooling method (Prins, 2015).

Despite the advances in cutting tool fluid, coatings, geometries and material, machining is still a process of intentional defect creation in a material to generate a specific surface. Surface generation in machining entails applying a cutting force through the cutting tool. This force affects the volume of the material directly located under the tool tip and its immediate vicinity. It also causes the contact zone between the tool and the workpiece to experience an elevated stress rate (Abdel-Aal, et al., 2009).

The surface from a topographical and a metallurgical point of view is important in the design and manufacture of critical hardware. Reduced surface integrity has the possibility to lead to reduced fatigue strength (Field, et al., 1997). As titanium alloys are often used in dynamic and load bearing operations and critical components in the aerospace industry, machined surfaces have to conform to aerospace regulations (Field, et al., 1997). Titanium components therefore require great reliability by the control of surface roughness and sub-surface damage (Ten Haaf, et al., 2008).

Due to the difficult to machine nature of titanium alloys, it is easy to damage the machined surface and difficult to achieve a satisfactory surface integrity (Che-Haron & Jawaid, 2005). Surface integrity involves the outermost surface layers of a machined component and is a function of tool material, sharpness, geometry, workpiece material, machining process, speed, feed, depth of cut and cutting fluid (Sun & Guo, 2009). Distinction is made between surface topography characteristics, and surface layer characteristics. Both surface topography and surface layer characteristics along with electrical (changes in conductivity) effects play a role in surface integrity (Van Trotsenburg & Laubscher, 2010). These effects may have a major influence on the failure of the workpiece and are commonly

interrelated, as fatigue failures typically nucleate at, or propagate, near the surface of a component (Field, et al., 1997).

Surface topography characteristics concern the geometric irregularities of the surface. It includes surface roughness (R_a), damage in the form of voids, microcracks, built-up edges, and heat-effected zones (Boyer, et al., 2007). During operation, these flaws in surface topography characteristics can lead to degraded fatigue strength and stress corrosion resistance (Donachie, 2000).

Surface layer characteristics, involves the metallurgical alterations of the surface and the sub-surface layer (Paul DeGarmo, et al., 2003). Milling influences the quality of the machined surface and subsurface by inducing anisotropic surface roughness, residual stress, surface microstructure alterations and microhardness alteration (Sun & Guo, 2009). Microstructural- or phase deformation is observed when machining titanium with deformed boundaries and elongated grains. The deformation layer is very thin when a sharp tool is used, while nearly worn tools result in a thicker layer (Che-Haron & Jawaid, 2005). Besides phase deformation, it is also observed that microstructural changes also appear close to the machined surface. One such example in titanium machining is the absence of beta phase close to the newly machined surface. It is suspected that the phase transformation from beta phase to alpha phase is due to the high temperatures resulting from the severe plastic deformation (Sun & Guo, 2009).

High degrees of surface integrity are, however, possible if the proper titanium machining techniques are used. Ezugwu et al. investigated the surface integrity of a Ti6Al4V workpiece after finish machining with PCD tools (Ezugwu, et al., 2007). The cutting speeds ranged between v_c = 175-230 m/min and conventional flood cooling was used. The surface roughness (R_a) was found to be well below the work piece failure criteria of R_a = 1.6μm. Micro-hardness analysis showed hardening of the top-machined surface, and the microstructure below machined surface had minimum or no plastic deformation for this cutting speed range. Micro-pits and re-deposited work piece material were found to be the main factors behind surface damage (Ezugwu, et al., 2007).

Surface integrity is a primary concern in titanium aerospace components. If surface integrity of a machined part does not meet the required specifications, the part is rejected as it may risk the safety of the aircraft and its occupants. In terms of this investigation however, surface integrity is negligible.

Alpha case removal through chemical milling is only a pre-forming process, and the dimensions and surface generated from this process are not the final outcome. Further component rough- and finish machining is executed after chemical milling, rendering the chemical-milled surface integrity extraneous. The same holds true for machining removal of alpha case from titanium samples with indexable tungsten carbide cutters. Although there is a strong emphasis on surface integrity in titanium machining, alpha case removal remains a pre-forming process.

2.5. Economic benefits

The primary objective of the study is the feasibility testing of alpha case removal from hot rolled Ti6Al4V samples using indexable tungsten carbide cutters. In the event that the feasibility is confirmed, the secondary objective is the scope of feasibility within the context of the South African manufacturing industry. South Africa already has an established machining industry. With little or no additional capital expenditure, titanium competency can be secured over a large portion of the market. Should alpha case machining removal be implemented in established machine shops, the expanded market would lead to an increase in exports. In addition, downstream beneficiation from additional titanium machining contracts would further expand the market.

The scope of feasibility must first be established and this can only be achieved by doing a cost comparison of chemical milling with machining removal. To do this, a basic understanding of milling economics is required. A general concept in milling economics is making the best use of the particular cutting tool. This means finding a balance between using high cutting speeds for milling productivity, and lower cutting speeds that promote sustainable tool life (Dimitrov, et al., 2013). Gilbert published the *Economics of Machining* in 1950, in which he derived the first mathematical formulae to determine optimal cutting speed for a machining operation, given that the various time and cost components of the operation are known (Gilbert, 1950).

Figure 22 depicts a basic minimum unit cost curve for machining operations such as milling. The two principal costs in milling are machine time- and tooling cost. An argument can also be made for material cost, as higher amount of material removal results in longer machining time and increased tooling cost. This can be minimised by preforming or near net shape technologies which pre-shapes the part, resulting in a reduction in material volume removal and cutting time. However the reduction in material cost is offset by the cost of additional manufacturing processes. For this particular investigation, preforming and near net shape utilisation is not applicable and can be omitted.

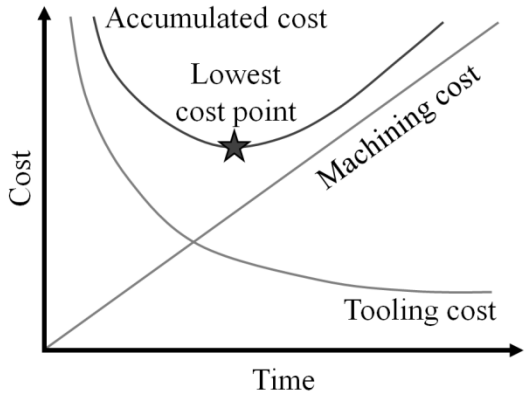

Figure 22: Minimum unit cost curve for milling operations where the minimum accumulated cost is dependent on the sum of the machining cost and the tooling cost – adapted from (Dimitrov, et al., 2013)

From Figure 22 it can be seen that high cutting speeds result in high tooling cost, although machine time cost are kept low. On the other hand, when low cutting speeds are utilised and tool life is at a

maximum, the low cutting speed results in increased cost of using the machining. The machining cost is an hourly or daily running cost of contracting the machine. It incorporates the cost of the initial machine purchase and the operational expenses of keeping the machine running. In order to determine the most economical removal method for alpha case by method of machining, a balance needs to be found between tooling cost and machining cost. Once the optimal and most economical milling strategy has been determined, that strategy must thereafter be compared with chemical milling. However, the two removal strategies are completely different and must be viewed as such.

Chemical milling and machining follow two completely different process chains, and two completely different removal strategies. In chemical milling, the area of the surface experiencing material removal is constant, and the depth is the variable factor. For machining, the depth remains constant and the cutter size in relation to the workpiece varies. Furthermore, the material removal rate for chemical milling is altered by factors such as solution temperature and solution strength, whereas in machining the material removal rate is influenced by cutting speed and feed rate.

It is commonly known that depth of cut has a lesser effect on tool wear compared to cutting speed and feed. Therefore an increase in cutting depth will provide a substantial increase in material removal rate without greatly influencing tool life (De Bruyn, 2014). In an alpha case removal setup, excessive depth of cut does not aid in the removal of scale. The additional material that is removed comes from the substrate beneath the alpha case. Although excessive depth of cut does not aid in the removal of alpha case, it may have other benefits.

In normal machining operations there are two methods used for measuring the total lifespan of a tool. They are the total cutting time, and total volume material removed. The cost of tools is calculated with regards to the total material removed throughout its cutting life. The result is a cost per cubic centimetre of material removed (ZAR/cm^3). This is the method that is to be followed for the cost calculations for this study. However, total volume removed is a redundant comparison in this investigation because a maximum amount of material removed from the workpiece is not the objective. The objective is alpha case removal on the surface of hot rolled titanium, the clearing of alpha case over the largest possible surface area. As mentioned, depth of cut has a minimal impact on tool wear. Depth of cut can hence be doubled which would result in nearly twice the amount of material removed, yet only a slight reduction in total surface area alpha case removal. The same can be said for a less aggressive depth of cut which would lower total material removed, but at a slight increase in total surface area alpha case removal. Applying a variation of depth of cut to titanium alpha case removal by machining will yield raw material of different geometrical sizes.

In an established machining production process, the varying depth of cut can be used to pre-machine a raw workpiece to a closer tolerance as required for subsequent machining processes. This may lower

the machine time of subsequent processes, and a reduction in the total amount of material removal for machining processes may lead to a reduction in cost.

One such example, shown in Figure 23, is the machining of an aerospace part by the Institute for Advanced Tooling at Stellenbosch University. The manufactured part has a final height of 30 mm. However, the raw titanium material from which the part is manufactured has a total height of 38.1 mm. The removal of 8.1 mm material is insignificant in most machining operations. However, in titanium aerospace manufacturing, this is a significant amount of material to be removed before actual part production takes place. With an initial baseplate dimension of 502 x 326 x 38.1 mm, more than MR = 1300 cm^3 material is removed to reduce the height to 30 mm before actual part roughing is executed. If this initial surface machining can possibly be avoided by utilising a more aggressive alpha case removal depth of cut, then overall machining will also be more economical, productive and environmentally friendly.

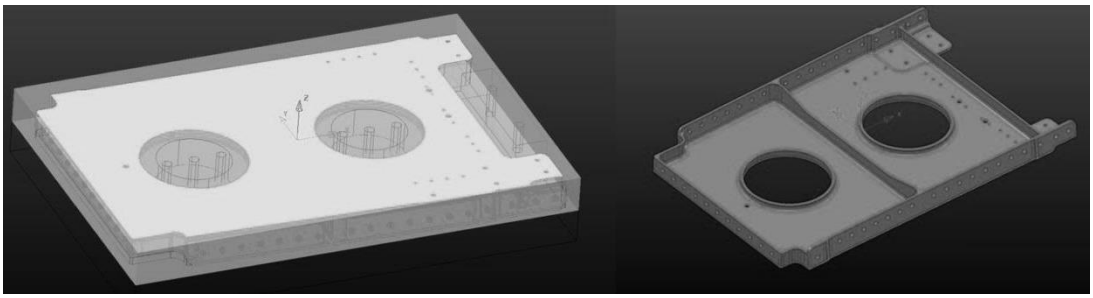

Figure 23: Computer-aided manufacturing (CAM) model of an Intercostal illustrating the total amount of material to be removed in the machining process

Performing face milling at a high depth of cut (a_p) greatly increases the required machine power and rigidity of setup. Those requirements will be highlighted even further if cutting tools with larger diameters are utilised. However, face milling is specifically suited for large surface area material removal. It is therefore capable of executing machining at high cutting depth. Alternatively, multiple shallow cuts can be employed to mill down the excessive material to a desired height. The disadvantages of using machining are also apparent and must be addressed before large scale alpha case removal is attempted. Firstly, components cannot exceed the size restrictions of the workspace in the milling machine. Milling machines come in a range of different sizes, but most milling machines have work areas smaller than one cubic metre in size. Even though larger machines capable of managing components up to four metres in length are available, these machines are expensive. The utilisation of more expensive machines results in higher hourly rates for machine time. This in turn increases the cost of alpha case removal. Additional cost modelling can therefore also be conducted depending on the size of the component, the size of the milling machine that is required, and the hourly cost of operating the machine.

Moreover, chemical milling removes material along the entire surface area of a component simultaneously. This effectively restricts the need for material repositioning and setup. Machining

removes material at a constant depth on one surface of the sample at a time. After one side of a component has been machined, a repositioning step must follow. Repositioning exposes new alpha case which is then subsequently machined. Repositioning adds additional processing time to a component, adding to the labour cost and ultimately the final cost. In five-axis machining this may be mitigated somewhat due to the milling machine table being capable of tilting the workbench, exposing the sides of the component to the cutting tool. However, additional weight restrictions are placed on components when attempting to machine in five-axis mode. Furthermore, the equipment cost per hour of five axis machining is more expensive than three axis machining. A comparison between a more versatile five-axis and a lower cost three-axis could easily be completed.

Finally, the repositioning of the workpiece component goes hand in hand with clamping, moving and changing the workpiece. Large workpiece sizes result in heavy workpieces. The additional size, as well as the additional weight, makes initial clamping difficult and the same goes for repositioning. Additional equipment and labour are required in order to move a large workpiece. However, the same applies for chemical milling where additional equipment is also required for the workpiece relocation.

The complications that arise from workpiece size, repositioning, and the number of axes, can be solved with the addition of a milling machine pallet changer. Pallet changers allow for the quick and easy setup of workpiece material with minimal hassle. The minimal amount of time that the operator is focused on workpiece repositioning will result in a higher machining efficiency which will eventually result in lower cost of production. The pallet changer itself will however, add to the initial capital expenditure and as a result, the ultimate operating cost of the machine. Therefore, as with the analysis of the optimum number of axes, there should also be an analysis to determine when, and with how many axes, a pallet changer increases productivity at a reduction in cost.

3. Experimental Setup and Design

The primary objective of this study is to determine the feasibility of machining removal of alpha case from Ti6Al4V hot rolled samples using indexable tungsten carbide cutters. In the event that this process is feasible, the secondary objective is to determine the scope of feasibility by doing a cost comparison between machining removal and chemical milling. The scope of feasibility must focus on a South African manufacturing industry where industrial machine shops are readily available and little or no knowledge of chemical milling is currently available.

3.1. Background experiments

Much has been documented on the formation and weight gain of alpha case as a function of heat and time. Each heat-treatment cycle used in academic studies is different and yields different alpha case formation. Before any alpha case removal experiments are to be conducted, it would be helpful firstly to understand what the exact hardness and depth of the alpha layer are for the specific heat-treatment regime used in this study. Subsequent machining experiments will be based on the results of the background study. This will increase the thoroughness of the investigation and ensure successful removal of alpha case from the primary machining trials.

3.1.1. Initial alpha case formation

The primary output of the groundwork experiments would be to characterise the physical and chemical properties of the alpha case layer. The focus would be on alpha case which represents what is commonly formed in industry. Therefore, the material to be investigated is grade five Ti6Al4V (6 wt.% aluminium, 4 wt.% vanadium) which is considered the workhorse titanium alloy, in that it is the most widely used titanium alloy. A full description is given in Table 1, Chapter 2.

To ensure the integrity of the material, samples are cut from a wrought titanium billet by means of abrasive waterjet cutting to dimensions of 15 x 15 x 2 mm. In total, 14 samples are used in five different heat-treatment conditions. Samples are cleansed with methanol and placed in a Gallenkamp Muffle Furnace (Accurate to 10°C at 900°C to be heat-treated in ambient atmosphere. An additional sample of dimension 100 x 15 x 15 mm, is also heat-treated under the same conditions. This sample is also cleansed, and placed on an Al_2O_3 plate within the furnace. The latter sample is weighed before and after heat-treatment using a Kern Analytical Balance with an accuracy of $\Delta w \pm 0.001$g for samples up to $w = 120$ g.

This trial focuses on alpha case formed on hot rolled titanium. However, newly rolled titanium with alpha case still present is not readily available in South Africa as titanium hot rolling is not performed in the country. An alternative must therefore be used which closely simulates industry standard alpha case. Hot rolling induces thermo-mechanical effects on the material, but it is the temperature which results in alpha case formation. Therefore, instead of using a thermo-mechanical heat-treatment

procedure, a purely thermal alternative will be used. The time and temperature combination to simulate hot rolling is recommended by an industry partner and used as part of this investigation.

To simulate the thermo-mechanical effect of hot rolling, a purely thermal alternative is used. Samples are placed in the furnace and heated to T = 950°C, where they remain for two hours to simulate the heat up prior to rolling. The furnace is then cooled with the samples still in the furnace, to T = 800°C at a rate of ΔT = 2.5°C per minute, and this temperature is maintained for another hour. This simulates the mill annealing afterwards. Thereafter the furnace is cooled to T = 650°C at a rate of ΔT = 2.5°C per minute, and then to T = 350°C at a rate of ΔT = 5°C per minute. The final stage is to let the heat-treated sample cool down to room temperature (RT = 25°C) in ambient air. A summary of the heat-treatment process can be found in Figure 24.

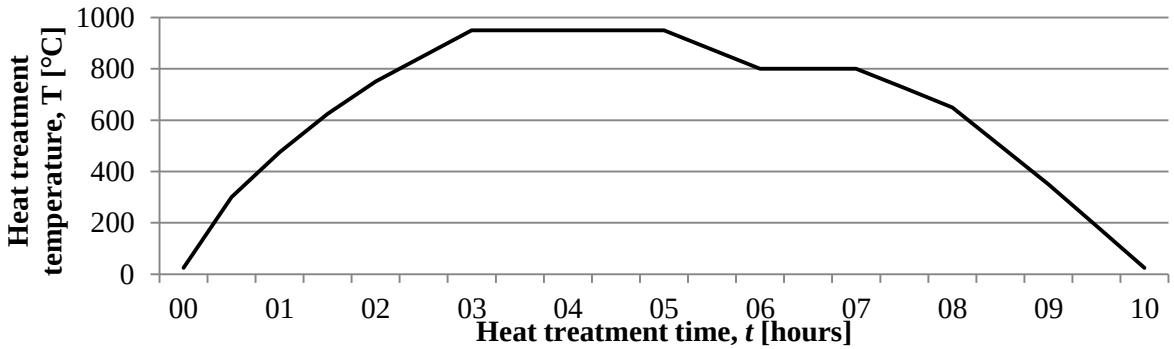

Figure 24: Heat-treatment profile of titanium samples to be followed for every heat-treatment cycle

The 14 samples are subjected to five different heat-treatment conditions, each with a different range of conditions as specified in Table 2. The different conditions are chosen to analyse the individual effects of each heat-treatment condition as experienced by the samples. Four samples will undergo the full heat-treatment regime, and four samples will undergo none at all. Two samples will only be exposed to T = 950°C for two hours, and a further two samples will be exposed to T = 800°C for two hours. The final two samples will be exposed to the full heat-treatment cycle in a vacuum. The vacuum heat-treated samples will be used to study the effect of the heat-treatment on the sample alone, without the effect of oxidation.

Table 2: Number of samples in each heat-treatment

Number of samples	No exposure	Atmospheric conditions	950°C for two hours	800°C for two hours	Vacuum conditions
4	X				
4		X	X	X	
2		X	X		
2		X		X	
2					X

3.1.2. Alpha case evaluation

Following heat-treatment, all samples are mounted in epoxy resin using Struers Epofix resin and hardener resin (containing 15 parts epoxy in addition to two parts hardener), and allowed to set over t = 24 hours in a hot box at T = 30°C. Thereafter, samples undergo surface grinding to remove the

topmost two millimetre of material using a Struers LaboOpl-1 semiautomatic polishing machine with. This foregoing grinding step is conducted to remove the alpha case layer from the surface under investigation, and to expose the substrate material. Samples are then metallographically polished in a three step process. The final polishing step uses a colloidal silica suspension to produce a mirror like finish of up to 0.01 μm (ASM International, 2002).

Selected samples undergo etching on the polished surfaces in order to observe the alpha case optically. Samples are immersed three times for five seconds in Weck's reagent, containing 40 parts distilled water to every 1 part ammonium hydrogen difluoride - $(NH_4)HF_2$. Optical microscopy is performed with an Olympus GX51 inverted metallurgical microscope. Samples are afterwards repolished, and subjected to microhardness testing along the outer perimeter of the mounted samples using an Emcotest DuraScan micro hardness testing machine with a Vickers indenter.

All heat-treated samples are indented with electronic load applications of 0.5, 0.3 and 0.1 HV (kg) and untreated samples are only subjected to 0.5 and 0.3 HV loads. Indentation spacing is done by hand and kept in excess of three diagonal lengths, and indentation sizes are in the range of 55 μm for a 0.5 HV load, and 20 μm for a 0.1 HV. Over 1500 hardness indentations are made on the various samples at the different indentation loads. The distance between indentation and sample edge is quantitatively measured from optical micrographs (Olympus GX51) and analysed with Stream Essentials software developed by Olympus. Indentations are then analysed and averaged across a group of samples to smooth out the curve. All sample preparation and hardness testing conform to guidelines recommended by Struers, a leading supplier of materialographic preparation equipment and consumables, hardness testers, and imaging software (Struers, 2010).

The polished heat-treated samples undergo further analysis under ZEISS EVO MA15VP scanning electron microscopy (SEM) which will reveal much of its composition and grain structure. SEM uses a focused beam of high-energy electrons to generate a variety of signals at the surface of solid samples. The signals that derive from electron sample interactions reveal information about the sample including crystalline structure, chemical composition and orientation of materials making up the sample. SEM therefore removes the need for an etchant in order to present the microstructure (Goldstein, et al., 2003).

Following the background experiments are the primary experiments of this investigation. The primary objective of this research document is to explore the possibility of using machining as a substitute to chemical milling in the removal of alpha case from hot, processed titanium, specifically Ti6Al4V. Standard machining techniques are used with indexable tungsten carbide cutting tools, to attempt the removal of the alpha case with the hope that these techniques can then be reapplied in industry. If successful, the knowledge gained by the study could further the South African titanium agenda by removing the need for the construction of costly and hazardous chemical milling facilities. Instead,

already established machine shops can be outfitted to perform alpha case removal. This is in the event that feasibility is confirmed and the scope of feasibility allows for actual implementation in the South African manufacturing industry.

3.2. Feasibility testing of alpha case machining removal

Successful tool life testing depends on establishing a test plan objective, designing the test, conducting the test, analysing the results and applying the results. The testing program requires metallurgical, manufacturing-process and experimentation knowledge (Kendall, 1997).

3.2.1. Establishment of test conditions

Preparation of material, tool and equipment must be done in such a way that the experiments reflect industry standards and that the experiments are repeatable. Experimental setup and design therefore follow the guidelines set out by ISO 8688-1 (Tool life testing in milling – Part 1: Face milling). This particular ISO has been developed for face milling operations utilising carbide tools and is recommended for both factory and laboratory testing. Important experimental design factors include:

- Workpiece material preparation (in this situation alpha case)
- Cutting tool material, geometry, edge and coating
- Cutting strategy
- Milling equipment

3.2.1.1. Workpiece material

The test piece to be used in this investigation is a grade five alpha beta alloy, Ti6Al4V. A full description of the chemical composition is given in Table 1, Chapter 2. The original workpiece material has been subjected to numerous experimentation and the resulting dimensions are therefore non-uniform. The identified block is first machined to remove surface wear marks left by previous experimentation. Thereafter the workpiece is cut in half via band saw. The resulting dimensions for the two blocks are given in Figure 25.

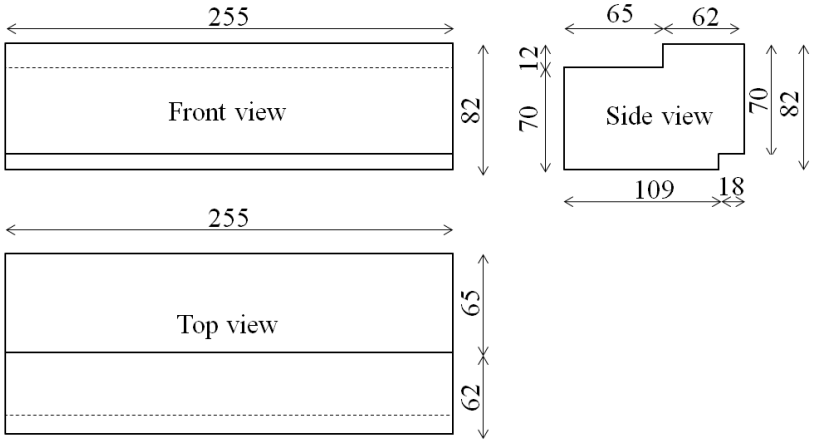

Figure 25: Final workpiece material dimensions of the titanium sample blocks to be used in the primary machining experiments

Hardness measurements, to determine benchmark hardness for the material before experimentation, were taken at various points along the centre line of the newly cleaned surface. The hardness of standard Ti6Al4V is 349 HV (Donachie, 2000). The resulting average hardness for the uncut testing section was 357 HV, which is close to the standard hardness of Ti6Al4V.

3.2.1.2. Cutting tool

According to ISO standards for tool life testing in face milling, the recommended workpiece for face milling shall be a bar or billet of rectangular cross-section with width 0.6 times the cutter diameter (ISO, 1989). Literature, on the other hand, suggests the cutter diameter may vary between 1.3 - 1.6 times the width of the workpiece (Smid, 2003). Furthermore, ISO suggests a minimum workpiece length of three times the cutter diameter is to be used for all face milling applications (ISO, 1989). As the workpiece size and dimensions are pre-set, it is decided to match the cutting tool size to the workpiece according to the above mentioned specifications. Two sides of the workpiece were identified as having a width of 70 mm and a length of 255 mm. These surfaces are to be used in the experimental phase. The 70 mm wide surface is too large to be cut in a single process, which is why two machining passes will be used to clear the alpha case layer. If the resulting a_e = 35 mm width of cut accounts for roughly 60% of the cutter width, or the cutter width selected is between 1.3-1.6 times the width of cut (a_e), then the cutter diameter should vary between 45.5-58 mm. To keep with the cutter sizes available by cutting tool manufacturers, a 50 mm cutter diameter is selected.

Generally, titanium face milling cutters exhibit positive radial rake angles ranging from $\angle_{RRA}$ = 5° to 20°, and negative axial rake angles between $\angle_{ARA}$ = -2° to -11°. However, a negative radial rake angle offers increased strength to the cutting insert and cutting edge compared to the alternatives (Smid, 2003). Due to the presence of the hard alpha case layer, the strongest possible cutting edge was selected for the cutting operation which is a double negative cutter. Additionally, double negative inserts offer twice the number of cutting edges because they are double sided. As a result, the cutting tool used in this investigation is an ISCAR SOF 45 out of the HELIDO 800 line. It is a multifunctional face milling cutter incorporating double negative orientated double sided octagonal inserts for the maximum number of 16 cutting edges per insert.

The particular ISCAR cutter to be used is shown in Figure 26. The cutter has a diameter of 50 mm and the experimental width of cut (a_e) will be 70% of the cutter diameter. The coated micro-grain cemented carbide insert has a sharp edge and is recommended for interrupted cutting and heavy operations on stainless steel and high temperature alloys. The multi-coating comprises TiN and TiAlN, and is applied by physical vapour deposition. The octagonal shape of the insert results in a $\angle_{CH}$ = 45° corner angle, which helps in the distribution of cutting forces across the tool edge.

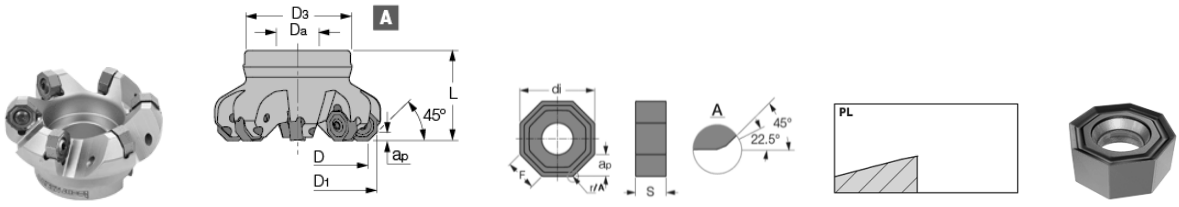

(a) **(b)** **(c)** **(d)** **(e)**

Figure 26: (a) Photo of ISCAR cutter to be use in machining experiments, (b) dimensions of cutter, (c) dimensions of inserts to be used in machining experiments (d) sharp shape of insert edge, (e) 3D model of carbide insert to be used – adapted from (ISCAR, 2015)

Tungsten carbide cutter material has proven its superiority in the machining of titanium alloys and still remains the first choice in turning and face milling. Nonetheless, limited amount of research has been conducted on face milling. Severe chipping and flanking of the cutting edge have been reported to be the main failure mode when milling titanium alloys with carbide tools. These types of failure modes are a result of a combination of various factors such as high thermo-mechanical and cyclic stresses. Others include the adhesion to work piece material, and the breaking off from the tool faces of work piece material (Jawaid, et al., 2000).

3.2.1.3. Machining equipment

Titanium machining requires a riged setup owing to the low modulus of elasticity and the toughness of the material. Rigidity is determined by a combination of factors such as spindle, workpiece, mounting and the machine itself. Low rigidity causes vibrations and chatter which result in poor surface finish and further tool wear. Furthermore, spindle load is also higher at the low cutting speeds used to machine titanium. The load is also amplified by the use of a negative radial cutter that adds additional power requirements to the setup. It is unknown if the alpha case layer will have any influence in the rigidity and power requirements of the machining operation.

Figure 27: Hermle C40U dynamic 5-axis CNC milling machine to be used in primary alpha case removal machining experiments

The machining trials are to be carried out on a Hermle C40 U Dynamic 5-axis CNC milling machine, such as the one shown in Figure 27. A full list of technical specs is listed in Table 3. No additional instrumentation is connected to the machine. Blaser B-Cool 755 will be used as coolant which will be applied via through spindle and high pressure cooling at 40 bar pressure.

Table 3: Hermle milling machine technical data (Hermle, 2008)

Machine model	**Hermle C40 U Dynamic 5-axis CNC milling machine**
Year	2006
Work area	850(X) – 700(Y) – 500(Z) mm
Spindle speed	18 000 rpm
Torque, τ	130 Nm
Main power, *P*	15 kW
Maximum table load	1 400 kg
Rapid linear traverse	60 m/min
Linear acceleration, a	10 m/s^2

3.2.1.4. Workpiece heat-treatment

The primary objective is the feasibility testing of alpha case machining removal from hot rolled titanium with the use of indexable tungsten carbide cutters. As there are no titanium hot rolling facilities in South Africa and newly rolled samples are not readily available, an alternative to the thermo-mechanical effects of hot rolling must be sought. A purely thermal alternative, recommended by an industry partner, is to be used to simulate the alpha case formation. The simulated heat-treatment cycle will expose titanium to high temperatures for a short period of time.

A wrought titanium block, which had been the subject of previous machining experiments, was cut in half by means of band saw, and residual machining marks were cleared with light pass machining at high cutting speed and low cutting feed under high pressure cooling. The resulting dimensions of the two blocks were roughly 255 x 70 x 127 mm. Samples are cleansed with ethanol and heat-treated one at a time in ambient air using a Gallenkamp muffle furnace as shown in Figure 28.

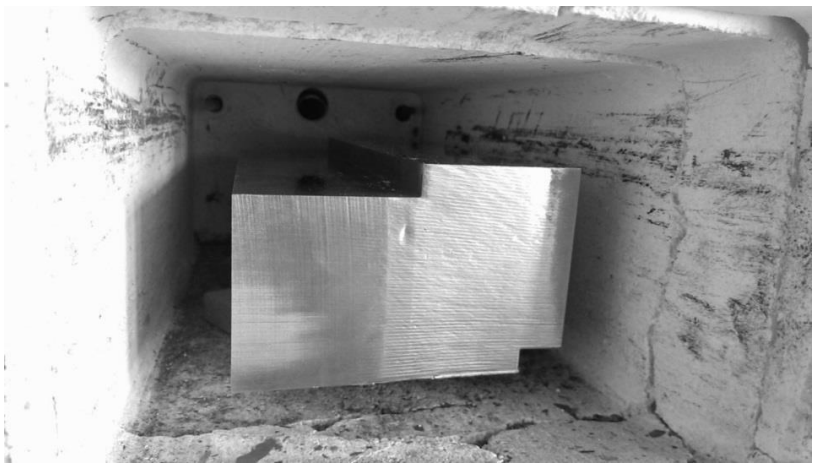

Figure 28: Titanium sample placed in Gallenkamp muffle furnace before heat-treatment begins

To simulate the thermo-mechanical effect of hot rolling, a purely thermal alternative is used. The heat treatment cycle for the primary experiments are kept the same as for the background experiments and are depicted by Figure 25.

3.2.1.5. Machine setup

There is no specific titanium component that is to be machined in this investigation, and there is no need for special milling operations such as slotting, plunging or ramping. The removal of a maximum

amount of material is the primary aim of the investigation. Straight line cuts will therefore be implemented. Figure 29 is a simplified representation of the planned machining strategy. The workpiece surface that is to be machined has a total width of 70 mm. As the cutter diameter (50 mm) is the limiting factor in determining the width of cut, one surface will be subject to multiple cuts of a_e = 35 mm width each. After one side of the block has been machined with two passes of width of cut a_e = 35 mm, the block will be flipped over and the other side will be subject to machining.

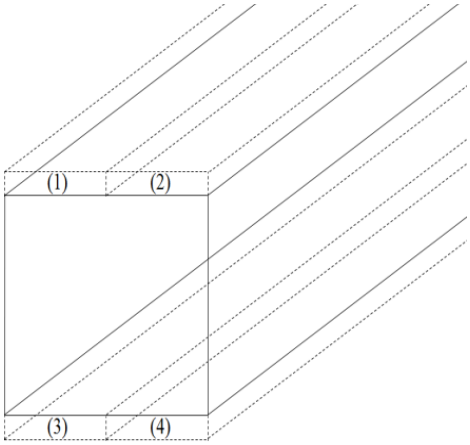

Figure 29: Rudimentary schematic of cutting strategy to be followed for the primary alpha case machining experiments

After the one titanium sample has been machined on both surfaces, the sample will be replaced by the second sample and machining commences similarly. Straight line cuts as close in accordance to ISO 8688-1 as possible are performed for experimentation. The workpiece and cutting tool setup is displayed in Figure 30.

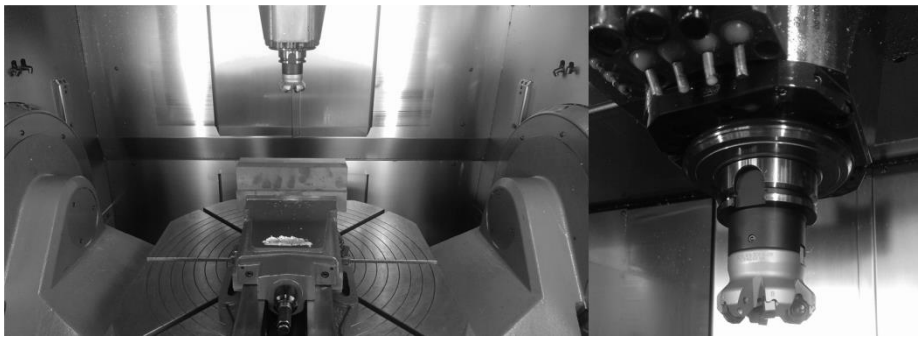

(a) **(b)**

Figure 30: (a) Machining setup of workpiece and cutting tool for experimentation, (b) cutting tool setup for machining experiments

3.2.2.Machining execution

The performance of unused carbide inserts will be investigated at various machining parameters based on the recommended parameters set by the cutter manufacturer. These parameters follow the accepted practice for titanium machining of using low cutting speeds in order to promote long tool life. Based on manufacturer recommendations, cutting speed will vary between v_c = 40, 60 and 80 m/min and cutting feed will vary between f_z = 0.1, 0.15 and 0.2 mm/z. As it is unknown what the extent of oxidation is for this specific heat-treatment regime, depth of cut (a_p) is the only parameter that is not

predetermined. This will be determined in the background experiments. Optical microscopy and the hardness indentations will be used to determine the depth to which oxygen, and therefore alpha case, penetrates into the sample. Down (climb) milling is used, causing chips to be formed from thick to thin, which in titanium milling promotes longer tool life. The cutting speed, feed, material removal rate, and cutter depths are listed in Table 4 and Table 5.

Table 4: machining parameters to be used in experimental procedure

Dimensional parameter	
Width of cut, a_e [mm]	35
Depth of cut, a_p [mm]	TBD
Length of cut [mm]	255
Cutting speeds, v_c [m/min]	40, 60, 80
Cutting feed, f_z [mm/z]	0.1, 0.15, 0.2
Number of inserts, z	6

Table 5: Cutting feed and speed combinations for machining experiments

ISCAR SOF 45								
Cutter D [mm]	**a_p [mm]**	**a_e [mm]**	**z [inserts]**	**L [mm]**	**f_z [mm/z]**	**v_f [mm/min]**	**v_c [m/min]**	**N [rpm]**
					0.1	153	40	255
					0.1	229	60	382
					0.1	306	80	509
					0.15	229	40	255
50	TBD	35	6	255	0.15	344	60	382
					0.15	458	80	509
					0.2	306	40	255
					0.2	458	60	382
					0.2	611	80	509

Tool entry and exit feed rate is different from normal cutting conditions. A slower entry speed v_f = 77 mm/min is used until the cutting tool is completely engaged in the workpiece material. Thereafter the feed speed returns to the experimental parameters as prescribed in Table 5. This is done to minimise the shock experienced by the cutter and to promote tool life at initial contact.

3.2.3. Sampling plan

In the process of determining the feasibility of the primary objective, a number of sub-objectives have been set. These sub-objectives will help to determine the feasibility of the primary objective by serving as measurable variables that can be used in analytics. These measurable sub-objectives will serve as dependant variables of the experimental process. The outcome of the dependant variables (tool life, mode of wear, surface roughness) is dependent on the experiments' independent variables, which in this case are cutting speed (v_c) and feed rate (f_z). Depending on the specific combination of independent variables under investigation, the wear rate (for example) of the carbide inserts will be different. The influence that each cutting parameter has on the dependent variables is to be evaluated and discussed. The measurement and study of wear rates, wear types and mode of failure will provide the necessary insight into the machining process.

3.2.3.1. Tool life criteria

Wear is measured at various test point intervals during the machining process. The test points are used to generate a wear curve for each combination of cutting speed (v_c) and feed (f_z). In order to determine the useful life of a tool, it is necessary to define the life of the tool in terms of wear. There are numerous types of wear which are dependent on cutting forces, temperature, material and the machine. ISO 8688:1 provides a detailed description of the predominant types of wear and provide standardised failure criteria for each type.

ISO 8688:1 also provides three different criteria for tool failure depending on the goal and the availability of resources. The criteria may vary from the final destruction of the cutting tool in order to determine the maximum life of the insert, normal deterioration intensity by compromising between reliability and cost of testing, and minimum capability testing whereby the cost of material is expensive (as is the case with highly wear resistant materials). For the purposes of this study, a compromise between reliability, cost of testing and normal deterioration intensity will be used as a tool failure criteria. According to ISO, the recommended tool life criteria are given in Table 6.

Table 6: Tool life criteria

Tool deterioration phenomena		**Length, [mm]**	**Criteria [mm]**
Flank wear (V_{max})	Uniform	N/A	0.35
	Non-uniform	N/A	1.2
	Localised	N/A	1
Chipping	Micro-chipping	< 0.3	0.25
	Macro-chipping	0.3 – 1.0	0.4
	Breakage	>1.0	-

3.2.3.2. Experimental cycle

The nine different machining trials (three cutting speeds, three cutting feeds) are performed on the newly heat-treated samples. Each of the two workpiece material billets have four possible machining sides, giving a total of eight machining sides per heat-treatment cycle. Once all eight sides are successfully machined, the sample is heat-treated once more in order to re-apply the alpha case layer. Samples are to be heat-treated and machined multiple times in order to accumulate a satisfactory amount of data. A total of MR = 100 cm^3 of material is to be removed for each combination of cutting speed (v_c) and cutting feed (f_z) before experimentation is stopped. This is unless tool failure criteria are met before the insert meets its quota. Tool wear is measured after every single straight line cut is performed. Due to the multitude of heat-treatment cycles to be performed, experiments will be randomised to help limit the small effect that variability in the heat-treatment cycle will have on the experiments.

After each machining trial, the newly generated surface of the workpiece and cutting inserts are measured and analysed via an Olympus SZX7 stereomicroscope. Tool wear and mode of wear for each individual cutting edge are documented and processed. Surface hardness testing of the newly

machined workpiece surface is used to determine whether all of the hardened alpha case is removed. Testing is conducted using an Emcotest DuraScan micro hardness testing machine with a Vickers indenter and a 1 HV (kg) load. Surface roughness measurements are also performed with a Mitutoyo Surftest-211. Machining chips are collected in order to study the morphology and colouration of the chips, as yellow or brown discolouration indicates towards high cutting temperatures (Kalpakjian & Schmid, 2013). A flow chart for the entire experimental procedure is provided in Figure 31.

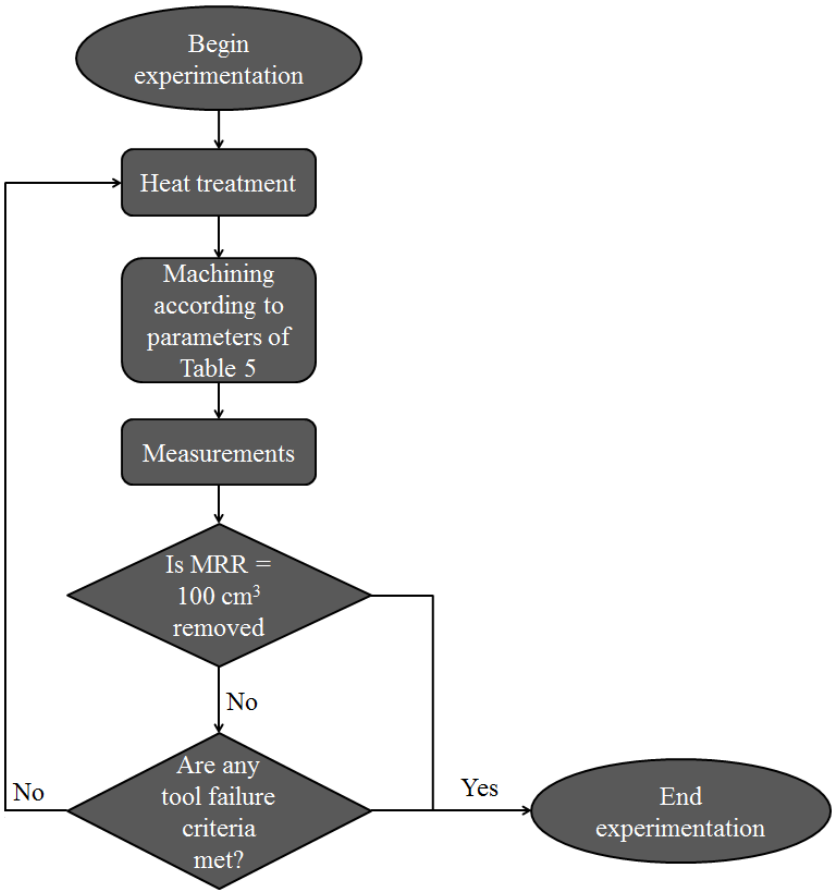

Figure 31: Experimentation flow chart to be used for all machining conditions from initial heat-treatment up until tool failure and end of experimentation

Furthermore, various cutting inserts used for experimentation purposes are to be subjected to scanning electron microscopy (SEM) from ZEISS EVO MA15VP. Under SEM the tool coating can be better studied than under stereoscopic microscopy, and EDX enables the study of adhesion wear as the chemical composition of the surface can be quantified. Statistical analysis of the experimental results is to follow the completion of the experiments. The analysis will be conducted, using Modde 10.1 Design of Experiments software by Umetrics. Analysis includes, but is not limited to, the determination of R^2, Q^2, repeatability, reliability, and coefficient plot.

3.3. Scope of feasibility testing

In the event that the feasibility of the primary objective is confirmed, additional analysis must be conducted to determine the secondary objective. The secondary objective and the final analysis will

concern the scope of feasibility of alpha case machining removal in a South African manufacturing context. First, the most economical machining parameters must be determined in the removal of alpha case. In this, some milling economics will be applied. Once the most economical method has been determined, a comparison is to be made between machining removal and chemical milling. The cost comparison will help to determine if, and under what conditions, machining removal is a viable economic option.

Viability can range from small batch production, to large scale implementation, or no production at all. In determining the feasibility of scope, the current market setup in South Africa must be considered as no chemical milling facilities are currently available. Such facilities must first be constructed at high capital cost. Furthermore, the operation of these facilities holds large safety implications, which adds substantial cost to the facility and endangers the safety of the operators. Processing of the used acids further adds to the cost of operation and the environmental risk attached to chemical milling should also be addressed. This is, however, only an overview analysis and not an in-depth look at the economics of the two processes.

4. Experimental Results and Discussion

4.1. Background experiments

Much is known about alpha case, including its physical and chemical properties. However, the heat-treatment cycle used in this specific analysis will produce unique alpha case formation. The resulting alpha case must first be investigated before removal is attempted. Information such as hardness, composition and depth of oxidation will be discussed in the background experimental results and discussion.

4.1.1. Alpha case evaluation and weight gain

The formation of alpha case is well documented and the weight gained over surface area is explained by equation 1 in Chapter 2. This equation, in combination with work performed by Du, et al., was used to create Figure 32, which estimates the weight gain per surface area of the larger sample during heat-treatment. Total weight gain after four hours of heat-treatment is w = 627 mg, in a sample with surface area of A = 65.6 cm^2. The majority of oxygen pickup is expected to have occurred at the higher temperature during the first half of the heat-treatment cycle. Thereafter oxidation slowed due to the reduction in temperature and the thickening of the alpha case.

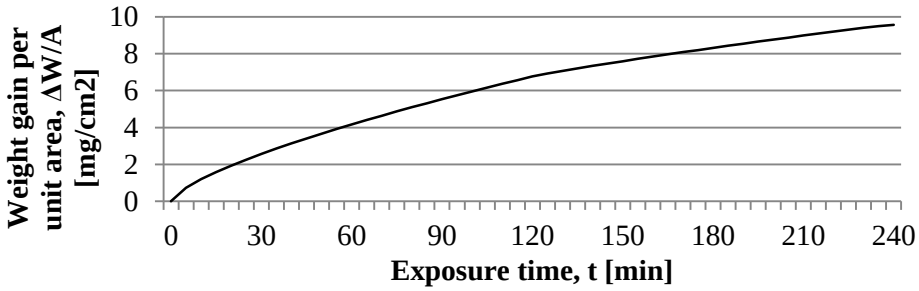

Figure 32: Weight gain representation for oxidised samples per square centimetre

Figure 33 (a) illustrates the visible alpha case on the samples etched with Weck's reagent, viewed through optical microscopy. The alpha case is only visible up to a maximum depth of 300 µm, although it rarely exceeds 200 µm. Furthermore there is no clear border dividing alpha case and non-alpha case substrate.

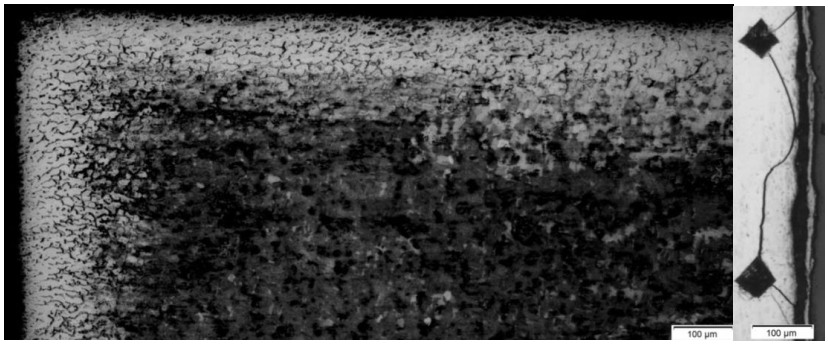

(a) **(b)**

Figure 33: Optical micrographs showing (a) white alpha case layer after etched with Weck's reagent (b) brittleness of alpha case when exposed to hardness tests

Figure 33 (b) depicts the crack formation resulting from indentations made by hardness tester in the brittle, heat-treated samples where alpha case is present near the edge. The formation, and later propagation, of surface cracks can cause components to fail in high stress environments. Traditional, untreated titanium does not form these brittle cracks when indentations are made close to the edge.

4.1.2. Hardness testing

Indentations made close to the edge serve only to indicate the brittleness of alpha case, and were not used to factor in hardness. Proper hardness testing procedures were followed in order to ensure accurate readings. According to Struers, a manufacturer of equipment and consumables for materialographic sample preparation, the sample thickness should exceed the indentation depth by eight times. For hard materials, the indentation spacing should exceed three diagonal widths and indentations should not come within two indentation spacings from the surface edge. The spacings are measured from indentation centre point to centre point. An illustration of the indentation and measurement methodology is given in Figure 34.

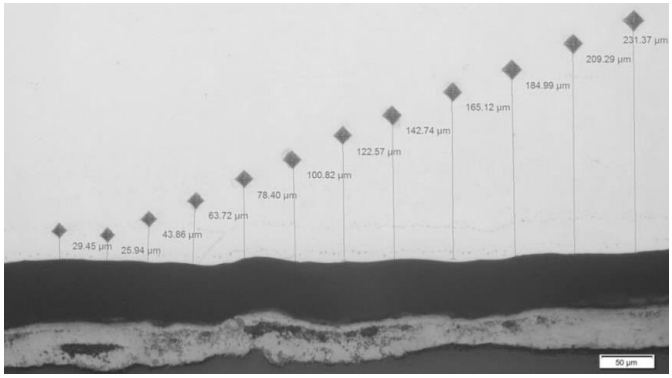

Figure 34: Optical micrograph illustrating hardness testing and measurement methodology

Figure 35 depicts the hardness profile for each of the five heat-treatment regimens illustrated in Table 2, Chapter 3, used for the 14 samples in the background experiments. Hardness testing was conducted to determine the extent of interstitial solid solution formation, which occurs because of the oxidising heat-treatment. Ti6Al4V exhibits a typical hardness of 349 HV, and Figure 35 shows that the return to typical titanium hardness is reached, albeit a distance from the edge. Close to the edge, the heat-treated samples – specifically those treated at T = 950°C – exhibit a two fold increase in hardness. High speed steel has a typical hardness of roughly 800 - 1000 HV, and the alpha case layer peak hardness is comparable to that. The peak of the hardness measurements is close to the edge, and return to normal hardness is achieved roughly 450 µm from the sample edge. The difference in alpha case depth displayed by optical microscopy in Figure 33 (a), compared to hardness testing in Figure 35 is therefore evident. This further suggests uncertainties in determining the border between alpha case and substrate.

In terms of the alternate heat-treatment cycles, it was observed that at T = 800°C only a small amount of oxidation resulted in alpha case formation. This is as a result of the lower oxidising temperature. In

terms of the vacuum heat-treatment, no oxidation was observed and the sample does not exhibit any increase in hardness close to the edge. Finally, the untreated titanium sample displays hardness values traditionally recorded in titanium.

Other than the samples that experienced the full heat-treatment cycle, only the sample exposed to T = 950°C exhibits a significant increase in hardness as a result of oxidation. The hardness profile is comparable to the samples exposed to the full heat-treatment regime. As a result, it can be concluded that the majority of the oxidation experienced by the sample undergoing the full heat-treatment cycle, is experienced in the first two hours at T = 950°C.

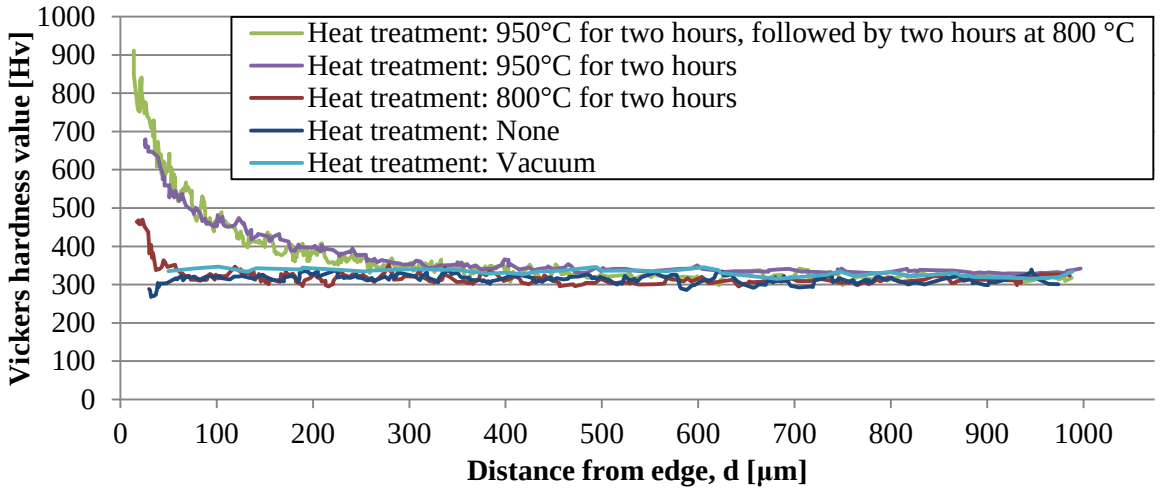

Figure 35: Variation in surface hardness of heat-treated samples, compared to untreated samples as measured from sample edge

The dimensions of the hardness indentations are a noticeable consequence of the varying hardness as depth from the edge is increased. Because of the declining hardness, indentations seem skewed towards the interior of the sample. This is demonstrated in Figure 36, whereby the shape of hardness indention is short towards the sample edge, illustrating the increased hardness compared to the side facing the interior. The longer, opposite half of the indentation clearly shows a decrease in hardness as distance from the edge is increased. Indentation shape returns to the more commonly known square shape further from the edge where sample hardness is similar for the entire surface area of the indentation. Strictly speaking, indentations made in the alpha case layer close to the edge often yield results that do not conform to normal hardness testing standards. This is because the two diagonal lengths of the indentation are often not within 10% of each other as prescribed by standards. However, there is no method available to counter the uneven shape of the indentation.

Figure 36: Disparity of hardness indentation shape close to the harder sample edge, compared to the customary substrate indentation shape

4.1.3. Composition

Figure 37 is a SEM micrograph of the edge of a heat-treated Ti6Al4V sample. It shows the transformation of the darker alpha grains close to the edge. As oxygen is an alpha stabiliser, extraction of oxygen from the surrounding atmosphere fuels the growth of the alpha grains. The visibly lighter beta phase suffers under the increasing size of the alpha grains. The abundance of oxygen also forces the lighter beta phase to absorb oxygen which starts phase transformation. The body-centred cubic structure of the beta phase therefore transforms into an alpha phase hexagonal closed packed structure. This causes the beta grains close to the edge to shrink in size and to greatly alter in composition. Oxygen diffusion into the titanium substrate decreases as distance from the edge is increased. Consequently, alpha grains are larger and more connected at the edge, and reduce in size further from the edge. Beta grains, however, are smaller at the edge and increase in size as distance from the edge is increased.

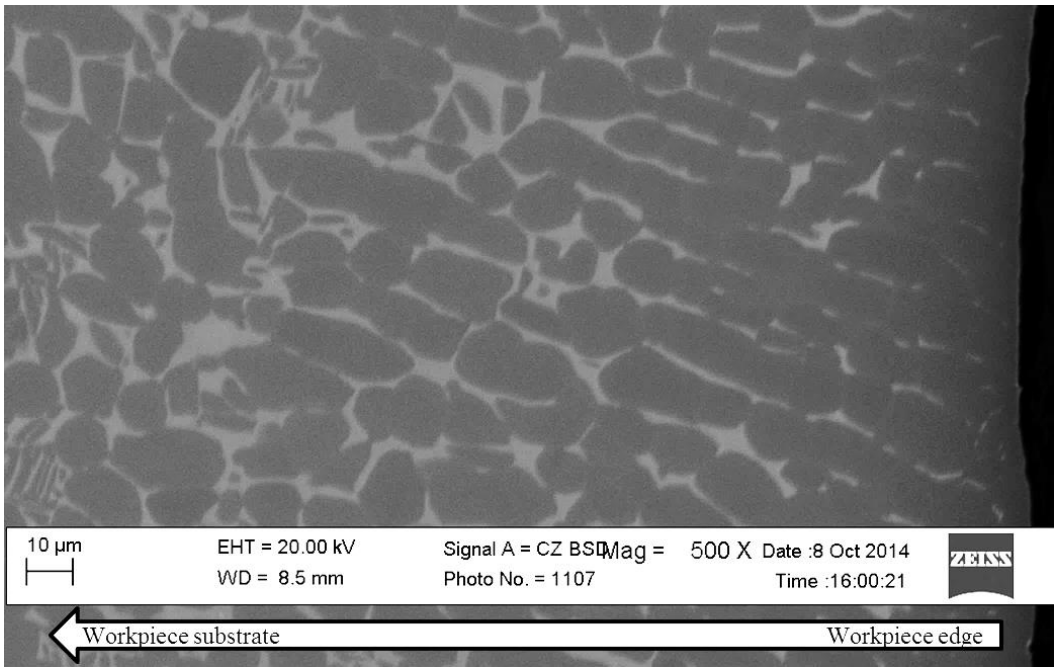

Figure 37: Scanning electron micrograph of the edge of the heat-treated sample that shows large dark alpha grain structures overwhelming the smaller and lighter beta phase structures, and the substrate where lighter beta grain and darker alpha gain structures return to normal sizes

Due to the allotropic nature of titanium, alpha and beta grains exhibit different compositions. Ti6Al4V (6 wt.% aluminium, 4 wt.% vanadium) represents the average weight percentage across the entire titanium sample for both phases. However, deeper analysis would show that alpha grains are richer in aluminium (±7 wt.%) than in vanadium (±2 wt.%). Alpha phase also exhibits a higher concentration of titanium (±91 wt.%). Beta phase is much richer in vanadium (±10 wt.%) than aluminium (±4 wt.%), and has a slightly lower titanium (±85 wt.%) content. Additionally, beta grains exhibit small quantities of iron (±1 wt.%), something which is completely absent in alpha phase.

SEM is not accurate in detecting low level oxygen content and therefore cannot perform oxygen depth profiling. However, it is capable of detecting intermediate levels of oxygen. To compromise,

compositional energy dispersive X-ray spectroscopy (EDX) and wavelength dispersive X-ray spectroscopy (WDX) analysis were conducted. An array of points was selected close to the edge for both a heat-treated sample (where oxygen should be present), and an untreated sample (therefore not containing alpha case). The compositions of the points were then compared.

Figure 38 depicts the measured composition of the two different phases in the heat-treated and untreated samples. Comparing the alpha phase under normal conditions to the heat-treated alpha phase, yields a substantial increase in oxygen content in the heat-treated sample. This increase in oxygen consequently lowers the weight percentage of the other elements such as aluminium and titanium in the heat-treated alpha phase. Furthermore, owing to the shrinking effect of the heat-treated beta phase close to the edge, the beta phase yields a significant decrease in titanium weight percentage and an equally significant increase in vanadium weight percentage. The lower titanium weight percentage is as a result of portions of the beta grain undergoing phase transformation to alpha phase. The phase transformation to alpha phase does, however, not absorb a large quantity of vanadium. As a result, the vanadium remains in the shrinking beta phase. The vanadium weight percentage increases in the shrinking beta phase close to the edge, resulting in almost equal amounts of titanium and vanadium in the heat-treated beta phase close to the edge.

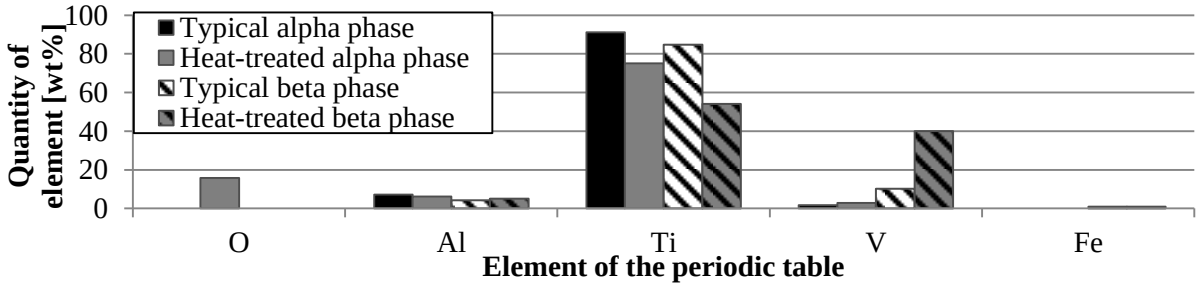

Figure 38: EDX analysis of heat-treated titanium sample at various sampling points

4.1.4.Background experiments conclusion

The investigation of the physical and chemical properties of alpha case is a crucial first step in investigating alternative removal methods. Alpha case must first be understood before it can be removed. The compositional and grain structure analysis provided insight into its microstructure, and visualises the otherwise arbitrary facts of an alpha case layer. Furthermore, the analysis in weight gained and the optical microscopy of the etched surface further builds on previous research. Most importantly for this investigation, is the hardness profile generated by the micro-hardness testing. It conceptualises the increase in hardness close to the edge, and determines the depth that the alpha case layer penetrates into the substrate. This knowledge will help in the preparation of the experimental setup for alpha case machining removal with tungsten carbide indexable cutters, as an alternative to chemical milling.

Optical microscopy of the alpha case layer yielded a maximum thickness of 300 µm. On the other hand, microhardness depth profiling yielded an alpha case depth of 450µm. There is however, a

strong possibility of oxidation further into the titanium substrate which still constitutes alpha case. To assure complete alpha case removal, the decision was made to remove double the amount of material indicated necessary by hardness testing. Depth of cut a_p = 1 mm will have a limited influence on tool life and should therefore not significantly wear more than a lesser depth of cut. Each machining operation with depth of cut a_p = 1 mm and width of cut a_e = 35 mm, over the length of the workpiece surface (255 mm) will therefore remove roughly MR = 9 cm^3 of material.

4.2. Primary objective

Herein follows the reporting and analysis of the experiments conducted in this study to fulfil the primary objective. It includes the workpiece inspection and surface hardness testing to confirm that the alpha case has been removed from all titanium samples by machining. Furthermore the analysis of the tungsten carbide indexable cutters are documented and includes aspects such as total wear, wear rates and type of wear experienced during experimentation. Some statistical analysis is also conducted based on the tool life exhibited by the carbide tools.

4.3. Workpiece sample inspection

Heat-treatment is performed on Ti6Al4V samples with the goal to form alpha case. The primary machining experiments will then attempt to remove the alpha case from the samples. The titanium samples used in this study were heat-treated to the specifications of **Error! Reference source not found.** in Chapter 3. The billet in Figure 39 (a) is an as yet untreated titanium sample. Each heat-treating cycle resulted in samples looking similar to what is exhibited in Figure 39 (b).

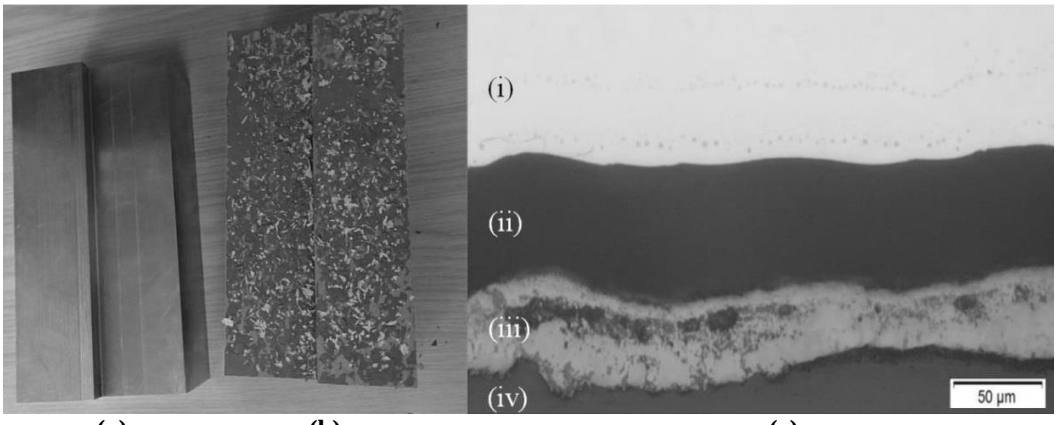

(a) **(b)** **(c)**

Figure 39: (a) Metallic appearance and colour of Ti6Al4V samples before heat-treatment (b) flaking of workpiece surface after heat-treatment (c) presence of alternating oxide layers with (i) the uppermost white representing titanium substrate (ii) dark TiO_2 layer is second from the top (iii) followed by the Al_2O_3 layer and (iv) the lowest layer representing the resin which is used to mount the sample

Figure 39 (b) exhibits severe flaking of the surface layer, similar to the double layered oxide scale theory described in Chapter 2 by Du, Datta, Lewis and Burnell-Gray. Furthermore, the colouration of the flakes and the oxide layer surrounding the titanium sample do not resemble normal titanium colouration, and instead resemble naturally occurring TiO_2. A micrograph of the alternating oxide

layers is shown in Figure 39 (c). The alternating layers of TiO_2 (ii) and Al_2O_3 (iii) are clearly visible. However, the loose flakes separated from the sample in Figure 39 (b) are not present in the micrograph, therefore only showing a single layer of TiO_2 and Al_2O_3 and not double layers.

4.4. Confirmation of alpha case removal

Figure 40 portrays a newly machined surface produced by face milling. The oxidised surface (a result of heat-treatment) is replaced with the more commonly found metallic colour with traditional wear marks. The newly machined surface is smooth, owing to the flat relief face of the carbide insert.

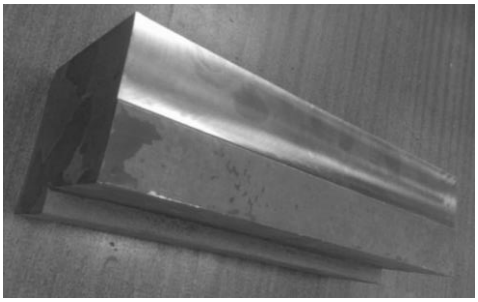

Figure 40: Oxidised surface is replaced by more common metallic surface after machining removal of alpha case

Figure 41 illustrates the average surface roughness of the newly machined surface measured in the length (X) and width (Y) direction. It shows higher roughness at increased feed rate, and declining roughness with increased speed. This is in agreement with the findings of literature.

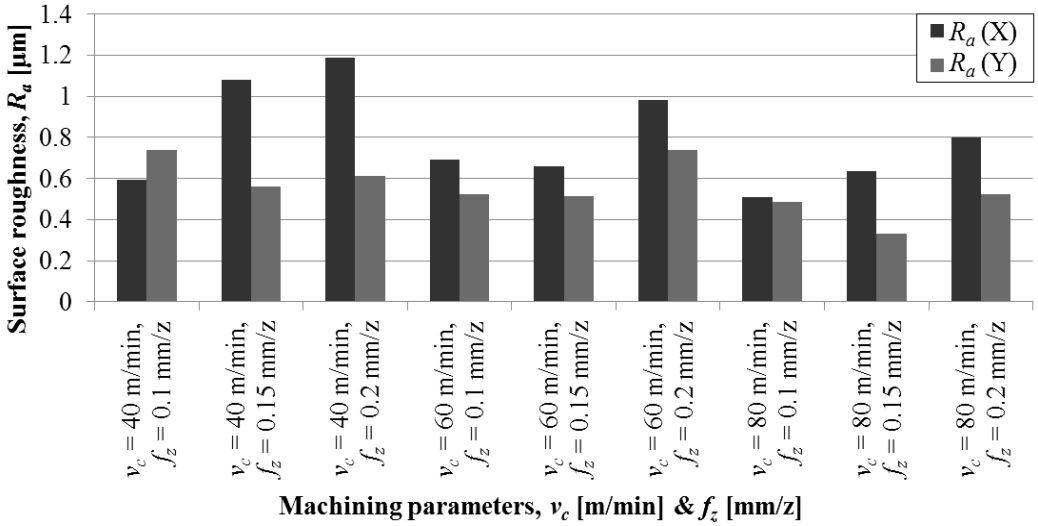

Figure 41: Surface roughness measurements of newly machined titanium in the X and Y direction

The primary focus of this study is the feasibility of machining removal of alpha case from hot rolled titanium. A primary factor, therefore, is the confirmation that the experiments were successful in the complete removal of alpha case from the samples.

Preliminary investigation of the newly machined surfaces suggests the alpha case layer has been removed by the chosen machining strategy at all machining conditions. However, visual inspection by itself is not a conclusive method of determining whether the alpha case layer has been removed or not.

A more accurate, albeit not totally comprehensive method of testing, consists of surface hardness measurements of the newly machined surfaces.

Alpha case is a hard material which is detrimental to tool life. This is the primary reason why it is removed before final component machining can commence. If the surface hardness of the newly machined surface emulates the surface hardness of normal titanium, then it is conceivable that the most detrimental (if not the total) portion of the alpha case must be removed. Even if the oxygen-affected zone penetrates deeper into the titanium substrate, the normalised hardness measurements indicate towards low oxygen content which does not alter the microhardness in a significant way. The remnants of the oxygen affected zone would therefore not have a measurable impact on further machining operations. However, the above assumption only holds true if further roughing operations are to take place. The removal of the alpha case serves only as a pre-machining step, aimed at the removal of scale from the billet before actual production. Oxidation and subsurface damage is possibly present in the newly machined surface, and therefore has to be removed in subsequent roughing and finishing operations. Figure 42 presents the average titanium surface hardness measurements taken from the newly machined titanium billet at various machining speeds and feeds after every machining trial.

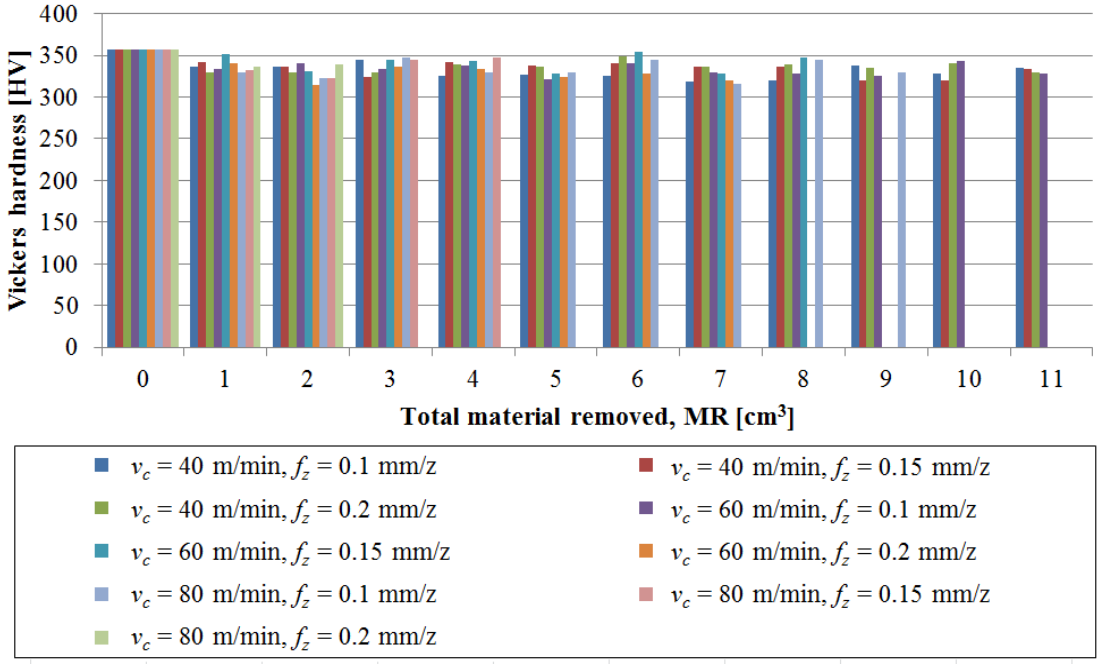

Figure 42: Surface hardness measurements before (0) and after (1-11) every experimental procedure

The initial hardness of the Ti6Al4V sample before heat-treatment was 357 HV. Samples of similar composition exhibit surface hardness measurements of 349 HV. This is similar to what is displayed in Figure 42. The values shown above indicate that the removal of the hardened oxygen enriched alpha layer was successful and that further roughing processes can commence. For a more accurate assessment, oxygen depth profiling needs to be conducted on newly machined samples in order to

confirm the absence of oxygen. However, because of the normalised surface hardness measurements, it can be assumed with a certain degree of accuracy that the alpha case layer has been removed.

4.5. Chip formation

At the conclusion of each machining trial, the chips were collected and examined under stereoscopic microscopy. Figure 43 depicts the chip morphologies of chips collected at three different cutting speeds, v_c = 80, 60 and 40 m/min, and feeds, f_z = 0.1, 0.15 and 0.2 mm/z respectively. Even though alpha case was present in the workpiece material, the collected chips resemble what is observed with traditional titanium machining.

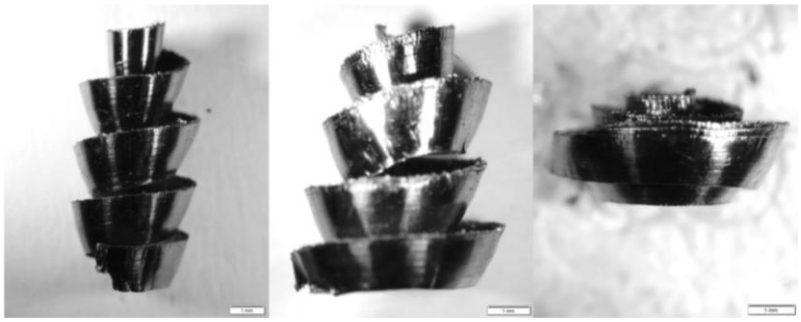

(a) **(b)** **(c)**

Figure 43: Various chip morphologies at (a) v_c = 40 m/min and f_z = 0.2 mm/z (b) v_c = 60 m/min and f_z = 0.15 mm/z and (c) v_c = 80 m/min and f_z = 0.1 mm/z

All the chips are spiralling and discontinuous, indicating the occurrence of serration. The length of the spiral is similar to the length of engagement, revealing little or no recutting of chips was experienced. Chip evacuation was therefore performed effectively. Excessive recutting of chips leads to increased tool wear, resulting in higher production cost. The different morphologies of chips observed in Figure 43 are consistent with literature as observed by (Li, et al., 2011). Slower cutting speeds produce longer, elongated chips while higher cutting speeds result in flat chips. The free surface (spiral interior) of all the chips possesses lamella structures. Differences in cutting speed result in a difference in lamella sizes, which may alter the morphology of the chips. Finally, no discolouration of the chips is observed.

The identical length of chips along with an identical depth of cut would result in the feed rate determining the volume of the chip. It is expected that doubling the feed rate would result in thicker chips, which would also result in an increase in volume. However, measuring the thickness of the chips is difficult owing to the inconsistent segmentation or saw-tooth formation.

Figure 44 illustrates the lamella (serration) effect in the metal cutting of titanium. Within a specific measuring distance, the number of lamella structures (serration) is different depending on the cutting speeds and feeds. The lamella structures are irregular, small and compacted at low cutting speeds, resulting in more lamella structures over a unit of measure. At higher cutting speeds there is clearer saw tooth visibility as height of the peaks becomes larger. This results in a decreasing number of

lamella structures within a unit of measure. The analysis also showed that feed rate has a measurable effect on lamella formation which is consistent with what was observed by Sun & Guo (2009) and Nurul Amin, Ismail & Nor Khairusshima (2007).

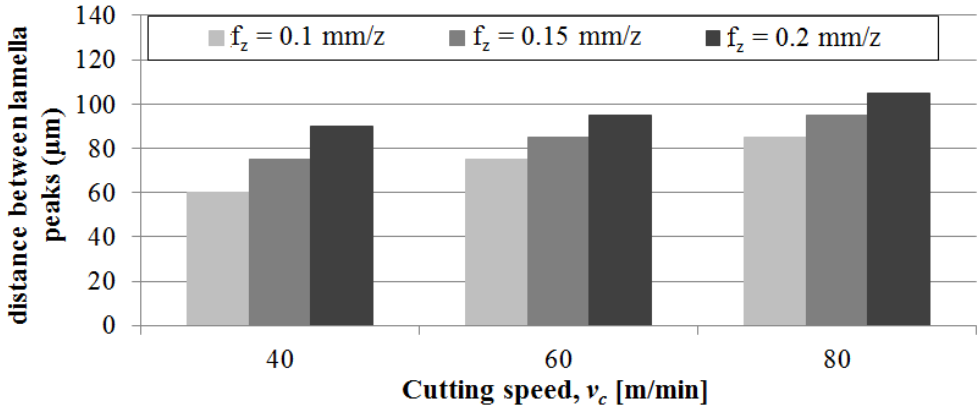

Figure 44: Rate of lamella formation on machining chips

4.6. Tool wear

After each machining experiment wherein MR = 9 cm^3 of material has been removed, the insert edges were analysed using an Olympus SZX7 stereomicroscope. Quantitative measurements of the micrographs were taken with Stream Essentials image analysis software. The different types and magnitude of wear were identified in accordance with ISO standards for face milling.

Figure 45 represents the wear curves of the different feed and speed combination over the total amount of material removed. It is clear from the start that the presence of alpha case has a measurable influence on the initial wear rate of the tool. In all nine combinations of feed and speed, it is observed that accelerated tool wear is experienced for the first machining trial of MR = 9 cm^3. Accelerated initial tool wear is common in titanium machining as is indicated in Figure 20. However, the degree of accelerated wear might be attributed to the sharp cutting edge, which is traditionally advised for titanium machining, yielding under the increased hardness of the alpha case surface layer. After the initial stages of tool wear, the wear rates for the majority of the feed and speed combinations subside, where after decreased wear rates are observed.

From Figure 45 it is clear that there are three different wear rate groupings in development: an accelerated, an intermediate, and a gradual wear rate. The first of the cutting tools not able to complete the prescribed MR = 100 cm^3 material removal are the most aggressive cutting speeds (MRR = 16-21.4 cm^3 per minute). After only MR = 18-36 cm^3 of material removal under the highest cutting speed of v_c = 80 m/min and feed rates of f_z = 0.2 and 0.15 mm/z respectively, the inserts already exhibit significant wear, almost fulfilling the failure criteria as set out by ISO. Due to the significant jump in wear experienced in the last machining runs of both these cutting conditions, it was decided to declare these tools as failed earlier. Both cutting conditions exhibited average wear of roughly V_B = 310 µm each, instead of the prescribed V_B = 350 µm. In keeping with consistency,

further failure criteria will henceforth be influenced based upon the premature declaration of tool failure. The new criterion is an average flank wear of roughly V_B = 300 µm across all six inserts.

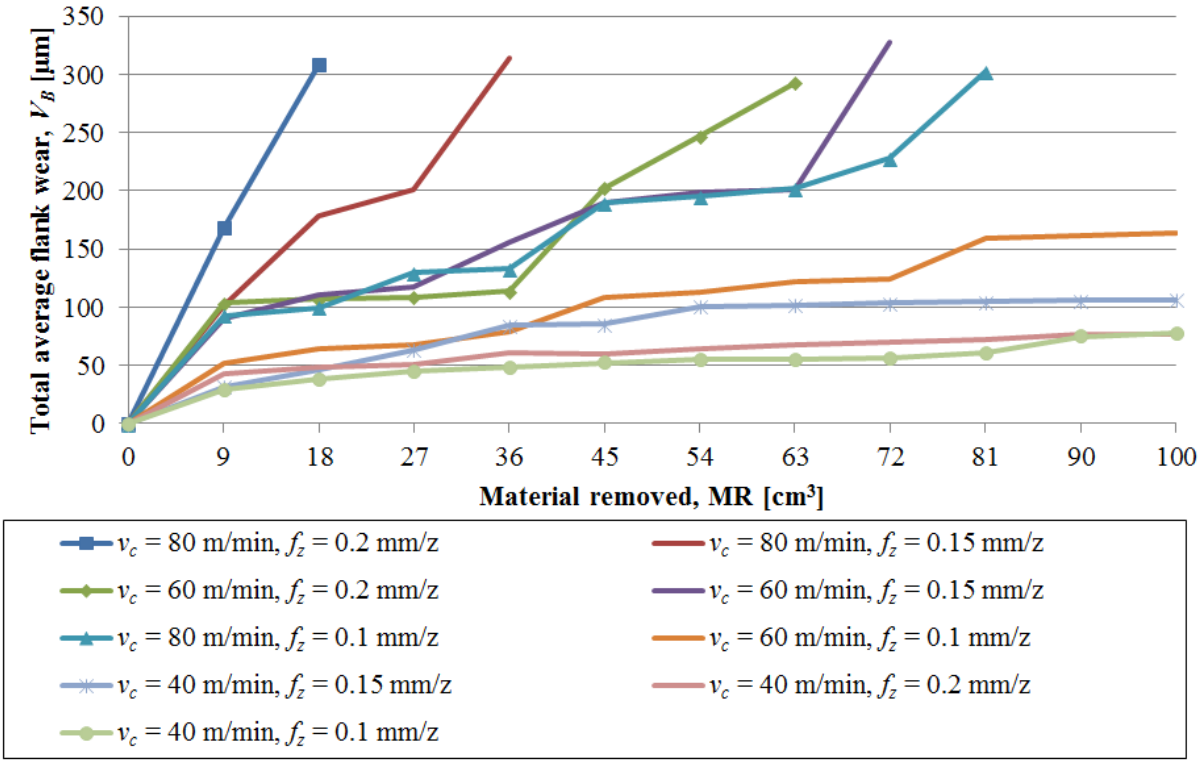

Figure 45: Wear curves for different feed and speed combinations

As the cutting feed and cutting speed is reduced, so does the wear rate. This is evidenced by the three intermediate wear curves displayed in Figure 45 (MRR = 10.7-16 cm^3 per minute). Carbide inserts exposed to these machining parameters, cutting speed v_c = 60 m/min and f_z = 0.2 and 0.15 mm/z, and v_c = 80 m/min and f_z = 0.1 mm/z, removed between MR = 63-81 cm^3 of material before they ultimately failed. Failure criteria were kept constant and these tools were also declared failed after experiencing roughly V_B = 300 µm of wear.

The final grouping observed showed much more gradual wear during the experimental phase. This is also the only group that does not meet any failure criteria before the experimental requirement of MR = 100 cm^3 material removal is met. The gradual wear rates come as a result of less aggressive material removal rates (MRR = 5.4-10.7 cm^3) whereby cutting parameters are at their slowest. Cutting speed vary between v_c = 40 m/min and f_z = 0.1, 0.15 and 0.2 mm/z, and v_c = 60 m/min and f_z = 0.1 mm/z.

4.6.1.Types of wear

Wear on the flank face of the carbide inserts is measured in the direction shown in Figure 46. Despite the fact that the corner angle of the edge is at $\angle_{CH}$ = 45° with the workpiece material, measurements are taken perpendicular to the flank face. From this angle, flank- and notch wear are the two most common types of observable wear. Flank wear, which is located on the relief surface of a cutting tool, is the most common type of wear generally observed in titanium machining. Such wear occurs due to

the gradual loss of tool material from the unwanted rubbing of the clearance face against the workpiece material. Notch wear, however, is observed in the form of chipping in the region of cutting edge adjacent to the workpiece surface.

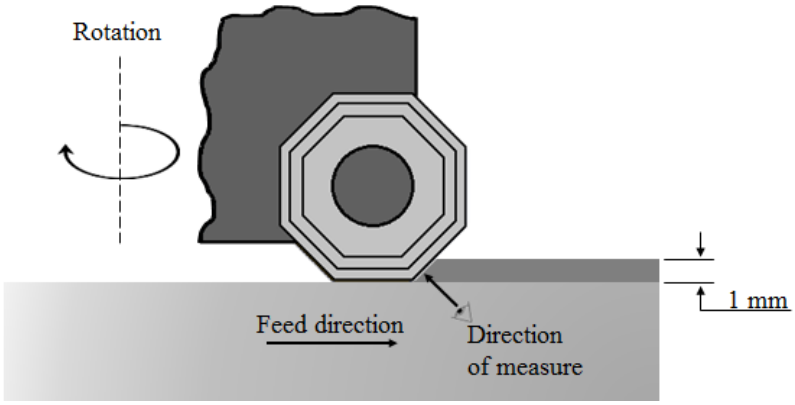

Figure 46: Schematic representation of the metal cutting operation and the direction from which tool wear is measured from the flank face

Figure 47 depicts the two distinctly different types of wear observed in the nine cutting parameters. The type of wear is related to the respective tool life, cutting speed, and total material removed. In general, utilising higher material removal rates results in notch wear and frequent chipping in the notch region adjacent to the hardened alpha case layer. Lower material removal rates are more often associated with uniform flank wear and minor, gradual notching. However, intermediate material removal rates resulted in both kinds of wear on respective inserts, leading to the conclusion that cutting speed has a severe impact on notching when machining alpha case titanium. An analysis of three different cutting parameters that result in similar material removal rates will be discussed below.

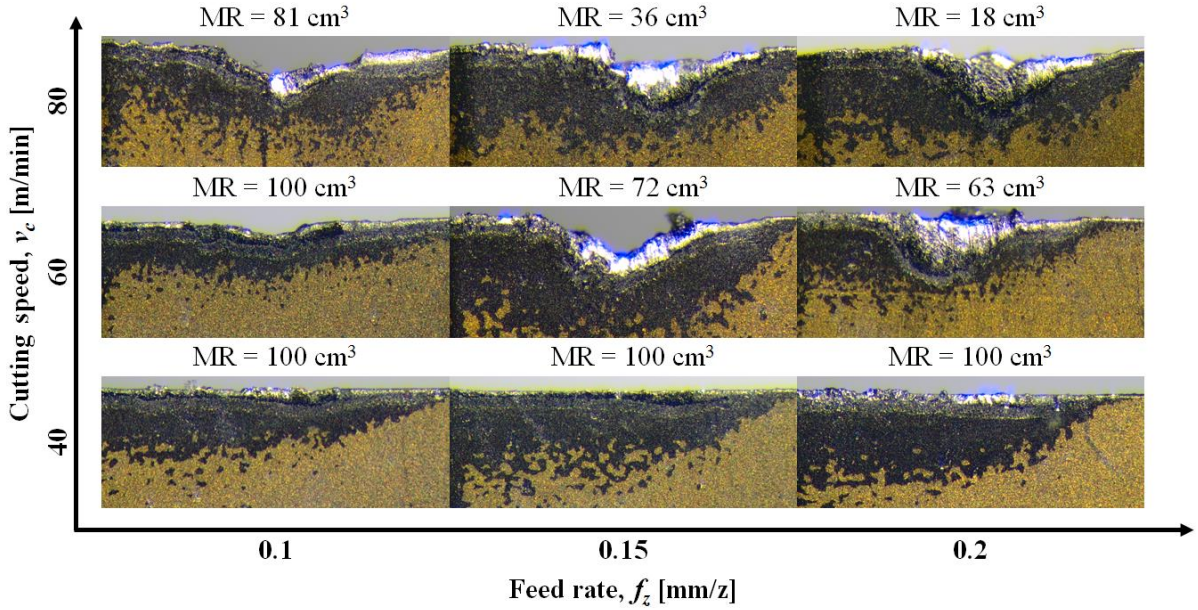

Figure 47: Final tool wear observed on various cutting edges with the correlating cutting speed v_c, cutting feed f_z and total material removed MR (see Figure 46 for direction of measurement)

Three cutting conditions were selected in order to study the wear rates and type of wear. The three cutting conditions were selected to analyse different cutting speeds, however at a constant material removal rate. Therefore, as the cutting speed is reduced, the feed rate is increased.

Figure 48 represents a collection of micrographs representing the progression of tool wear experienced by the carbide inserts at certain intervals of the machining experimentation process. This specific insert was exposed to a cutting speed of v_c = 80 m/min and f_z = 0.1 mm/z, which resulted in a material removal rate of MRR = 10.70 cm^3/min. Each micrograph is separated by the material removal of MR = 9 cm^3.

Severe notching is visible in the collection of micrographs and it is also clear that no significant wear is evident in the region just below the notch area. This leads to the conclusion that the alpha case is solely responsible for the severe notching and that the titanium substrate is readily removed. Similar wear patterns are also evident in a number of other aggressive cutting speeds.

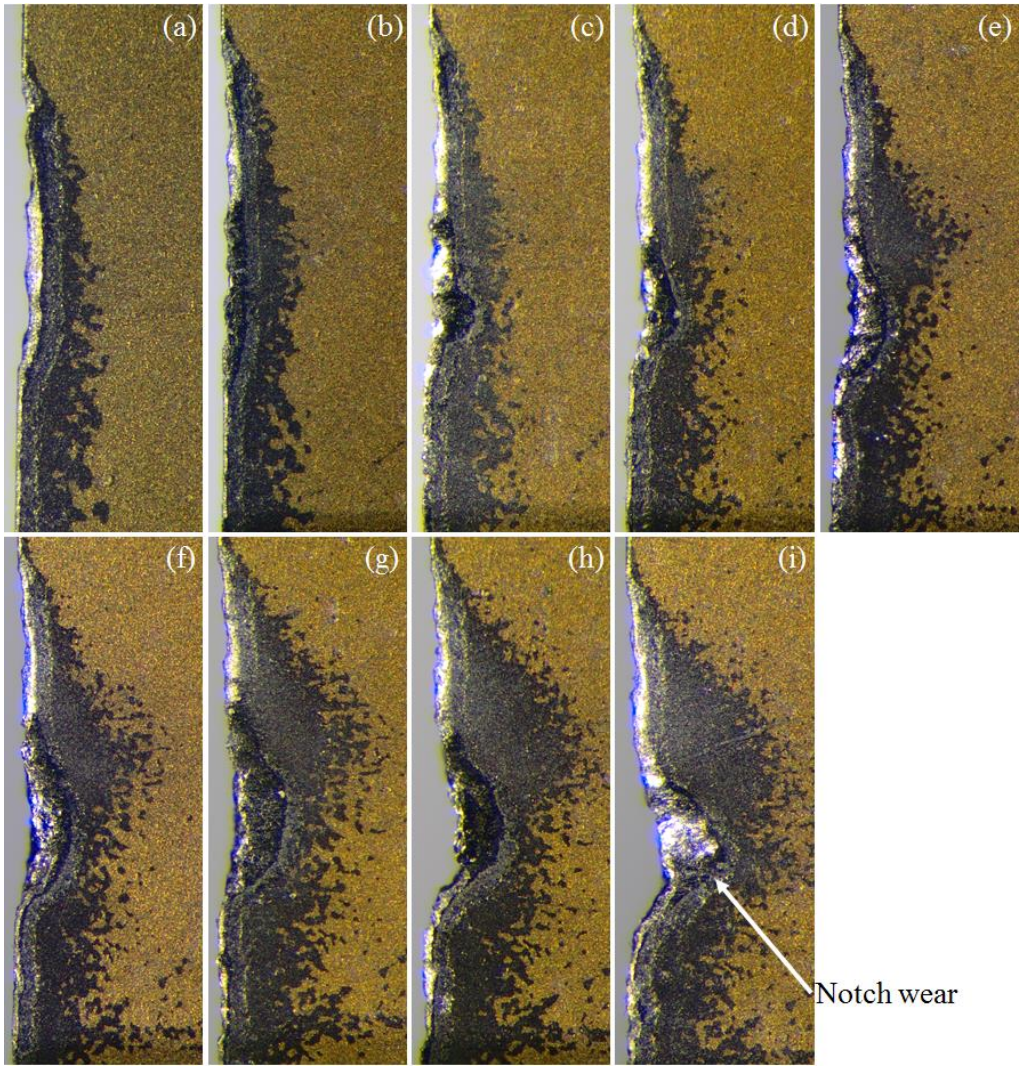

Figure 48: Collection of stereoscopic micrographs of carbide insert exposed to cutting parameters of v_c = 80 m/min at f_z = 0.1 mm/z. Shows the progression of tool wear in the removal of alpha case from (a) MR = 9 cm^3 – (i) MR = 81 cm^3

Figure 49 illustrates micrographs of the wear experienced from a lower cutting speed of v_c = 60 m/min at a slightly higher feed rate of f_z = 0.15 mm/z. The resulting material removal rate is slightly higher at MRR = 12.03 cm^3/min. The wear observed is similar to what is visible in Figure 48. It is commonly known that notching and chipping in the notch region are caused by machining parts with severe (hard or oxidised) surfaces.

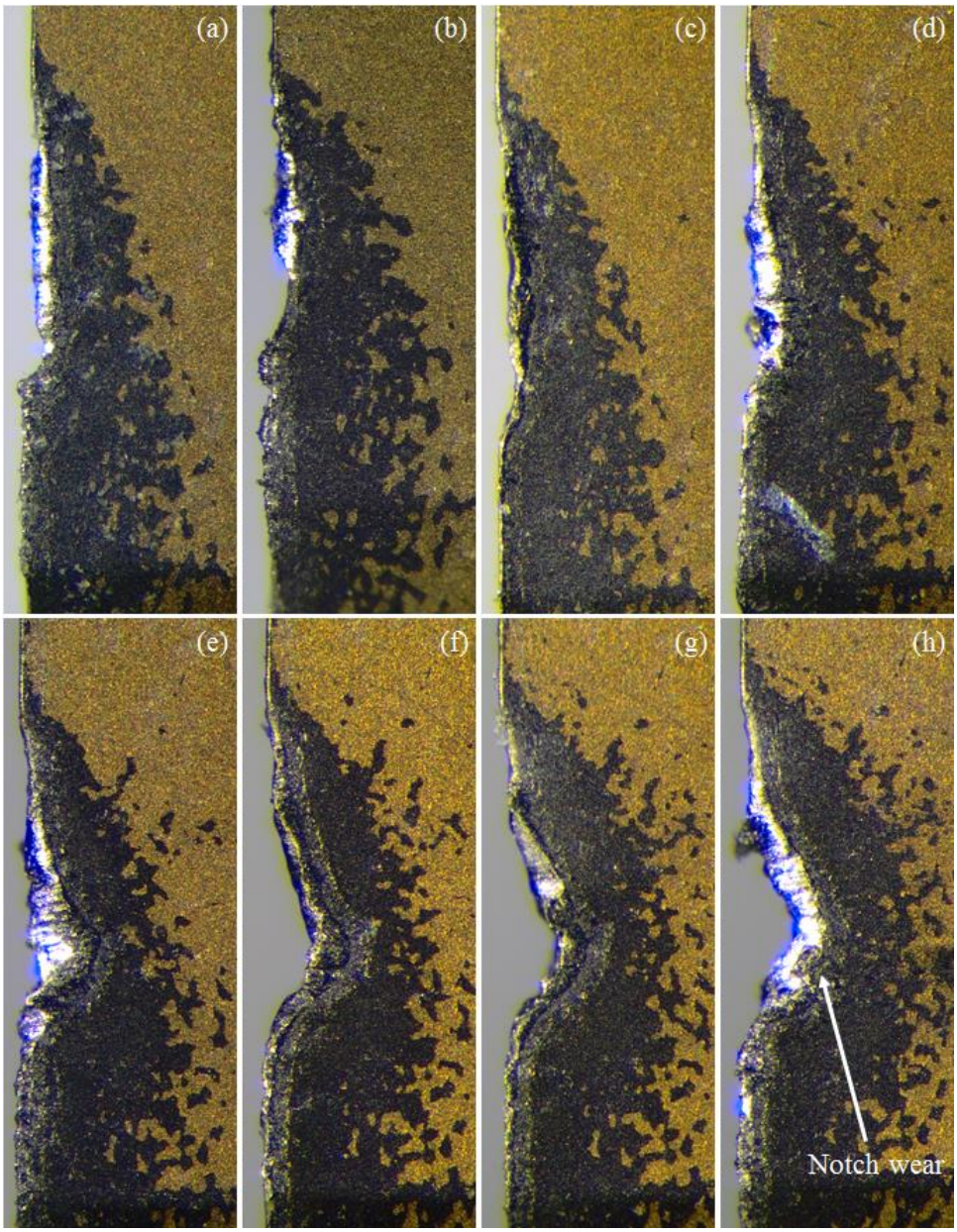

Figure 49: Collection of stereoscopic micrographs of carbide insert exposed to cutting parameters of v_c = 60 m/min at f_z = 0.15 mm/z. Shows the progression of tool wear in the removal of alpha case from (a) MR = 9 cm^3 – (h) MR = 72 cm^3

A closer inspection of Figure 48 and Figure 49 would result in the observation that the wear revealed by the micrographs extends well beyond the a_p = 1 mm depth of cut. The use of a CH = 45° corner angle in the carbide insert results in a 75% larger contact area, as opposed to the use of a CH = 90° corner angle. The larger contact length results in cutting forces experienced by the carbide insert to be

distributed over a longer contact area. This helps in the distribution of wear over a longer contact length which increases tool life.

As a result of the 45° corner angle, the wear scar on the flank face of the cutting tool also lies at the same angle. The length of the wear scar for cutting speeds of v_c = 60 m/min and f_z = 0.15 mm/z, is in some cases up to 1480 µm. This length is measured from the point where the flank face is at a 45° angle with the workpiece material. If the corner edge of the carbide insert did not include a 22.5° nose radius as shown in Figure 50, the contact length of the flank face would be an additional 396 µm. The contact length of the wear scar on the flank face at a 45° angle would therefore have a total length of 1876 µm. On the other hand, the prescribed a_p = 1 mm depth of cut projected on the 45° flank face of the carbide insert, would result in a contact length of 1414 µm. The wear scar therefore extends significantly higher than the prescribed depth of cut. This is as a result of the notching effect experienced by the cutting edges. The notching chips removed material above and below the workpiece surface.

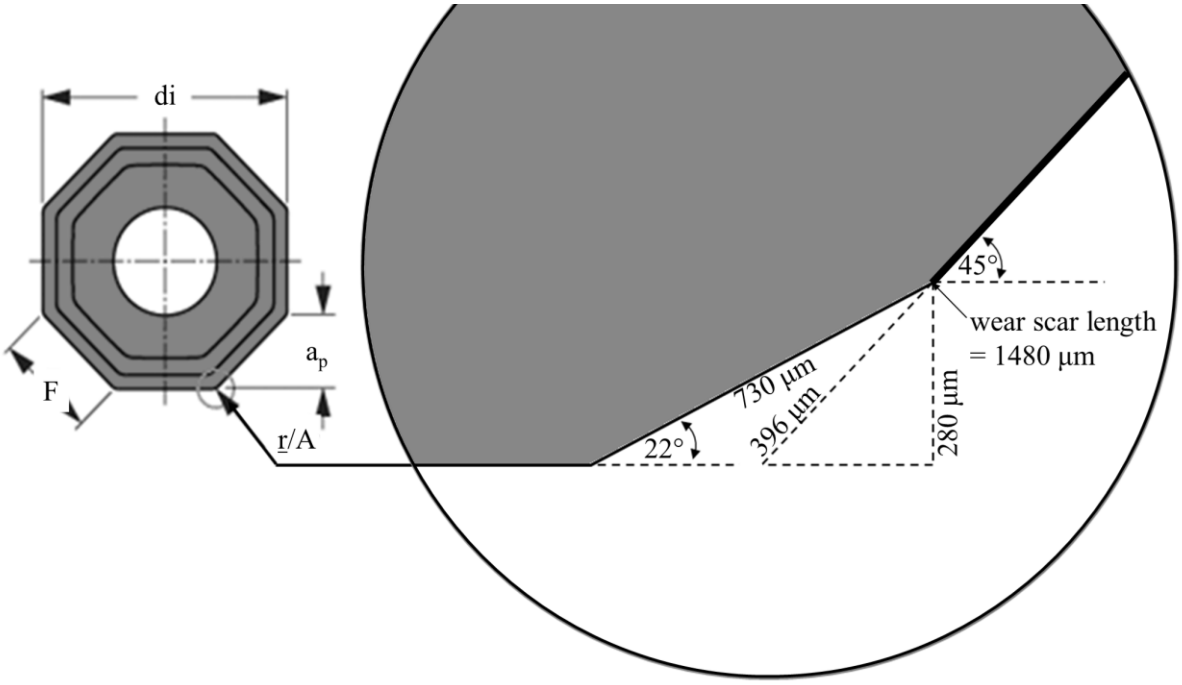

Figure 50: Schematic of the corner edge of the carbide inserts which shows the corner landing

Figure 51 is a schematic showing the shape and length of the average wear experienced by the carbide insert at cutting speeds of v_c = 60 m/min and f_z = 0.15 mm/z. This is the centre point in terms of the cutting parameters chosen in this investigation. It is clearly observable that the wear extends beyond the a_p = 1 mm depth of cut. It can also be observed that the majority of wear on this particular cutting condition is experienced in the harder portion of the alpha case layer. The softer substrate does not experience any significant wear that might be detrimental to tool life.

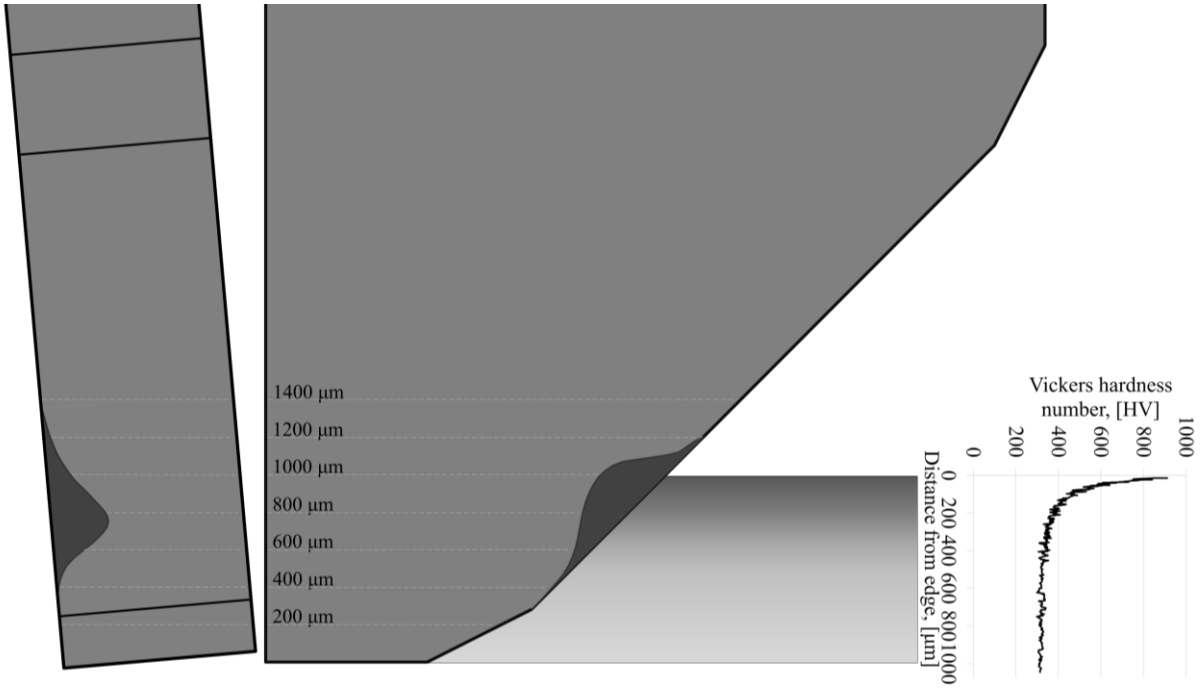

Figure 51: Schematic of average tool wear as a function of depth on a carbide insert at cutting speed of v_c = 60 m/min and f_z = 0.15 mm/z feed rate

Lower material removal rates, and by association lower cutting speeds, result in less aggressive wear rates and less severe notching. Figure 52 again illustrates the wear experienced by the carbide inserts exposed to cutting conditions of v_c = 40 m/min and f_z = 0.2 mm/z, which results in a material removal rate of MRR = 10.70 cm^3/min.

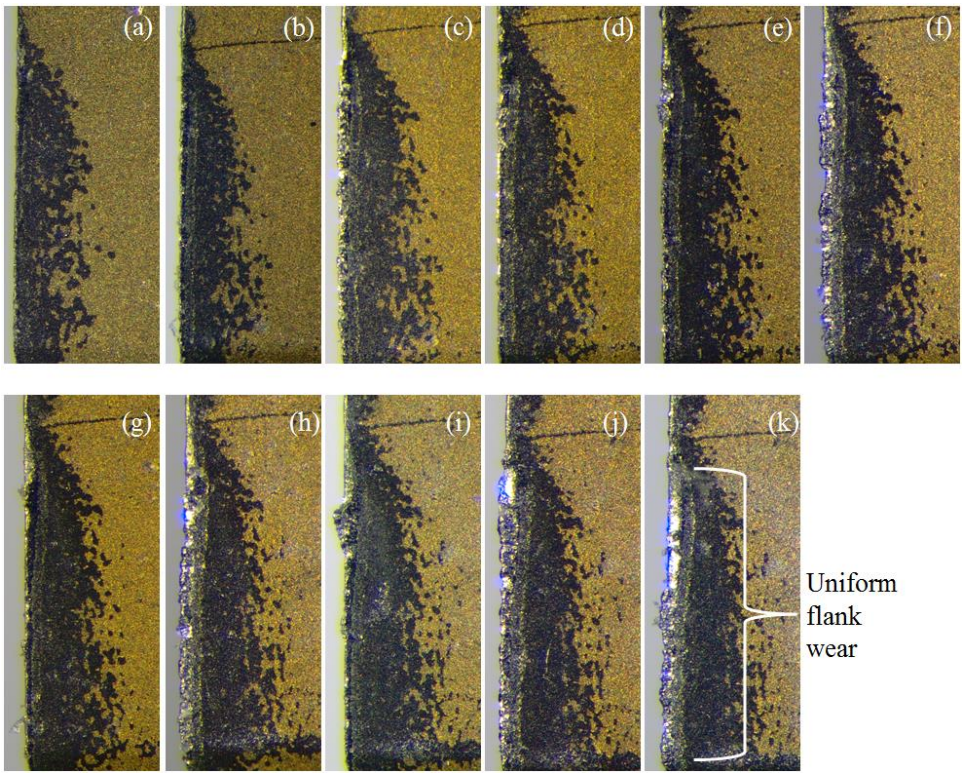

Figure 52: Collection of stereoscopic micrographs of carbide insert exposed to cutting parameters of v_c = 40 m/min at f_z = 0.2 mm/z. Shows the progression of tool wear in the removal of alpha case from (a) MR = 9 cm^3 – (k) MR = 100 cm^3

The inserts used in the experimentation as revealed in Figure 48, Figure 49, and Figure 52, yielded similar material removal rates despite the vastly different wear rates and patterns. The more aggressive cutting speeds (v_c = 60 and 80 m/min) resulted in high degrees of notching, which are absent at lower cutting speeds (v_c = 40 m/min). Figure 52 exhibits more gradual and varying degrees of uniform and non-uniform flank wear as the primary wear phenomenon. In other words, the wear experienced in the region directly adjacent to the alpha case wears at a similar rate as the substrate. This is more in line with what is expected in traditional titanium machining processes (Jawaid, Sharif & Koksal, 2000).

Flank wear is a common phenomenon in titanium machining and not much can be done to restrict wear on the flank face. However, in terms of notching there may be a couple of alterations in the machining process that can have a measurable effect in tool life. According to the Kennametal titanium machining guide the following should be incorporated in order to minimise notching (Kennametal, 2015):

- Avoid built-up edge
- Increase the lead tool angle
- Use tougher grades of carbide cutters
- Use chamfered (stronger) edge
- Maintain speed and decrease feed rate
- Increase coolant concentration
- Depth of cut should be greater than work hardening layer
- Use strongest insert shape possible
- Program a ramp to vary depth of cut

Some of these recommendations can be implemented to some extent, and others seem to be contradictory to what is experienced in the experimental procedure. Increasing tool lead angle may increase tool life by making sure the first part of the carbide edge to come in contact with the workpiece is not in the region adjacent to the hardened alpha case layer. This may reduce notching by first making contact in softer substrate material, and work its way up to the harder surface. This would, however, be at the expense of double-sided inserts, as the inserts would instead only be able to machine on one side of the insert, halving the number of cutting edges (Kennametal, 2015).

Tougher grades of tungsten carbide cutting tool material may cause less severe chipping, and chamfered edges would result in stronger edges better capable of combatting the alpha case hardness. Maintaining cutting speed and decreasing cutting feed are directly contradictory to what is observed in this study, though this may be due to the hardness of alpha case. The programming of a ramp in order to vary the depth of cut would result in a shift in the region of the cutting tool that is adjacent to the workpiece surface as shown in Figure 53.

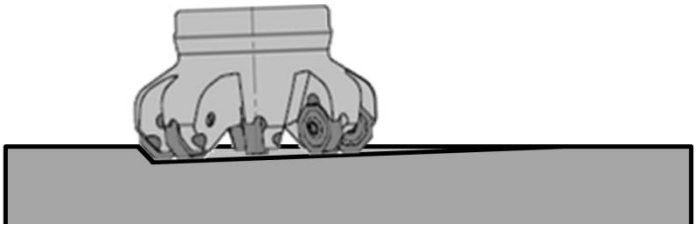

Figure 53: Programme a tool ramp into the workpiece in order to minimise notch wear on a localised point of the carbide insert

Programming a ramp would spread the effect of notching evenly along the cutting edge which would ideally lower the extent of notching and therefore increase tool life. Only certain face milling cutters are designed to allow a ramp down toolpath. One drawback of using a ramp down, or ramp up toolpath, is that the resulting surface would not be uniform. This may make subsequent milling more difficult (Kennametal, 2015).

4.6.2.Stair-formed wear pattern

Notch wear is a common phenomenon with hard materials such as titanium. It is very common when machining forgings with very tough surfaces, and the removal of scale. In this particular investigation, lower cutting speeds exhibited similar wear curve profiles to the one depicted in Figure 20. Accelerated wear is experienced at the beginning. This followed by gradual wear for the remainder of the experimentation period. During experimentation, cutting tools used at low cutting speeds did not experience tool failure. It is possible that the wear rate experienced by the cutting tool would again increase near the end of the tool's useful life. At higher cutting speeds, however, the wear pattern did not reflect what is depicted in Figure 20, owing to the notching of the cutting tool in the region adjacent to the workpiece surface.

In this cutting operation, the first contact between cutting tool and workpiece material is directly on the hardest part of the alpha case layer on the surface of the workpiece. This is the same for every carbide insert with every revolution. At high cutting speeds, the velocity that the cutting tool edge enters into the hard workpiece material puts cutting edge under severe stress. Chipping, which removes a portion of the cutting tool in that region, is therefore a frequent phenomenon in the region adjacent the workpiece surface. The chip that breaks away, changes the geometry of the cutting edge. As a result, the first portion of the cutting tool that makes contact with the workpiece material is different. Instead, first contact is made just below the chip in a region experiencing lesser amounts of wear. The shift in first contact therefore 'protects' the region adjacent to the workpiece surface which limits wear in the particular area.

Continual machining results in the formation and growth of a chip in the cutting edge. The area of first contact is altered with the formation and growth of every new chip. At first, the area of first contact moves down the cutting edge, owing to the angle of the cutting edge in relation to the workpiece. The downwards movement of first contact prevents the cutting tool from making first

contact with the workpiece material in the hardest part of the alpha case in the notch region adjacent to the workpiece surface. This therefore prevents the area currently experiencing the maximum amount of wear to accumulate additional wear. At some point, the length of the chip will become so great that the cutting edge adjacent to the alpha case in the hardest part of the workpiece material will again make first contact. As a result, a chip is eventually formed and the process repeats itself, until tool failure criteria is met. Figure 54 provides a visual representation of the stair formation phenomenon.

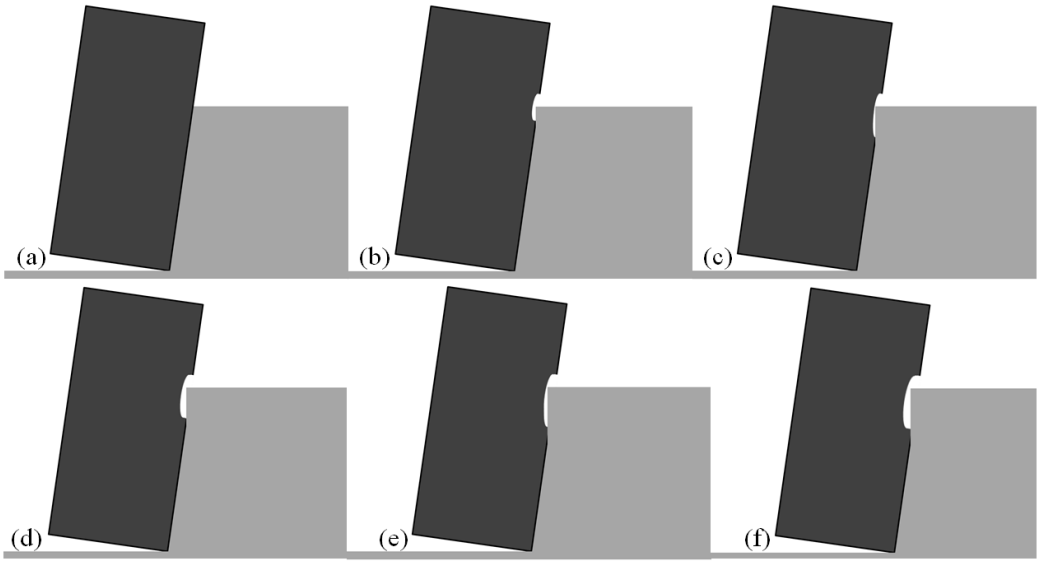

Figure 54: Visual representation of stair form notching (a) new tool engages in workpiece material (b) chip is formed in notch region adjacent to the workpiece surface (c) chip length is increased in order to expose material adjacent to the workpiece (d) chip depth is increased (e, f) process is repeated until tool failure

This is by no means a proven hypothesis and will require further experimental analysis to confirm. At high cutting speeds the hardened alpha case layer does however seem to result in wear phenomena similar to what is presented in Figure 54.

4.6.3.Projected tool life

Tool failure on the flank face of the cutting tool is defined as V_B =350 μm. Owing to the large jump in tool wear experienced by cutting edges close to tool failure, it was deemed appropriate to redefine tool failure to V_B = 300 μm. This was done in order to avoid potentially catastrophic tool failure of the already worn tools after the removal an additional MR = 9 cm^3 of material. Furthermore, only five out of the nine prescribed machining conditions experienced failure in terms of the new failure criteria (V_B = 300 μm). Strictly speaking, these tools can potentially still be used in titanium machining as tool failure is not met according to ISO standards. Some predictions can be made for the total material removal in the tools that did not meet any failure criteria. This can be achieved by extrapolating the available data until tool failure criteria is met, based on the ISO for tool life testing in face milling. The extrapolated data is based on the results of Figure 45.

The accuracy of applying extrapolation is not flawless. However, regression testing of all nine cutting conditions proved to be insufficient and does not show adequate similarities to the derived function. Full regression analysis is conducted in Appendix A. The lack of an alternative forced simple linear extrapolation, although this will also not provide an accurate fit to the data. Based on the ISO recommended failure criteria and the extrapolated tool wear curves, the following tool life curves are established in Figure 55.

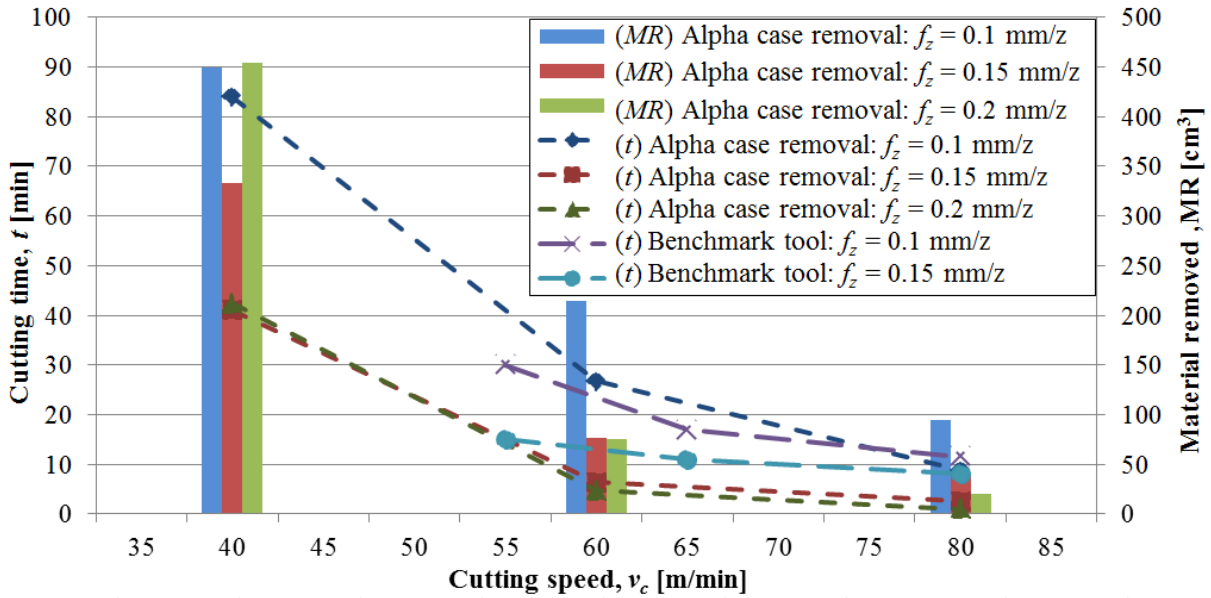

Figure 55: Tool life projection curve based on extrapolated data observed in experiments compared to benchmark data by (Jawaid, et al., 2000)

Firstly, when comparing the tool life results to literature, it is clear that tool life is adversely affected by the presence of alpha case. This is specifically true for high cutting speeds where the alpha case layer caused rapid deterioration of the cutting edge. Jawaid et al. performed face milling experiments at similar cutting speeds and observed longer tool life at higher cutting speeds. At lower cutting speeds however, the alpha case has a smaller effect on the wear rate. At low cutting speeds alpha case machining removal more closely resembles what is experienced in literature. Furthermore the tool life curve of alpha case machining also resembles that of the benchmark observations.

Figure 55 illustrates the total tool life and material removed, as a factor of cutting speed and feed rate. It is clear that cutting speed has a measurable influence on tool wear. The more aggressive feed rates (f_z = 0.15 mm/z and f_z = 0.2 mm/z) result in very similar cutting times across all cutting speed ranges. The projection of total amount of material removed by each cutting condition also resembles the tool life projection curve.

At the lowest cutting speed (v_c = 40 m/min) two cutting conditions result in similarly high total material removal. This is however at vastly different total cutting times. The higher material removal rate exhibited by utilising a higher feed rate (f_z = 0.2 mm/z) results in shorter cutting time for similar amount of material removal. This increases the efficiency by removing similar amounts of material in

a shorter amount of time. A more detailed analysis will, however, be required in order to determine the most efficient cutting condition in terms of cost.

Most notable, is the tool life at cutting parameters of v_c = 40 m/min while varying cutting feed between f_z = 0.15 and 0.2 mm/z. The tool life in each case is almost identical despite the difference in feed rate. There is however a large difference in total material removal by these cutting conditions. This is also visible in Figure 45 whereby the lower feed rate experiences more wear over the MR = 100 cm^3 material removal than the more aggressive feed rate. The reason for this is the method of wear experienced in one of the carbide inserts at v_c = 40 m/min and f_z = 0.15 mm/z.

Figure 56 displays a series of micrographs taken of one of the carbide insert edges that underwent machining at v_c = 40 m/min and f_z = 0.15 mm/z. Figure 56 (b), is taken after MR = 18 cm^3 of material removal and shows the formation of a crack stretching nearly the length of the tool contact area. After the removal of MR = 36 cm^3 of material, significant chipping is experienced by the insert as a result of the crack. This chipping in one of the carbide inserts results in the measurement being classified an outlier which greatly increases the average tool wear experienced at this specific cutting condition.

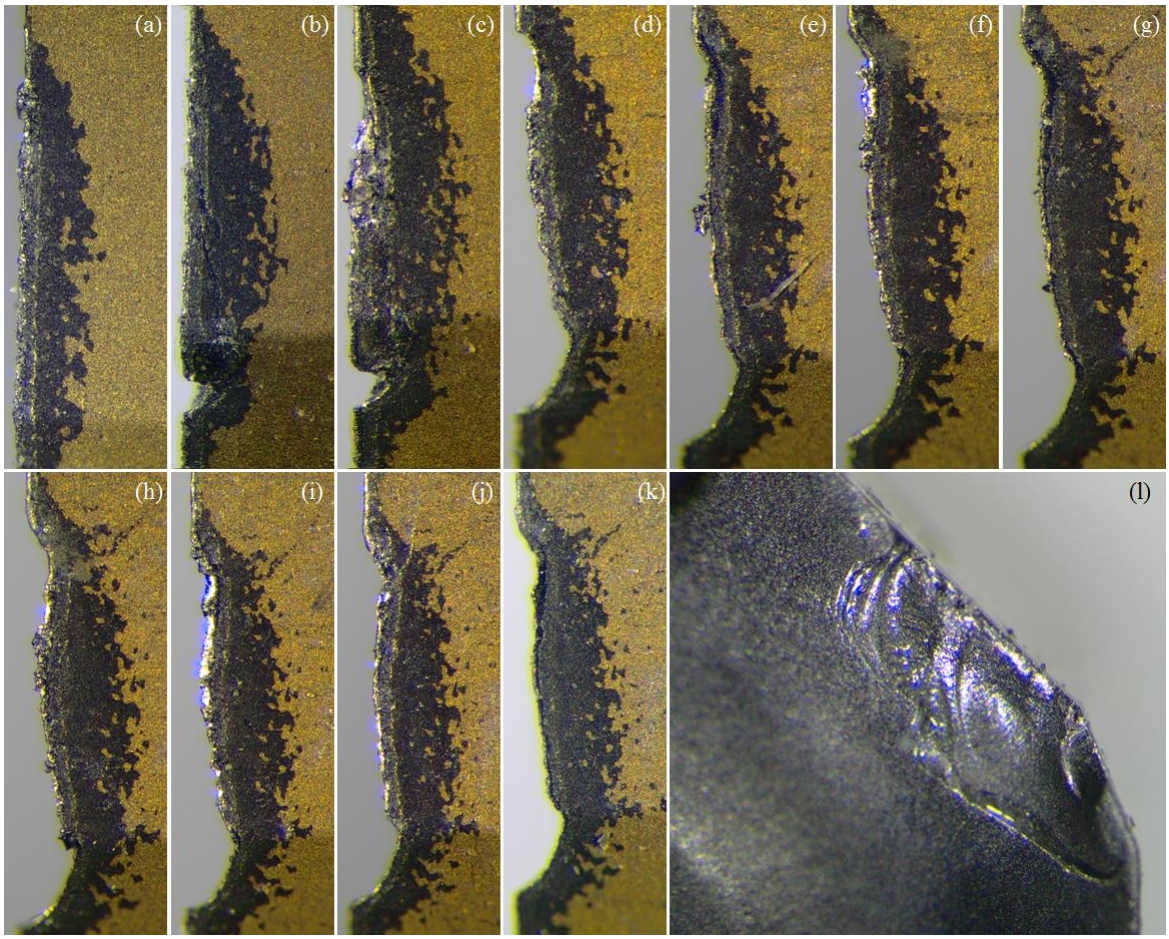

Figure 56: Collection of stereoscopic micrographs of carbide insert exposed to cutting parameters of v_c = 40 m/min at f_z = 0.15 mm/z. Shows the progression of tool wear in the removal of alpha case from (a) MR = 9 cm^3 – (k) MR = 81 cm^3, and (l) portrays the extent of chipping experienced by this particular insert edge after MR = 81 cm^3

Although the crack is substantial on the rake face, it does not meet any failure criteria, and the tool is suitable for further machining. The tool completed the prescribed removal of MR = 100 cm^3 and showed no significant additional chipping or wear as machining continued. Choosing to disregard the chipped insert when calculating the average tool wear, results in a wear rate similar to that shown when machining at cutting speeds of v_c = 40 m/min, at either f_z = 0.1 or 0.2 mm/z. After the prescribed MR = 100 cm^3 material removal, all three feed rates at v_c = 40 m/min exhibit identical wear. This leads to the belief that at low cutting speeds, feed rate has a negligible influence on wear. On the other hand, at high cutting speeds, feed rate does have a noticeable effect on tool wear. This conforms to what is observed by the cutting tool manufacturer.

Figure 57 illustrates the tool wear measured from each individual carbide insert at cutting speed v_c = 40 m/min for all three feed rate ranges (f_z = 0.1, 0.15 and 0.2 mm/z). A total of 100 cm^3 of material has been removed by all three conditions. Figure 57 (a) encapsulates the individual measurements of all the cutting edges alongside a box and whiskers plot.

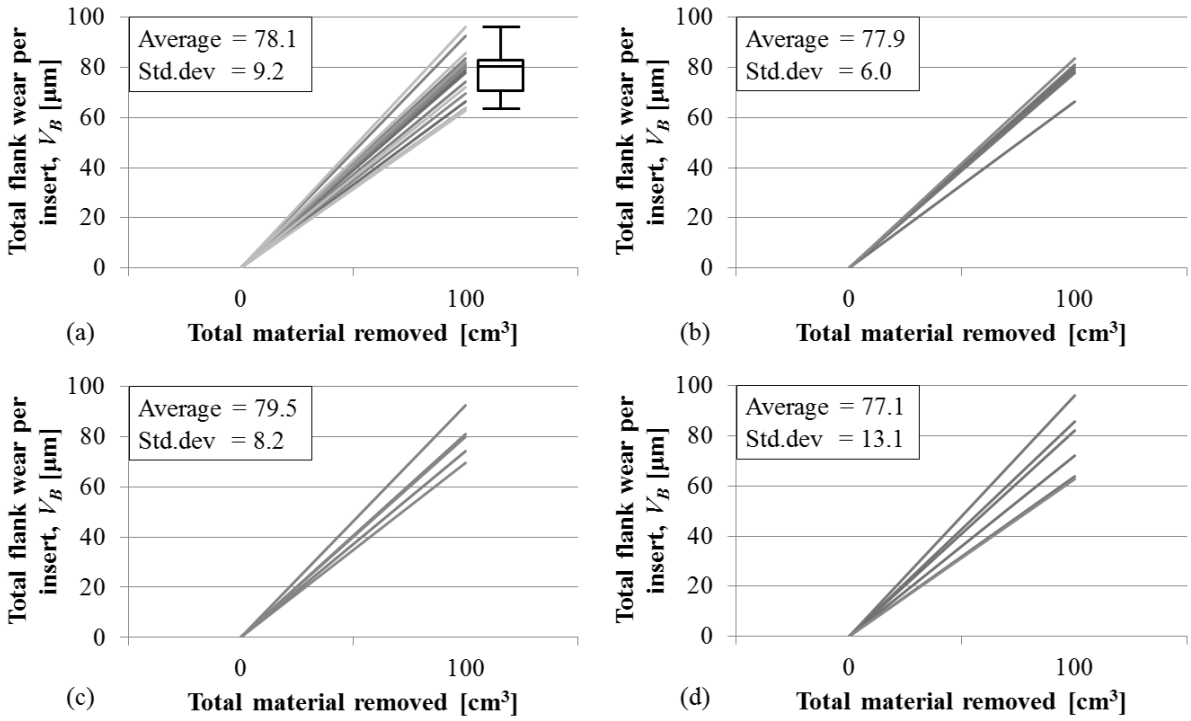

Figure 57: Spread of tool wear as measured from (a) all the carbide inserts combined (b) individual carbide inserts that underwent machining at v_c = 40 m/min and f_z = 0.1 mm/z (c) individual carbide inserts that underwent machining at v_c = 40 m/min and f_z = 0.15 mm/z (d) individual carbide inserts that underwent machining at v_c = 40 m/min and f_z = 0.2 mm/z

The standard deviation of Figure 57 (b) (v_c = 40 m/min and f_z = 0.1 mm/z) is very small with only one measurement falling a little outside the grouping. In Figure 57 (c) (v_c = 40 m/min and f_z = 0.15 mm/z) and (d) (v_c = 40 m/min and f_z = 0.2 mm/z) the measurements are a little more scattered, which results in a slightly higher standard deviation. However, the averages for all three graphs are very similar. For all measurements in Figure 57 (b, c and d) there is a possibility of minor errors in the measurement of wear. This may lead to more aggressive feed rates exhibiting less aggressive wear rates. For Figure 57

(c) it was decided to omit the significant outlier which was caused by chipping at conditions of v_c = 40 m/min at f_z = 0.15 mm/z.

4.6.4. Statistical interpretation

The following section outlines the most basic statistics that can be derived from the experimental results. However, because not all machining experiments were conducted until tool failure, varying combinations of tool wear and total material removal are experienced for the individual observations. In order to compensate for this variation, section 4.6.3 extrapolated the data in order to estimate total tool life. The statistical inference in this section is based on that extrapolation, and significant variations in the derived (versus actual) data, would lead in amplified variation in the statistical analysis. Furthermore, the extrapolated data omitted the outlier wear measurement as a result of significant chipping in machining parameters of v_c = 40 m/min at f_z = 0.15 mm/z.

Experimentation did not follow a full factorial analysis; nevertheless, valuable analysis can still be conducted with the help of certain data analytical tools such as Modde 10.1 Design of Experiments software by Umetrics. Analysis of the statistics includes R^2, Q^2, coefficient plots and contour plots. The observation numbers are represented in Table 7.

Table 7: Experiment number

Experiment number	Cutting speed, v_c [m/min]	Feed rate, f_z [mm/z]	Total material removed, MRR [cm^3]
1	40	0.1	449.25
2	60	0.1	214.54
3	80	0.1	93.66
4	40	0.15	440.01
5	60	0.15	77.01
6	80	0.15	40.16
7	40	0.2	453.67
8	60	0.2	75.26
9	80	0.2	20.45

The replicate plot in Figure 58 allows for a quick raw data inspection by showing the variation in results for all experiments. The plot is used to predict the variation present in the results on an overview level. The ideal outcome is that the variability of repeated experiments is much less than the overall variability. Experiments deviating significantly from the others should be checked. This specific investigation did not include any repeated experiments which could show variability, therefore limiting the impact of the replicate plot.

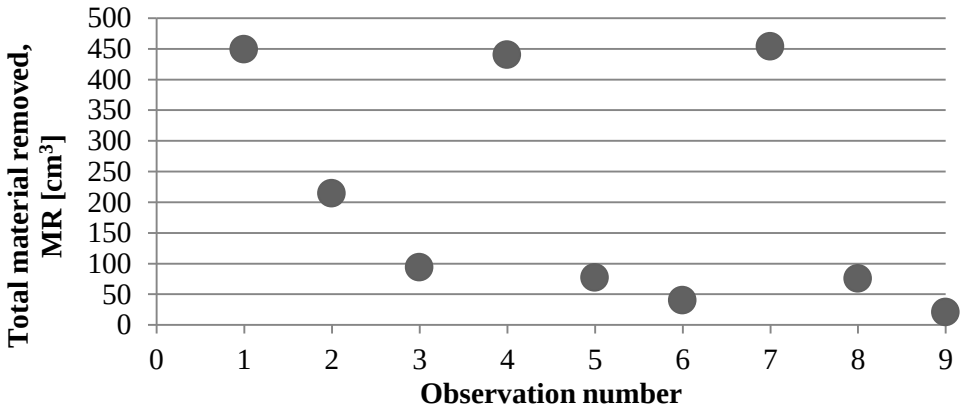

Figure 58: Repricate plot of total material removed

The response distribution in Figure 59 shows the shape of the experimental results. The ideal distribution is a bell-shaped normal distribution. A proper estimate of the distribution requires a minimum of 11 observations; as this investigation only constitutes nine observations, it is not complete. It does, however, show that even with two additional observations, the distribution would not show a bell shaped curve. In general, normally distributed responses will give better model estimates and statistics. Because this investigation does not meet the sample size requirements, no further analysis of the response distribution can be conducted.

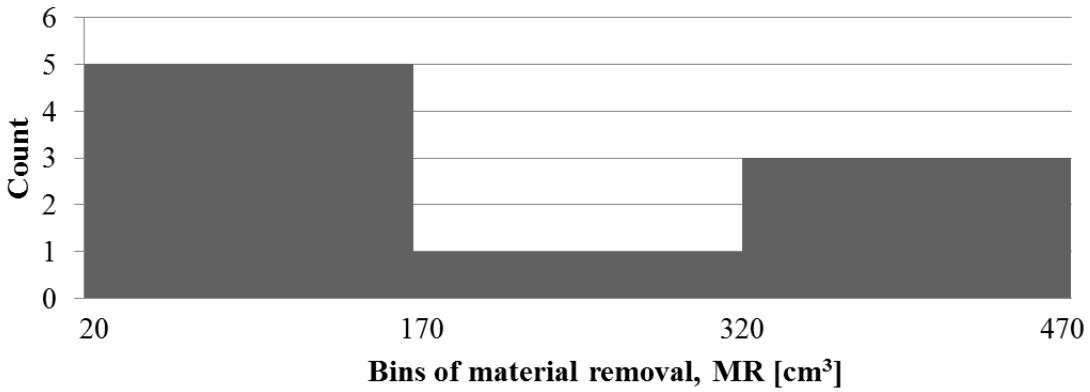

Figure 59: Response distribution once data is placed in bins

The summary of fit encapsulates the basic model statistics into a single diagram. Each of these values is evaluated between one and zero, with one being a perfect fit. Ideally, model validity and reproducibility are also included, but these statistics require a minimum of 11 data points and repeated experiments. The coefficient of determination (R^2) is used to determine how the data fits the statistical model. This investigation shows an R^2 value of 0.85, which shows a relatively good model fit to the regression line. A good R^2 value in itself is not sufficient to predict a good model. It is possible to have a high R^2 value but have a bad model. This is especially true when the reproducibility or model validity statistics are poor, which is not available in this model.

The predictive squared correlation coefficient (Q^2) is the percent of variation of the response predicted by the model according to cross validation. Q^2 is related to how well the model predicts new data. A useful model should have a large Q^2, as Q^2 shows and estimates the future prediction precision. In a

model with a good R^2, and moderate model validity with a design with many degrees of freedom, it is possible to have a poor Q^2 due to insignificant terms in the model. Q^2 should be greater than 0.1 for a significant model and greater than 0.5 for a good model. This model exhibits a Q^2 of 0.71 which shows relatively good repeatability. The model fit is therefore adequate for the R^2 and Q^2 values, but incomplete owing to a lack of model validity and reproducibility.

The coefficient plot exhibited in Figure 60 displays the regression coefficients with confidence intervals. For process factors, the effect plot displays the change in the response when a factor varies from its low level to its high level when all other factors are kept at their averages. As the coefficients are the change in the response when the factors vary from the average to the high level, the effects are twice the coefficients. By default the coefficient plot shows coefficients relating to scaled and cantered variables which make the coefficients comparable. The coefficient is significant (different from the noise) when the confidence interval does not cross zero.

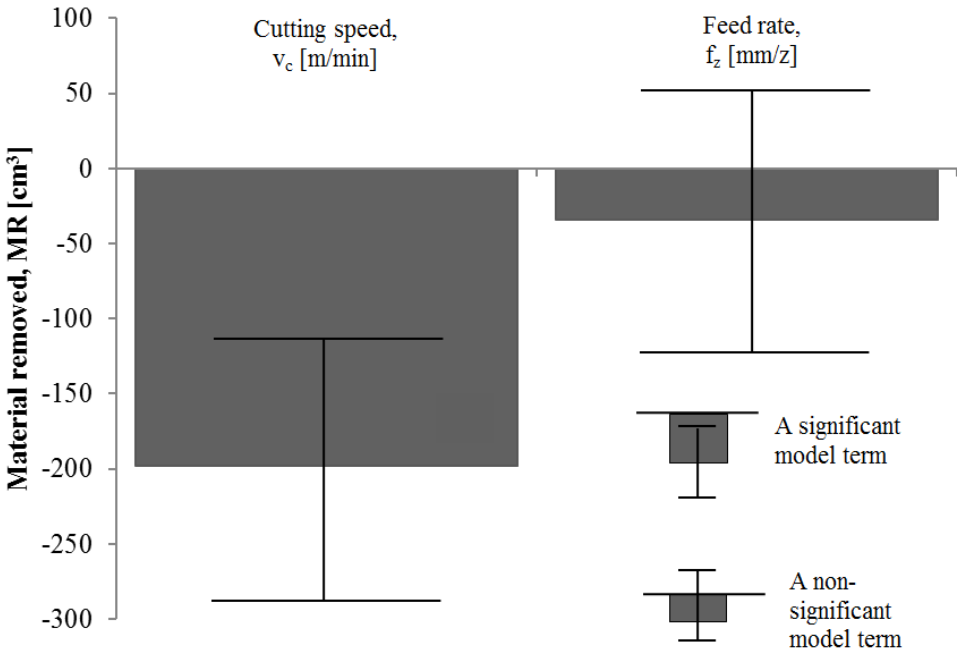

Figure 60: Coefficient plot comparing the effect of the two indipendant variables Cutting speed, v_c [m/min] and feed rate, f_z [mm/z]

In this particular investigation, cutting speed has the most substantial effect on total material removed. This was observed in experimentation and is also verified in the coefficient plot in Figure 60. In terms of percentages, increasing cutting speed accounts for 85% of the reduction in total material removal. On the other hand, increasing feed rate accounts for the remaining 15% reduction in total material removal. Cutting speed is therefore the significant model factor in this particular case. This is possibly as a result of the high degree of notching experienced at high cutting speeds, which accelerates tool wear. At the lowest cutting speed, tool wear is limited to uniform flank wear and show similar amounts of material removal regardless of cutting feed. The varying degree of effect that feed rate has on the model is a large contributor to why the model is not accurate in predicting future trends. At

high cutting speeds, the effect of feed rate on total wear is more prominent, and at low cutting speeds the effect of feed rate is negligible. However, according to the coefficient plot, the effect of feed rate is constant regardless of cutting speed, which is not the case in reality.

Figure 61 illustrates the observed versus predicted values according to the regression analysis. With a good model, all the points will fall on the 1:1 line. With less good models, the points are scattered around the 1:1 line. Figure 61 falls into the latter category and the observed versus predicted plot is less than ideal, although rough estimations can be made with the model if a high degree of tolerance is awarded. What is especially incorrect is the predicted removal rate of observation #9, as a negative removal is not possible. This is further incorrectly shown in the 3D response contour plot below.

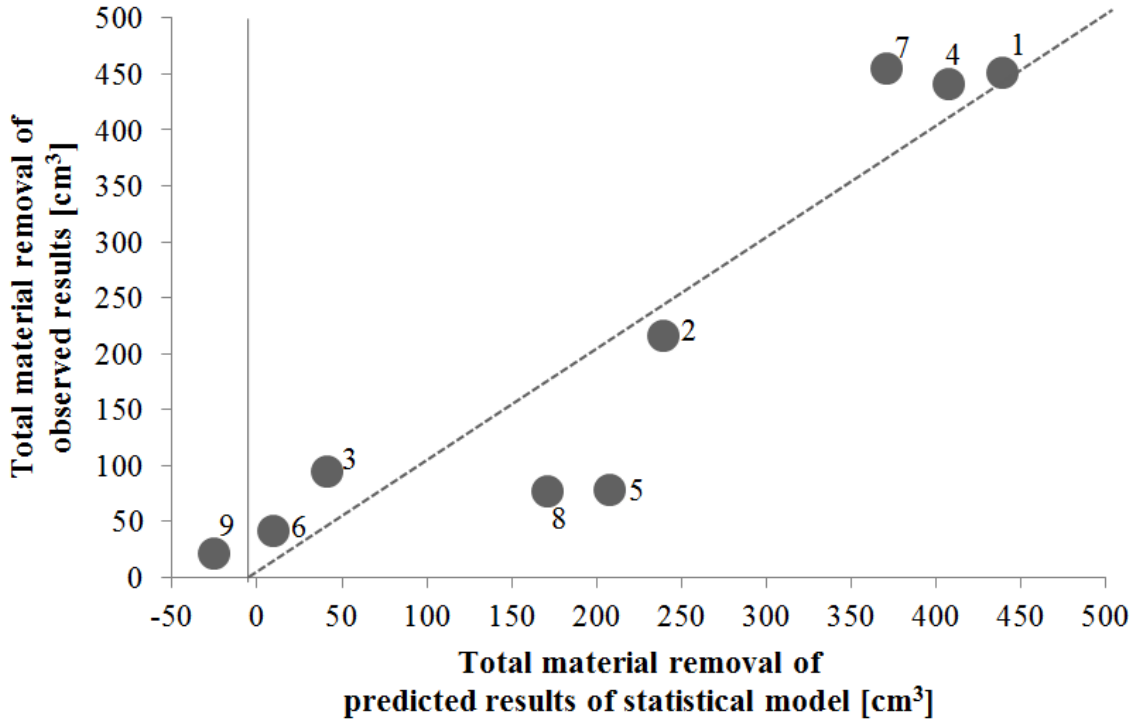

Figure 61: Observed data versus predicted regression plot as determined by the statistical model

Figure 62 illustrates the three dimensional response contour plot for the predicted model. Contour plots display the three dimensional relationship in two dimensions. The x- and y-factors (predictors) are plotted on the x- and y-scales respectively, and response values are represented by contours. In the case above, a desirable response (total material removed) can be selected from the colour axis on the right hand side. Thereafter a corresponding set of cutting speed and cutting feed parameters can be determined from the x- and y-axes. From the range of identified cutting parameters, simple calculations can then determine the most adequate cutting speed and cutting feed parameters for a specific goal. That goal can range from maximum material removal, minimum cost, to minimum cutting time.

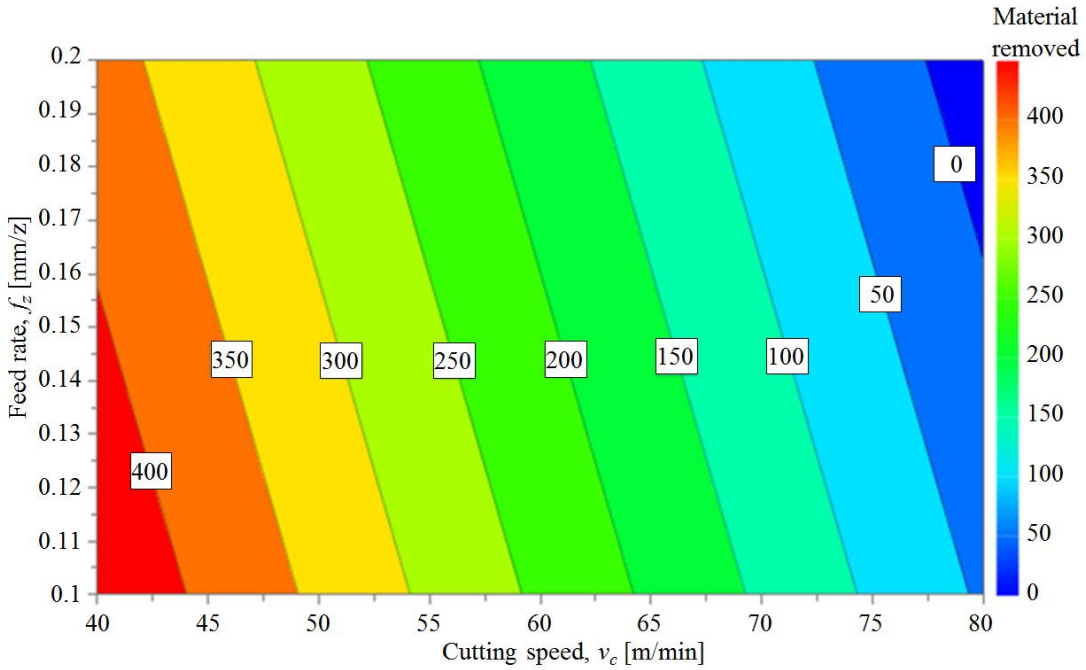

Figure 62: 3D response contour plot for the predicted model (material removed) as a function of cutting speed, v_c [m/min] and cutting feed, f_z [mm/z]

In conclusion, the model above provides deeper insight into the underlying statistics of the experimentation results. As not all cutting parameters experienced tool failure, some assumptions had to be made in order to acquire functional data. This will decrease the model validity. However, the underlying results of the statistical analysis are similar to the observed results. Cutting speed has a much larger effect on total material removal than cutting feed. Nevertheless, the resulting regression analysis did prove to be unsatisfactory and does not adequately reflect the observations of the experimentation. This can possibly be ascribed to cutting feed having a negligible effect on total material removed at low cutting speeds, and a relatively higher effect at higher cutting speeds. This skews the results of the regression and prevents the accurate use of a simple linear regression.

4.6.5. The effect of repeated heat-treating

Instead of the thermo-mechanical manner in which titanium is normally formed during hot rolling, this study removed alpha case which was formed in a purely thermal manner. Also, alpha case was only removed on two of the surfaces of the heat-treated blocks. The alpha case on the remainder of the sides was not removed before additional heat-treatment took place. These surfaces were therefore repeatedly heat-treated in the process of growing new alpha case on recently machined surfaces. In total, each titanium block experienced nine heat-treatment cycles. The surfaces that did not experience machining in order to remove the alpha case layer, should therefore exhibit excessive alpha case formation as depicted in Figure 63.

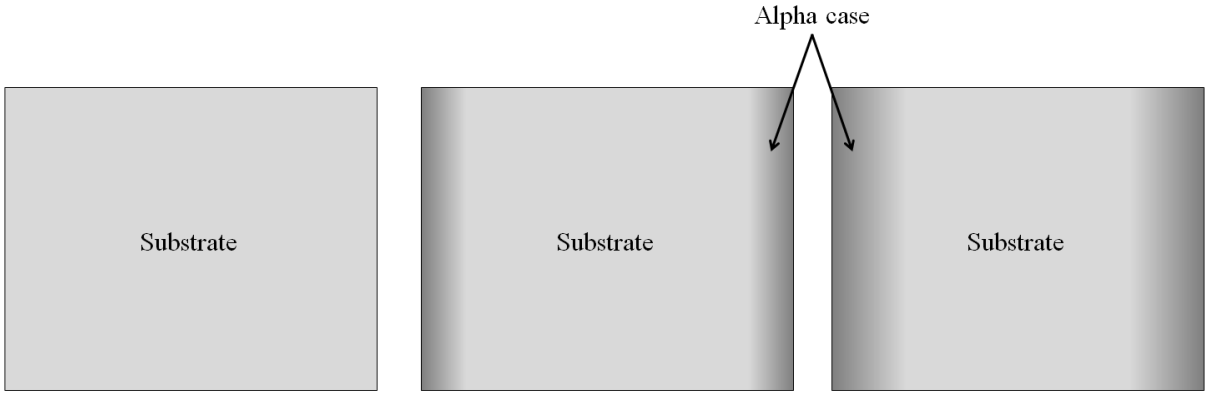

Figure 63: Alpha case formation for repeated heat-treatment whereby (a) represents a yet untreated sample (b) after initial heat-treatment alpha case has formed (c) after a number of heat-treatment cycles the alpha case depth will reach its maximum

Offcut samples were heat-treated along with the primary titanium samples in anticipation of this phenomenon. These samples were used to determine the extent of excessive alpha case formation brought on by the continuous heat-treatment, and to determine if the excessive alpha case formation has any effect on the sample hardness, or depth of hardness increase. After the final heat-treatment cycle, a small sample is cut from the offcut sample via electrical discharge machining. As with previous hardness measurements; the sample is mounted in resin and polished in the same manner as described in section 3.1. The sample is subjected to the same hardness testing regiment as before using the same equipment. The resulting hardness profile is illustrated in Figure 64. It illustrates the hardness of a sample undergoing a single heat-treatment cycle, compared to the hardness of a sample undergoing multiple heat-treatment cycles.

From Figure 64 it is clear that there is no significant variation in hardness experienced by the two samples. The maximum singular hardness indentation of both samples is relatively the same (912 HV and 916 HV for single and multiple heat-treatment cycles respectively). Hardness equilibrium is reached at around 450 μm from the sample edge for both samples. The only difference between the samples (one sample undergoing a single heat treatment cycle, one sample undergoing nine heat treatment cycles) is not in hardness itself, but in the penetration, or depth, of the hardening effect. Multiple heat-treatment cycles slightly increased the depth of hardness penetration at some depths. In other words, hardness measurements taken from the sample that experienced multiple heat-treatment cycles is slightly harder than a measurement of the singularly heat-treated sample. This is the case even though the measurements are taken the same distance from the edge.

The significant increase in time exposure could allow for additional oxygen diffusion into the sample. Further analysis would be needed to settle the matter. An alternative possibility is that a slightly higher furnace temperature resulted in the increased oxidation. Figure 35 in section 4.1.2 determined that the heat-treated samples experiencing higher temperatures, showed significant increase in hardness compared to samples at lower temperatures. This shows that at the exposure temperature has

a large influence on alpha case formation for the short time periods that these samples are heat-treated. This may be the reason for the increased hardness in the sample experiencing multiple heat-treated in Figure 64. One of the multitudes of heat-treated cycles may have resulted in a slightly higher furnace temperature, which may have accelerated oxidation.

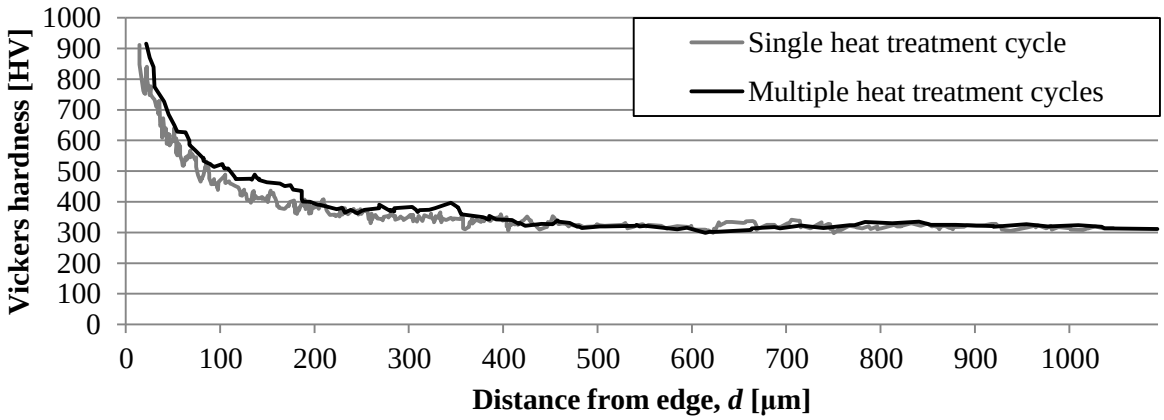

Figure 64: Hardness values measured from sample edge comparing a single heat-treatment cycle with multiple heat-treatment cycles

From this analysis it can be concluded that the multiple heat-treatment cycles did not significantly influence the alpha case layer hardness. As a result, the machinability of the alpha case layer does not alter significantly with each heat-treatment cycle.

4.7. Deeper carbide insert analysis

Stereoscopic microscopy of the carbide inserts was performed in order to analyse wear and to determine mode of failure. Further analysis of the carbide inserts was also performed in order to study additional effects. Inserts were cleansed with ethanol and the worn flank faces of selected inserts were subjected to SEM (ZEISS EVO MA15VP) for further imaging and to study composition.

Figure 65 represents a worn insert that did not exhibit any significant notching or chipping when observed with stereoscopic microscopy. Instead, the carbide insert experienced gradual flank wear similar to traditional titanium machining. This type of wear is for this investigation only experienced at the lowest cutting speed v_c = 40 m/min, regardless of feed rate. The numbered blocks from one to five in Figure 65, represent areas selected to undergo energy-dispersive X-ray spectroscopy (EDX) analysis over the area of the square. The five areas were selected based on their different appearance. A summary of the weight percentages of the five selected areas are given in Table 8.

The first area selected is right on the cutting edge, in a portion directly exposed to the extreme forces of machining. As is visible in Table 8, a high quantity of tungsten is present which is only possible if the coating has been removed from the cutting edge, and the substrate material is exposed to the harsh environment of machining. The second most abundant element is titanium. Both TiN and TiAlN coatings contain high levels of titanium, but it appears as though the coatings have been removed in this area, as evidenced by the high tungsten quantity. Furthermore, low levels of aluminium and

vanadium are also present. An alternative possibility is that titanium from the workpiece has been deposited on to the carbide edge through adhesive wear. The titanium present in the measurement is therefore a consequence of the workpiece material Ti6Al4V being deposited onto the carbide edge and not the titanium in the coating.

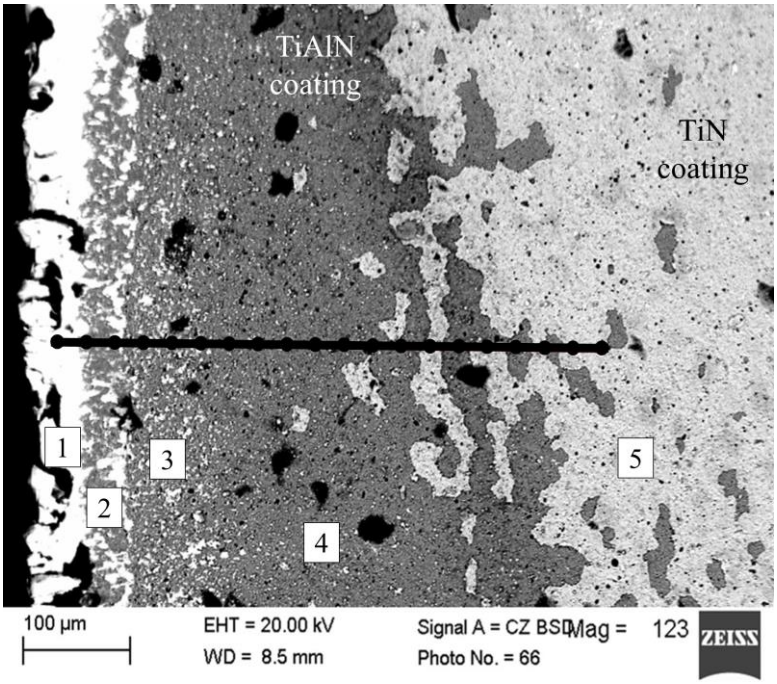

Figure 65: SEM of carbide edge flank wear at v_c = 40 m/min and f_z = 0.2 mm/z, showing five points of measure used the area composition analysis of Table 8, and 20 points in a linear line used in compositional analysis in Figure 66

Area number two is selected because of what appears to be the coating deposited with titanium onto the carbide edge through adhesion. The specific area selected is limited purely to the TiAlN coating in order to determine if there is significant difference in composition close to the edge, as compared to the coating further from the edge. These results of observation number two, compared to the observations in number three and four show no significant change in coating composition as distance from the edge is increased. Coating adhesion to the underlying material is therefore not diminished over time. Instead the coating adheres to the carbide substrate until it is completely removed. This is not the case with the top most TiN coating, which is at some places readily removed from the carbide edge up to 500 µm from the carbide edge.

Table 8: Compositional analysis of numbered areas represented in Figure 65

	Weight percentage of element [wt.%]						
Spectrum	**Aluminium**	**Titanium**	**Vanadium**	**Cobalt**	**Tungsten**	**Carbon**	**Nitrogen**
1	3.57	28.82	1.49	8.46	44.53	2.86	10.27
2	35.00	50.39	0.66	0.23	0.00	1.32	12.40
3	34.24	51.35	0.46	0.00	0.37	1.61	11.97
4	35.34	51.12	0.34	0.00	0.68	1.63	10.89
5	16.72	66.90	0.00	0.00	0.58	1.16	14.64

The final compositional area analysis is executed on the topmost TiN coating. It appears to exhibit slightly higher quantities of nitrogen and titanium, and a high a level of aluminium which is not listed

as a property of the coating. This may be owing to the thin nature (± 7 µm) of the coating, in that some aluminium is picked up in the spectrum. Alternatively, some aluminium may have diffused into the topmost coating during its manufacture.

Apart from certain surface areas being measured in order to determine composition, an array of points was also selected to determine the compositional difference as distance in a linear direction is increased. As far as accuracy is concerned, this is less reliable as only a certain spot is analysed instead of a larger area; however, it will still result in useful data. The array of points is represented by the red line in Figure 65, where the 20 spots along that line are analysed. The resulting compositions are given in Figure 66.

Initially, a high quantity of titanium is picked up, and aluminium and vanadium levels are also similar to what is expected in the workpiece alloy Ti6Al4V. This further proves that material from the workpiece is deposited on to the carbide edge. No tungsten or cobalt is measured, which only indicates that the specific area of measure is completely concealed by the adhered titanium workpiece material. Moving away from the edge and on to the TiAlN coating decreases titanium content, and an increase in aluminium and nitrogen is experienced.

At only the third point in the series does the composition seems to have normalised. For the remainder of the array of data points the resulting composition remains constant. Trace amounts of cobalt, tungsten and carbon are picked up throughout the array of points. Regardless of the fact that the final two data points cross into the topmost TiN coating, composition is maintained at similar levels as before the coating. It may be possible that machining has an eroding effect on the topmost coating, and that further away from the machining operation the composition is closer to what is typically expected.

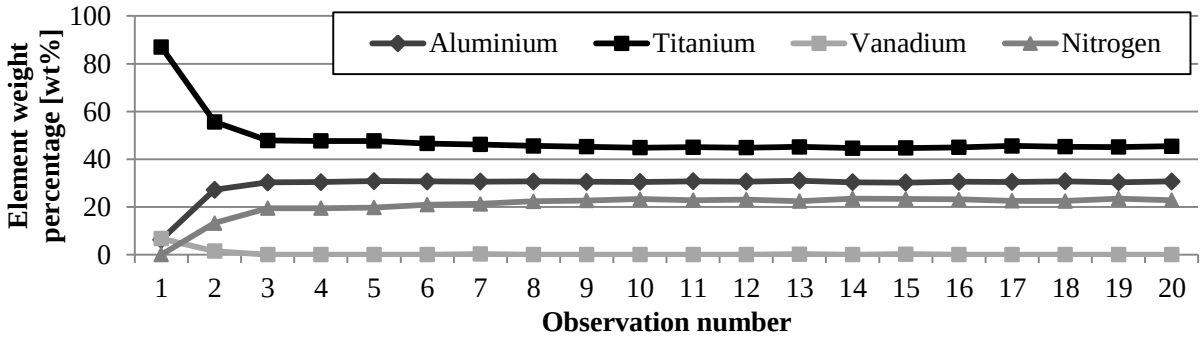

Figure 66: Compositional analysis of array of data points represented by the red line in Figure 65

A worn carbide insert edge which experienced notching as the primary mode of wear looks similar to Figure 67, when subjected to SEM. Uniform flank wear is replaced with a chip in the region of the cutting edge adjacent to the workpiece surface, which is large enough to constitute tool failure.

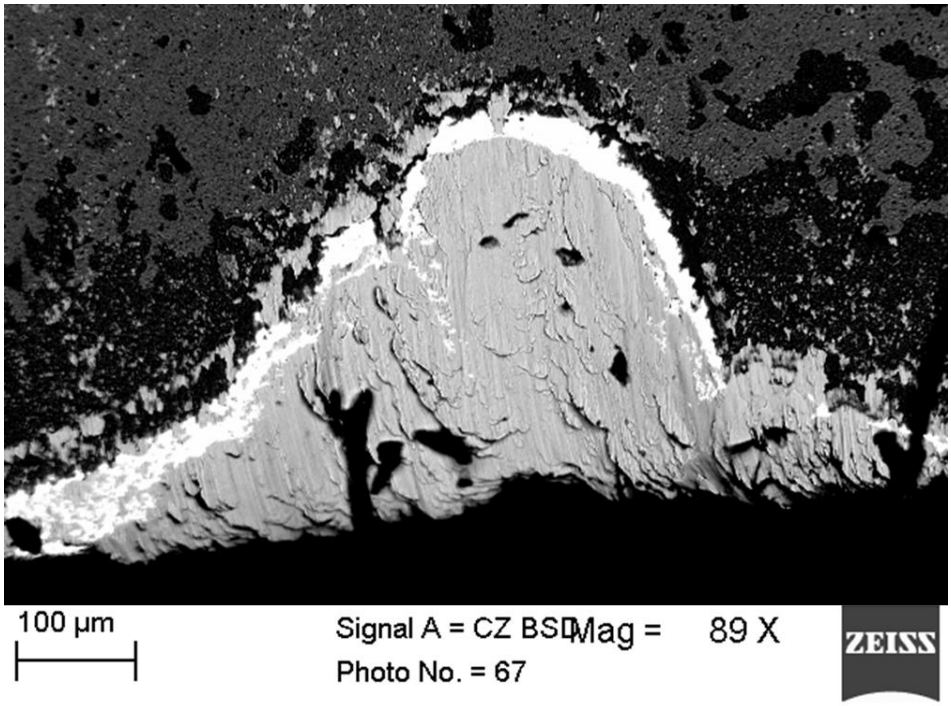

Figure 67: Scanning electron microscopy of carbide edge notch wear at v_c = 60 m/min and f_z = 0.15 mm/z, showing a near catastrophic chip in the notch region adjacent to the workpiece surface

Figure 68, similar to Figure 65, depict the array of points to be analysed for composition weight percentages. The results are illustrated in Figure 69.

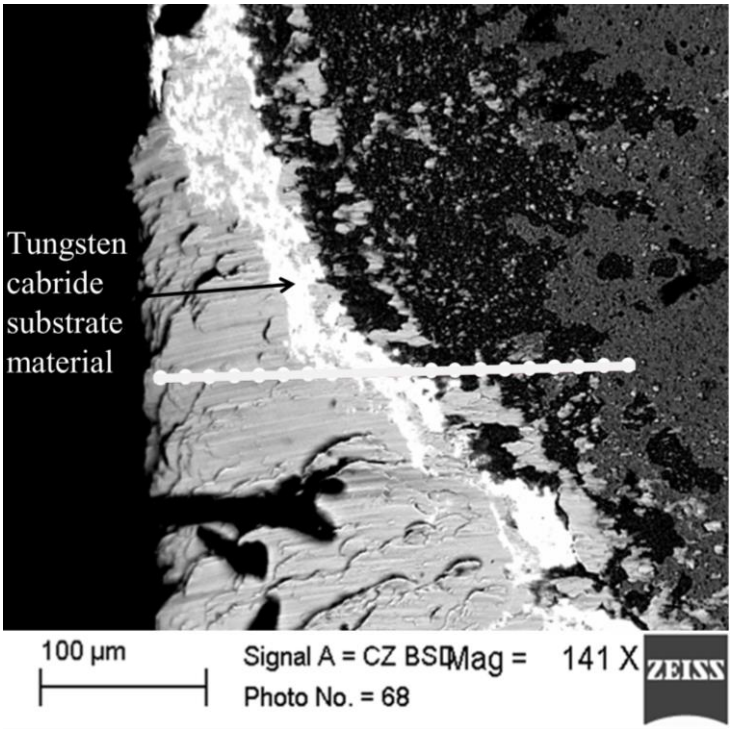

Figure 68: SEM of a specific area above the notch wear at v_c = 60 m/min and f_z = 0.15 mm/z with the line indicating the 20 points of measure in a linear line for compositional analysis dipicted in Figure 69

The array of data points begins on a portion of the chip close to the carbide edge, and moves towards the interior of the tool until it reaches the topmost TiN coating. As with the previous sample in Figure 65, the first couple of data points exhibit high quantities of titanium along with vanadium and

aluminium. This is constant with Ti6Al4V workpiece material being deposited onto the carbide edge. Even though the chip completely exposes the tungsten carbide substrate, little or no tungsten or cobalt is measured. For the first six observations this remains constant, likely owing to the entire chip being deposited with the workpiece material through adhesion. Thereafter an elevated amount of tungsten and cobalt are measured and a drop in titanium and vanadium is experienced. This is evident for the next five measurements, which indicates that the coating has therefore been eroded from this area and titanium adhesion has not yet taken place. The tungsten-rich area represents the interior tungsten carbide cutting tool and on Figure 68, this region is represented by the white area in the centre of the red line indicating the array of data points. Moving past this area and into the darker coating yields high quantities of titanium, nitrogen and aluminium that represent the TiAlN coating. The final data point is positioned on the topmost TiN coating and a slight increase in nitrogen is experienced along with a decrease in aluminium.

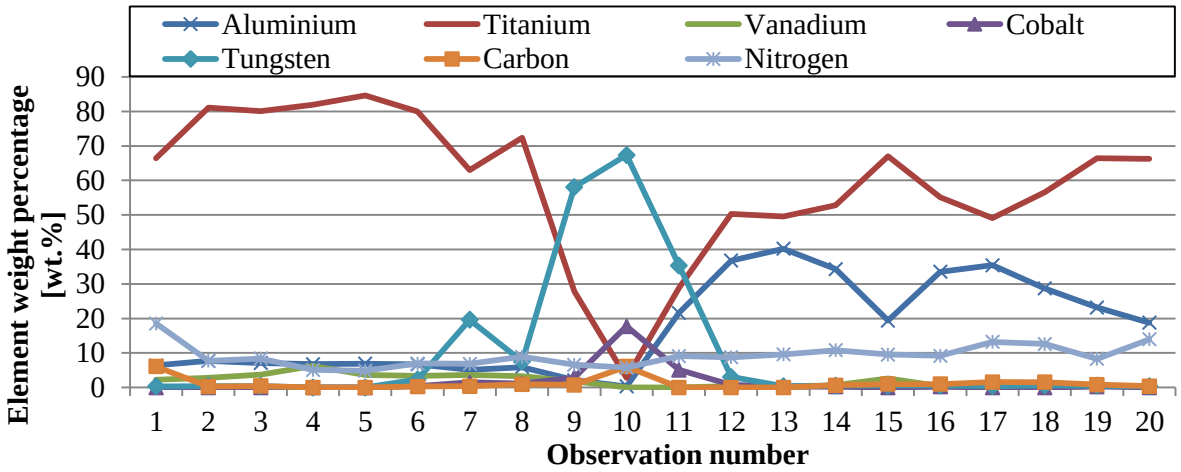

Figure 69: Compositional analysis of array of data points represented by the red line in Figure 68

What should be specifically noted from the deposited or adhered titanium is that it is readily adhered to what appears to be the tungsten carbide substrate. Vanadium is only present in the workpiece material and can therefore be used as an indicator for when adhesion of the workpiece material has taken place. In Figure 68, for the entire length of the measurements which were taken on the chip, high levels of titanium and an elevated level of vanadium are measured. This indicates that the entire chip is likely covered with a titanium workpiece adhesion layer owing to titanium's high chemical reactivity and affinity towards the tungsten carbide substrate.

4.8. Completion of primary objective

There are two objectives for this study. Up to now, the primary objective has been investigated: Determining the feasibility of alpha case machining removal of hot rolled titanium by using indexable tungsten carbide cutters. Firstly, the physical and chemical properties of heat-treated titanium were investigated in section 4.1. Next, machining removal was based on the background experiments and machining removal was executed. It was determined that machining successfully removes alpha case

from heat-treated titanium samples in section 4.4. At high cutting speeds, the tungsten carbide cutting inserts experienced high degrees of notching in the region adjacent to the workpiece surface. At lower cutting speeds, notching was replaced with gradual, more common flank wear. This type of wear resulted in longer tool life, which greatly increases the total amount of material removal. At low cutting speeds, total material removal is similar to what is experienced in research literature. The feasibility of machining removal of alpha case using indexable tungsten carbide cutters has therefore been confirmed for low cutting speeds. At high cutting speeds the predominant type of wear was chipping in the notch region, and at low cutting speeds more traditional flank wear was experienced. Adhesion of titanium workpiece material was also present no matter the type of wear experienced.

4.9. Cost model

Following the confirmation of the feasibility of machining removal of alpha case from hot rolled titanium using indexable tungsten carbide cutters, the secondary objective must be investigated. The secondary objective involves investigating the scope of feasibility in the context of the South African manufacturing industry. In short, can machining removal realistically be applied to either small batch manufacturing, large scale implementation, or not at all. This can be determined by identifying the most economical machining technique, and comparing this with alpha case removal through chemical milling. To follow is a basic analysis of the costs involved in titanium alpha case removal by means of machining. This is by no means a comprehensive analysis, and only serves as an illustration on which further analysis could build.

4.9.1. Cost calculations of alpha case titanium machining removal

From the experiments performed in the alpha case removal investigation, tool life data has been acquired. This tool life data can be used to calculate the total machine time and tooling cost which will then yield a price per removal of a certain volume of material. Table 9 and Table 10 summarise the resulting price per unit removal of a certain amount of material (ZAR/cm^3). For the tool life calculation of cutting at cutting speed v_c = 40 m/min and feed rate f_z = 0.15 mm/z, the near catastrophic chip was omitted. As has been mentioned, this is only an analysis of the most basic costs associated with machining removal.

Table 9: Machine time and total material removed for 10 inserts of 16 edges each

Cutting parameters, v_c [m/min], f_z [mm/z]	Total machine time, t [hours] per 10 inserts	Total material removed, MR [cm^3] per 10 inserts	Total machine cost [ZAR 500/hour]
80, 0.2	0.42	545	212
80, 0.15	1.11	1071	556
60, 0.2	2.09	2006	1 042
60, 0.15	2.85	2053	1 422
80, 0.1	3.89	2497	1 945
60, 0.1	11.89	5720	5 944
40, 0.15	24.38	11733	12192
40, 0.2	18.84	12097	9 422
40, 0.1	37.32	11979	18 660

Table 10: Cost calculations for cutting tools displaying individual cost for the removal of MR = 1 cm^3

Cutting parameters, v_c [m/min], f_z [mm/z]	Machine cost per cubic centimetre [ZAR/cm^3]	Tooling cost per [ZAR/cm^3], R2500 per 10 inserts	Cost [ZAR/cm^3]
80, 0.2	0.39	4.58	4.97
80, 0.15	0.52	2.33	2.85
60, 0.2	0.52	1.25	1.77
60, 0.15	0.69	1.22	1.91
80, 0.1	0.78	1.00	1.78
60, 0.1	1.04	0.44	1.48
40, 0.15	1.04	0.21	1.25
40, 0.2	0.78	0.21	0.99
40, 0.1	1.56	0.21	1.77

Table 9 and Table 10 are arranged by ascending projected tool life across the various cutting parameters. They also provide numeric values to the information depicted in Figure 70. A full explanation of the cost calculation can be found in Appendix C. The most economical cutting condition is at v_c = 40 m/min and f_z = 0.2 mm/z. This yields a projected tool life of t = 42.40 minutes after which MR = 453.67 cm^3 of material has been removed. Total cost per cubic centimetre of material removal is calculated at R0.99/cm^3.

Figure 70 provides a visual representation of the results obtained in Table 9 and Table 10. It describes the unit cost curve calculated for the removal of one cubic centimetre of material for each cutting condition. It also shows the machine cost per cubic centimetre, tooling cost per cubic centimetre, and the total cost per cubic centimetre. Once more, the lowest cost of operation can be found at the lowest point in the cost curve. This is located at the second longest machining tool life which is obtained at cutting parameters of v_c = 40 m/min and f_z = 0.2 mm/z.

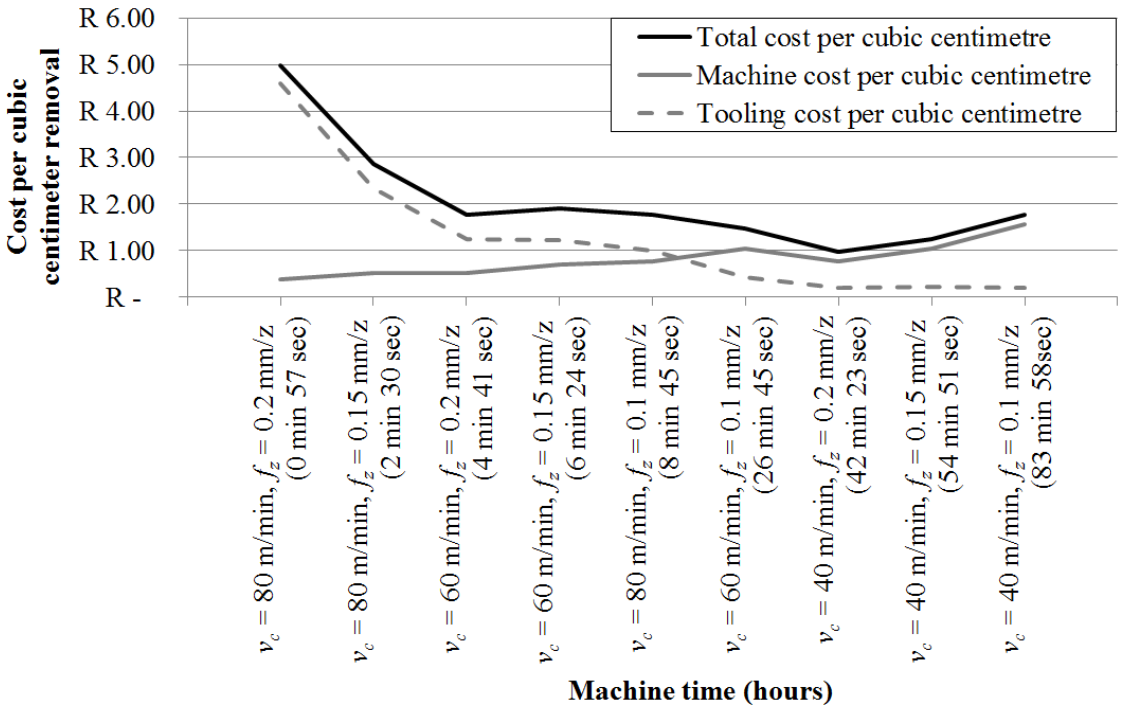

Figure 70: Basic estimation of the minimum cost curve for the removal of one cubic centimetre of material through milling. For illustration purposes only

There are some considerations to be noted: Firstly, this is only an abbreviated theoretical calculation and by no means represents the true cost associated with the operating cost. The material removal rate is calculated based on the machining parameters and cutter dimensions. Furthermore, tool life is not established by normal machining experimentation guidelines, owing to the very short intervals of machining. Ideally, cutting time should be measured in order to verify the duration. Calculations are thereafter based on the measured machining time and not on the predicted or calculated time. However, owing to the brief and stop-start nature of the experiments, the longest cutting operation is calculated to take 100 seconds, and the most aggressive cutting operation is calculated to take only 25 seconds per machining trial. It was therefore decided that the accuracy of time measurements would have been difficult to establish and was therefore omitted. However, calculated machining time and actual machining time is very similar when utilising only three-axis CNC milling.

Moreover, apart from the fact that only theoretical machining time is being utilised, other omissions were also made. Internal tool travel, the time that the cutting tool is not engaged in the workpiece material, is omitted. Furthermore, no approximation for tool- workpiece- and machine handling time has been made. These factors will further increase machine time, lower productivity and ultimately increase cost. The cost estimation in Table 9, Table 10 and Figure 70, is therefore the lowest bound cost that can possibly be attained. Realistically, cost per cubic centimetre of material removal would be higher than estimated. The only estimation which may accurately describe cost per cubic centimetre material removal, is tooling cost. Tooling cost is independent of material handling time and only dependent on extrapolated tool wear measurements. Although some assumptions are made regarding a fixed tool wear curve, tool life is based on more accurate estimations and therefore more closely represent the true cost as compared to machine cost.

4.9.2. Break even analysis

Having identified the most economical alpha case machining removal technique, the specific method must be compared with chemical milling. As no chemical milling facilities are present in South Africa, information on the process is limited and hard to come by. Thorough investigation is needed in order to accurately compare the costs associated with the two processes which would accurately reflect the South African market space. As the cost comparison is a secondary objective, only the most basic comparison of alpha case machining removal will be made with chemical milling in the context of the South African marketspace.

For machining removal of alpha case to become a viable alternative to chemical milling in South Africa, it must be profitable. In favour for going the route of machining removal is the fact that machine shops are already available in South Africa. With only minor technological and intellectual advances, titanium machining competency can be obtained by the machine shops if it is not already available. Furthermore, the purchase of additional milling equipment, to expand alpha case removal

capabilities, is easily accomplished. The supplementary milling equipment can additionally be used for further finishing of titanium components, or be used for completely different tasks. The equipment is therefore multi-purposed. The majority of the expenses associated with machining removal will be limited to consumables and labour (variable cost). There is no requirement for high capital expenditure and start-up costs for new facilities. Furthermore, no training, safety equipment or additional safety requirements are necessary. Machining using the prescribed guidelines can start immediately as soon as the need arises. The costs of machining removal are therefore illustrated in Figure 71 (a).

There are no chemical milling facilities currently in South Africa. Such facilities therefore, first need to be constructed. Additionally, equipment must be sourced, disposal techniques for used acids must be determined, and the skills and practical know-how required for chemical milling is also absent in South Africa. These would need to be sourced from outside our borders, adding to the eventual cost. Furthermore, extensive training would be required for new labourers (with special emphasis on safety). The requirements listed above must first be met at high initial capital investment and the milling facilities will take a long period of time to fully establish. However, in favour of chemical milling is its low variable and maintenance cost. Once the facilities are up and running, and a constant flow of projects is secured, chemical milling becomes a viable option. The relation between the required capital investment and its variable cost is depicted in Figure 71 (b).

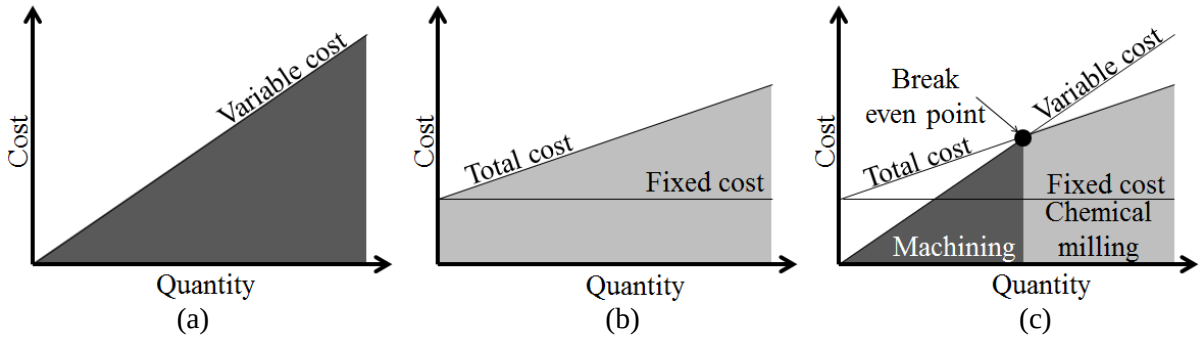

Figure 71: Hypothesised cost comparison of (a) machining removal, (b) chemical milling and (c) combined comparison of machining removal and chemical milling for small, medium and large theoretical quantities. For illustrative purposes only

Owing to the costly nature of the initial capital investment required for chemical milling, it is not deemed a viable option for low to medium quantities. Only at high quantities can the cost allocated to fixed costs be recuperated through normal operation. The question, therefore, is where and when exactly the profitability of chemical milling becomes apparent. True and long term profitability of chemical milling is only possible when the variable cost of machining becomes more expensive than the combined fixed and variable cost of chemical milling. In other words, at low to medium quantities, machining remains the most economical option. However, at medium to high quantities, chemical milling could become more attractive financially. This break-even schematic is shown in Figure 71 (c).

The risks of chemical milling are great as well. The solutions used for chemical milling are highly acidic and therefore highly dangerous. Safety of the labourers and safety of the equipment must be of primary concern. Medical equipment and trained medical personnel must be readily available for emergencies. Solutions must be properly stored in sealed containers before and after use. Used solutions must be properly processed and disposed of in a manner that will endanger neither the operators nor the environment. Finally, proper procedures should be in place in case of a chemical spill, either at the facilities or in the transportation of the chemicals. An extensive cost/benefit analysis should be completed in order to determine if at a specific profitability, the risk of chemical milling might not outweigh the possible benefits.

5. Conclusion

This study had two objectives; the first was to establish the feasibility of alpha case removal of hot rolled titanium by method of machining using indexable tungsten carbide cutters. The second was to determine the scope of feasibility in the context of the South African manufacturing industry.

Groundwork experiments subjected Ti6Al4V samples to isothermal heat-treatment at temperatures above T = 800°C in ambient air and atmospheric pressure. This was done in order to study the effects of oxidation on hot rolled titanium. Alpha case formation close to the edge exhibited hardness comparable to high speed steel. The hardness returned to normal Ti6Al4V values 450 μm from the sample edge. Furthermore, the distance of alpha case formation as measured microscopically, was roughly half the distance of oxidation as determined by microhardness testing. Finally, the hardened alpha case layer also experienced increased brittleness.

The heat-treated samples underwent scanning electron microscopy analysis which revealed a significant change in microstructure close to the edge. As oxygen is an alpha stabiliser, oxygen ingress into the substrate material increases the size of alpha phase grains. The increasing quantities of alpha stabiliser (oxygen) caused titanium to be extracted from the beta phase and used to augment the growth of the alpha phase. The beta phase close to the edge therefore suffered, becoming smaller and less frequent. Further from the edge, the alpha grains returned to their normal size and beta grains became larger and more frequent, returning to the natural state of an alpha beta alloy.

In terms of the composition of the heat-treated sample, alpha grains close to the edge experienced a slight drop in titanium and aluminium weight percentage because of the significant increase in oxygen content, up to 16.7 wt.%. Close to the edge the beta phase experienced a significant drop in titanium weight percentage, and an equally significant increase in vanadium concentration. This is as a result of titanium being extracted from the beta grains, which increases the vanadium weight percentage. Vanadium is not extracted by the growing alpha phase on account of it being a beta stabiliser. It remains in the diminishing beta grains where concentration steadily increases as titanium is extracted.

The primary objective successfully removed alpha case through machining at all cutting conditions. This was verified by surface hardness testing which revealed a new machined surface with hardness comparable to that of traditionally recorded titanium alloys. The tungsten carbide indexable cutters readily removed the alpha case layer for all machining parameters. However, different wear rates and types were observed for differing cutting parameters. Machining resulted in severe notch wear in the region adjacent to the workpiece surface for high cutting speeds, leading to short tool life. More gradual flank wear was experienced at lower cutting speeds, which showed wear rates more commonly associated with titanium machining. At the lowest cutting speed (v_c = 40 m/min), identical wear rates were observed regardless of the feed rate (f_z) being used.

The length of the wear scar in the carbide cutters greatly exceeded the expected length at the specific depth of cut (a_p). This was ascribed to chipping in the notch region, which often extends well beyond the region of the cutting tool adjacent to the workpiece surface. SEM analysis of the tungsten carbide cutters yielded a degree of adhesion wear on the carbide edges. It also showed that the topmost TiN coating is readily removed in the machining operation, but that the lower TiAlN coating performs well. Statistical analysis of the results concluded that cutting speed had the largest effect on total tool wear (up to 85%) and that the effect of feed rate marked up the remaining 15%. This does however not take into account the varying effect that feed rate has at high cutting speeds compared to lower cutting speeds. The statistical model, as a result, does not adequately fit the observed data. Based on the above-mentioned results, it was concluded that within the current body of knowledge, alpha case machining removal with the use of indexable tungsten carbide cutters is feasible. For the most economical removal of alpha case it is advised to use low cutting speeds, with the highest possible feed rate in order to promote a longer tool life and reasonable material removal rates.

Following the confirmation of the primary objective, the secondary objective, an investigation into the scope of feasibility of alpha case removal through milling in a South African manufacturing industry, was pursued. A comparison was made between mechanical removal and chemical milling in terms of processes, cost, and equipment. This was by no means a comprehensive model and should not be taken as such. However, it did highlight the larger themes.

South Africa already has an established and competitive machining industry and the expansion of the industry to include alpha case machining removal would greatly expand downstream revenue. The cost comparison found that the high capital expenditure that new chemical milling facilities would entail makes it uneconomical for small batch production. This is especially true when considering the high safety and environmental concerns associated with chemical milling. Machining removal does not require high initial capital investment and is therefore viable for small batch production. At high production volumes however, machining removal will not make economic sense due to the high cost of tooling. Chemical milling is therefore a viable option at medium to high production volume over the long term. For this to be confirmed, a detailed analysis of the chemical milling start-up and running costs from a South African perspective would need to be conducted.

Future work should investigate making machining removal more economical, by achieving higher material removal rates. High cutting speeds lead to high wear rates which make it uneconomical. Experimentation should also be conducted on actual hot rolled titanium as mechanical deformation will influence the diffusion of oxygen and as a result the alpha case formation to what is investigated in this study. Experiments should also be conducted for longer periods of time instead of the stop-start nature of this investigation. Prolonged testing may yield different results that will more closely resemble what is experienced in industrial manufacturing.

References

Abdel-Aal, H., Nouari, M. & El Mansori, M., 2009. Influence of thermal conductivity on wear when machining titanium alloys. *Tribology International,* pp. 359-372.

Abdel-Aal, H., Nouari, M. & Mansori, M., 2008. The effect of thermal property degradation on wear of WC-CO inserts in dry cutting. *Wear,* pp. 1670-1679.

Abele, E. & Fröhlich, B., 2008. High Speed Milling of Titanium Alloys. *Advanges in Production Engineering & Management,* pp. 131-140.

Arrazola, P. et al., 2012. *Machining of Titanium Alloys Used in Aviation,* Mondragon: Mondragon University.

Arredondo, J., Colleary, B., Miskell, S. & Sweet, B., 2010. *Chemiclal Milling and the Removal of Alpha Case,* Worcester: Worchester Polytechnic Institute.

Arsecularatne, J., Zhang, L. & Montross, S., 2006. Wear and tool life of tungsten carbide, PCBN and PCD cutting tools. *International Journal of Machine Tools & Manufacture,* pp. 482-491.

Askeland, D., Fulay, P. & Wright, W., 2010. *The Science and Engineering of Materials.* s.l.:Cengage Learning.

Barcza, N., 2000. *Foresight mining and metallurgy report,* s.l.: Department of Science and Technology (South Africa).

Barnett-Ritcey, D., 2004. *High-speed Milling of Titanium and Gamma-Titanium Aluminide: An Experimental Investigation,* McMaster, Canada: Ph.D. Thesis, McMaster University.

Barry, J. et al., 2006. Application areas for PCBN materials. *Industrial Diamond Review,* 66(3), pp. 46-53.

Bawa, A. et al., 2013. *Review of the DST-NRF Centres of Excellence Programme,* s.l.: National Research Foundation.

Bedinger, G., 2015. *Titanium and Titanium Dioxide,* s.l.: U.S. Geological Survey, Mineral Commodity Summaries.

Boettinger, W. et al., 2000. Alpha Case Thickness Modeling in Investment Castings. *Metallurgical and Materials Transactions B,* pp. 1419-1427.

Boyer, R., Collings, E. & Welsch, G., 2007. *Materials Properties Handbook: Titanium Alloys.* Materials Park: ASM International.

Chandler, H., 1989. Machining of Reactive Metals. In: *ASM Handbook Volume 16: Machining.* s.l.:ASM International.

Chan, K., Koike, M., Johnson, B. & Okabe, T., 2008. Modeling of Alpha-Case Formation and Its Effects on the Mechanical Properties of Titanium Alloy Castings. *Metallurgical and Materials Transactions A*, pp. 171-180.

Che-Haron, C. & Jawaid, A., 2005. The effect of Machining on surface integrity of titanium alloy Ti-6% Al-4% V. *Journal of Material Processiong Technology*, pp. 188-192.

Choi, B.-J. & Kim, Y.-J., 2013. Effect of Reacted Compounds in Al2O3+Ti Investment Mold on Alpha-Case Formation for Ti Casting. *Metals and Materials International*, pp. 439-444.

Davies, J., 1997. *ASM Handbook Volume 16: Machining.* s.l.:ASM International.

De Bruyn, R., 2014. *Improving and implementing advanced milling techniques for the manufacture of selected titanium aerospace parts,* Stellenbosch: Stellenbosch University.

Dechezleprêtre, A. & Sato, M., 2014. *The impcats of environemental regulations on competitiveness,* London: Grantham Research Institute on Climate Change and the Environment.

Department of Science and Technology, 2000. *FORESIGHT SYNTHESIS REPORT: DAWN OF THE AFRICAN CENTURY,* Pretoria: Department of Science and Technology (South Africa).

Department of Water Affairs and Forestry, 1998. *Minimum requirements for the handeling, classification and disposal of hazardous waste,* Pretoria: Department of Water Affairs and Forestry.

Dimitrov, D., Conradie, P. & Oosthuizen, G., 2013. *A Process Planning Framework for Milling of Titanium Alloys.* Stellenbosch, COMA'13, pp. 209-215.

Donachie, M. J., 2000. *Titanium: a technical guide.* s.l.:ASM International (OH).

du Preez, W., 2014. *Beneficiation of South Africa's Titanium Resource A Long Term Vision is the Key to Success.* [Online] Available at: https://www.thedti.gov.za/parliament/2014/TiResource.pdf [Accessed 04 08 2015].

Du, H., Datta, P., Lewis, D. & Burnell-Gray, J., 1994. Air Oxidation Behaviour of Ti6Al4V Alloy Between 650 and 850°C. *Corrosion Science,* 36(4), pp. 631-642.

Ezugwu, E., 2005. Key improvements in the machining of difficult-to-cut aerospace superalloys. *International Journal of Machine Tools & Manufacture,* pp. 1353-1367.

Ezugwu, E., Bonney, J., Da Silva Rosemar, B. & Cakir, O., 2007. Surface integrity of finished turned Ti-6Al-4V alloy with PCD tools using conventional and high pressure coolant supplies. *International Journal of Machine Tools and Manufacture,* Volume 47, pp. 884-891.

Ezugwu, E., Bonney, J. & Yamane, Y., 2003. An overview of the machinability of aeroengine alloys. *Journal of Materials Processing Technology,* pp. 233-253.

Ezugwu, E. O., 2004. High speed machining of aero-engine alloys. *Journal of the Brazilian Society of Mechanical Sciences and Engineering.*

Ezugwu, E. & Wang, Z., 1997. Titanium alloys and their machinability - a review. *Journal of Material Processing Technology*, pp. 262-274.

Field, M., Kahles, J. & Koster, W., 1997. Surface Finish and Surface Integrity. In: *ASM International Volume 16: Machining.* s.l.:ASM International.

Flight Safety Foundation, 1998. *MD-88 Has Uncontained Engine Failure on Takeoff Roll Following Fan-Hub Fracture,* Alexandria: Flight Safety Foundation.

Frangini, A., Mignone, A. & De Riccardis, F., 1994. Various aspects of the air oxidation behaviour of a Ti6Al4V alloy at temperatures in the range 600-700C. *Journal of Materials Science*, pp. 714-720.

Gaddam, R., Sefer, B. & Pederson, R., 2013. *Study of alpha-case depth in Ti6Al2Sn4Zr2Mo and Ti6Al4V.* Luleå, IOP Publishing.

Gilbert, W., 1950. Economics of Machining. In: *Machining - Theory and Practice*. Ohio: American Society for Metals, pp. 465-485.

Goldstein, J. et al., 2003. *Scanning electron microscopy and x-ray microanalysis.* New York: Springer.

Grote, K.-H. & Antonsson, E., 2008. *Springer Handbook of Mechanical Engineering.* New York: Springer Science and Business Media.

Grzesik, W., 2003. Friction behaviour of heat isolating coatings in machining: mechanical, thermal and energy-based considerations. *International Journal of Machine Tools & Manufacture*, pp. 145-150.

Grzesik, W. & Nieslony, P., 2003. A computational approach to evaluate temperature and heat partition in machining with multilayer coated tools. *International Journal of Machine Tools & Manufacture,* pp. 1311-1317.

Grzesik, W. & Nieslony, P., 2004. Prediction of friction and heat flow in machining incorporating thermophysical properties of the coating–chip interface. *Wear,* pp. 108-117.

Guilin, Y., Nan, L., Yousheng, L. & Yining, W., 2007. The effects of different types of investments on the alpha-case layer of titanium castings. *The Journal of Prosthetic dentistry,* pp. 157-164.

Gurrappa, I. & Gogia, A., 2001. High performance coatings for titanium alloys to protect against oxidation. *Surface and Coatings Technology*, pp. 216-221.

Haynes, W. M., Lide, D. R. & Bruno, T. J., 2012. *CRC Handbook of Chemistry and Physics.* s.l.:CRC Press.

Henry, S. et al., 1995. *ASM Speciality Handbook. Tool materials.* United States of America: ASM international. The materials Information Society.

Hermle, 2008. *Hermle C40 The Dynamic Technical Data,* Gosheim: Hermle.

Hong, H., Riga, A. T., Cahoon, J. M. & Scott, C. G., 1993. *Machinability of steels and titanium alloys under lubrication.* San Francisco, Elsevier Sequoia, pp. 34-39.

Hong, S. Y. & Ding, Y., 2001. Cooling approaches and cutting temperatures in cryogenic machining of Ti6Al4V. *international journal of machining tools & manufacture design, research and application,* pp. 1417-1437.

International Organization for Standardization, 1989. *Tool life testing in milling - Part 1: Face milling,* Switzerland: International Organization for Standardization.

Isakov, D. E. & Ohlund, D., 2009. Tackling Titanium. *Cutting Tool Engineering*, June, 61(6).

ISCAR, 2015. *ISCAR SOF 45.* [Online] Available at: https://www.iscar.com/eCatalog/Family.aspx?fnum=2541&mapp=ML&app=61&GFSTYP=M [Accessed 15 03 2015].

Jawaid, A., Sharif, S. & Koksal, S., 2000. Evaluation of wear mechanisms of coated carbide tools when face milling titanium alloy. *Journal of Materials Processing Technology,* pp. 266-274.

Kalpakjian, S. & Schmid, S., 2013. *Manufacturing Engineering & Technology.* s.l.:Prentice Hall.

Kalpakjian, S. & Schmid, S., 2013. *Manufacturing, Engineering and Technology.* s.l.:Prentice Hall.

Kendall, L., 1997. Tool Wear and Tool Life. In: *ASM Handbook Volume 16: Machining.* s.l.:ASM International.

Kennametal, 2015. *Titanium machining guide.* [Online] Available at: https://www.kennametal.com/content/dam/kennametal/kennametal/common/Resources/Catalogs-Literature/Industry%20Solutions/Titanium_material_machining_guide_Aerospace.pdf [Accessed 06 May 2015].

Kikuchi, M. et al., 2003. Grindability of cast Ti–Cu alloys. *Dental Materials,* p. 375–381.

Koen, D., 2011. *Investigation of novel cooling methods to enhance aerospace component manufacturing practices,* s.l.: s.n.

Komanduri, R., 1982. Some clarifications on the mechanics of chip formation when machining titanium alloys. *Wear,* pp. 15-34.

Komanduri, R. & Hou, Z., 2001. A review of the experimental techniques for the measurement of heat and temperatures generated in some manufacturing processes and tribology. *Tribology International*, pp. 653-682.

Komanduri, R. & Reed, W., 1983. Evaluation of carbide grades and a new cutting geometry for machining titanium alloys. *Wear*, pp. 113-123.

Komanduri, R. & Von Turkovich, B., 1981. New Observations on the Mechanism of Chip Formation When Machining Titanium Alloys. *Wear*, pp. 179-188.

Kuljanic, E., Sortino, M. & Totis, G., 2010. *Machinability of Difficult Machining Materials.* Mediterranean Cruise, TMT.

Landers, R., Galecki, G., Young, K. & Hanks, R., 2011. Peripheral milling of thin titanium plates: modelling analysis, and process planning. *Proceedings of the Institution of Mechanical Engineers, Part B: Journal of Engineering Manufacture*, pp. 783-798.

Langworthy, E., 1989. Chemical Milling. In: *ASM Handbook - Vol 16 - Machining Processes.* s.l.:ASM International, pp. 579-586.

Li, A., Zhao, J., Zhou, Y. & Chen, X., 2011. Experimental investigation on chip morphologies in high-speed dry milling of titanium alloy Ti6Al4V. *International Journal of Advanced Manufacturing Technology*, pp. 933-942.

Lopez de lacalle, L., Perez, J., Llorente, J. & Sanchez, J., 2000. Advanced cutting conditions for the milling of aeronautical alloys. *Journal of materials processing technology*, pp. 1-11.

Lütjering, G., Williams, J. & Gysler, A., 2000. Microstructure and Mechanical Properties of Titanium Alloys. In: *Microstructure and Properties of Materials (Volume 2).* Singapore: World Scientific, pp. 1-77.

Machado, A. R. & Wallbank, J., 1990. Machining of titanium and its alloys-a review. *Proceedings Institution of Mechanical Engineers, Journal of Engineering Manufacturing*, pp. 53-60.

Machado, A. & Wallbank, J., 1990. Machining of Titanium and its Alloys- a Review. *Journal of Engineering Manufacture*, pp. 53-60.

Marinov, V., 2008. *Manufacturing Processes for Metal Products.* s.l.:Kendall Hunt Publishing Company.

Mc Evily, A., 2003. Failures in inspection procedures: case studies. *Engineering Failure Analysis*, pp. 167-176.

Mitsubishi Carbide, 2015. *Function of tool features for face milling: Corner andle and chip thickness.* [Online]
Available at:

http://www.mitsubishicarbide.net/contents/mmus/enus/html/product/technical_information/information/f_kougu.html
[Accessed 04 May 2015].

Montgomery, D. & Runger, G., 2010. *Applied Statistics and Probability for Engineers.* s.l.: John Wiley & Sons, Inc..

Mutombo, K., Rossouw, P. & Govender, G., 2011. *Chemically Milled Alpha-Case Layer from Ti6Al4V Alloy Investment Cast.* Lüneburg, Trans Tech Publications, pp. 477-480.

Nabhani, F., 2001. Wear mechanisms of ultra-hard cutting tool materials. *Journal of Material Processing Technology,* pp. 402-212.

Nachtman, E., 1997. Metal Cutting and Grinding Fluids. In: *ASM Handbook Volume 16: Machining.* s.l.:ASM International.

National Transportation Safety Board, 1996. *Aircraft Accident Report: Uncontained Engine Failure Delta Air Lined Flight 1288 McDonnell Douglas MD-88, N927DA,* Washington, DC: National Transportation Safety Board.

Nouari, M. & Ginting, A., 2006. Wear characteristics and performance of multi-layer CVD-coated alloyed carbide tool in dry end milling of titanium alloy. *Surface & Coatings Technology,* pp. 5663-5676.

Nurul Amin, A., 2012. *Titanium Alloys - Towards Achieving Enhanced Properties For Diversified Applications.* Rijeka: InTech.

Nurul Amin, A., Ismail, A. & Nor Khairusshima, M., 2007. Effectiveness of uncoated WC–Co and PCD inserts in end milling of titanium alloy—Ti–6Al–4V. *Journal of Materials Processing Technology,* pp. 147-158.

Odelros, S., 2012. *Tool wear in titanium machining,* Uppsala: Uppsala Universitet.

Oosthuizen, G., 2009. *Innovative cutting materials for finish shoulder milling Ti-6Al-4V Aero-engine alloy,* Stellenbosch: Stellenbosch University.

Oosthuizen, G., 2010. *Wear characterisation in milling Ti6Al4V - A wear map approach,* Stellenbosch: Stellenbosch University.

Oosthuizen, G., Akdogan, G., Dimitrov, D. & Treurnicht, N., 2010. A Review of the Machinability of Titanium Alloys. *R & D Journal of the South African Institution of Mechanical Engineering,* pp. 43-52.

Oosthuizen, G., Akdogan, G. & Treurnicht, N., 2011. The performance of PCD tools in high-speed milling Ti6Al4V. *The International Journal of Advanced Manufacturing Technology,* pp. 929-935.

Park, K. et al., 2014. Eco-Friendly Face Milling of Titanium Alloy. *International Journal of Precision Engineering and Manufacturing*, pp. 1159-1164.

Patankar, S., Kwang, Y. & Jen, T., 2001. Alpha casting and superplastic behavior of Ti6Al4V. *Journal of Materials Processing Technology*, pp. 24-28.

Paul DeGarmo, E., Black, J. & Kohser, R., 2003. *Materials and Processes in Manufacturing.* Wiley: s.n.

Prins, C., 2015. *Through Spindle Cooling: A Study of the Feasibility of Split Tool Titanium Machining,* Stellenbosch: Stellenbosch University.

Rao, B., Dandekar, C. & Shin, Y., 2011. An experimental and numerical study on the face milling of Ti–6Al–4V alloy: Tool performance and surface integrity. *Journal of Materials Processing Technology*, pp. 294-304.

Ray, K., 1996. *A study on hot rolling of CP titanium,* s.l.: University of British Columbia.

Ribeiro, M., Moreira, M. & Ferreira, J., 2003. Optimization of titanium alloy (6Al-4V) machining. *Journal of Materials Processing Technology*, pp. 458-463.

Richmond Sarpong, 2013. *Standard operating procedure,* s.l.: UC Center for Laboratory Safety.

Richt, C., 2011. *Using High-pressure Coolant.* [Online] Available at: http://www.cimindustry.com/article/tooling/using-high-pressure-coolant [Accessed 04 May 2015].

Rossouw, P., 2015. *Chemical milling infromation* [Interview] (20 07 2015).

Santhanam, A. & Tierney, P., 1997. Cemented Carbides. In: *ASM Handbook Volume 16: Machining.* s.l.:ASM International.

Sharman, A., Aspinwall, D., Dewes, R. a. B. & P., 2000. *Tool life when turning gamma titanium aluminide using carbide and PCD tools with reduced depths of cut and high pressure fluid.* s.l., s.n., pp. 161-166.

Shaw, M. & Vyas, A., 1993. Chip Formation in the Machining of Hardened Steel. *Annals of the CIRP*, pp. 29-33.

Siekmann, H., 1955. How to Machine Titanium. *Tool Engineer,* pp. 78-82.

Smid, P., 2003. *Cnc Programming Handbook: A Comprehensive Guide to Practical Cnc Programming.* New York: Industrial Press, inc.

Sobiyi, K. K., 2011. *Machining of powder metal titanium,* s.l.: Stellenbosch University.

Soboyejo, W. & Srivatsan, T., 2007. *Advanced Structural Materials: Properties, Design Optimization, and Applications.* Boca Raton: CRC Press.

Solar Manufacturing, 2015. *Furnace products, parts and services.* [Online] Available at: http://solarmfg.com/products/ [Accessed 06 May 2015].

Struers, 2010. *Hardness Testing and Sample Prepartaion,* Esbjerg : Rosendahls.

Sung, S.-Y., Han, B.-S. & Kim, Y.-J., 2005. Formation of Alpha Case Mechanism on Titanium Investment Cast Parts. *Materials Science & Engineering,* pp. 173-177.

Sun, J. & Guo, Y., 2009. A comprehensive experimental study on surface integrity by end milling Ti6Al4V. *Journal of Materials Processing Technology,* pp. 4036-4042.

Sun, S., Brandt, M. & Dargusch, M., 2009. Characteristics of cutting forces and chip formation in machining of titanium alloys. *International Journal of Machine Tools & Manufacture,* pp. 561-568.

Ten Haaf, P., Mielnik, K. & Lauwers, B., 2008. *Development of HSC strategies and tool geometries for the efficient machining of Ti6Al4V.* University College Dublin (UCD) Belfield Campus, s.n., pp. 753-761.

The Institute for Molecular Engineering, 2014. *Standard Operating Procedure for Hydrofluoric Acid (HF),* Chicago: The Institute for Molecular Engineering.

The National Research and Technology Foresight Project, 1999. *Mining and Metallurgy Foresight,* s.l.: DACST.

Trent, E., 1988. Metal cutting and the tribology of seizure: I seizure in metal cutting. *Wear,* pp. 29-45.

Tufts University, 2015. *Tufts University Standard Operating Procedures (SOP) for Hydrofluoric Acid,* Medford: Tufts University.

University of the Witwatersrand, 2015. *Overview: Carbides and Cermets.* [Online] Available at: http://www.wits.ac.za/academic/ebe/strongmaterials/4525/carbides_and_cermets.html [Accessed 17 11 2015].

Van Noort, R., 1987. Titanium: the implant material for today. *Journal of Material Science,* Volume 22, pp. 3801-3811.

Van Trotsenburg, S. & Laubscher, R., 2010. *The effect of high speed machining on the surface integrity of certain titanium alloys.* Stellenbsoch, s.n., pp. 186-190.

Van Vuuren, D., 2009. *Keynote address: Titanium—an opportunity and challenge for South Africa.* Champagne Sports Resort, Drakensberg, The Southern African Institute of Mining and Metallurgy, pp. 1-8.

Wang, X., Hwang, K. & Koopman, M., 2013. Mechanical properties and wear resistance of functionally graded WC-Co. *International Journal of Refractory metals and hard metals,* pp. 46-51.

Watson, D., Bayha, T., Hoffmann, T. & Festeau, G., 2007. Titanium Takes Off. *Cutting Tool Engineering Magazine*, 59(3).

Winegard, B., 2012. *The Positives and Negatives of Cutting Tool Geometries.* [Online] Available at: http://cuttingedgeconversation.blogspot.com/2012/04/positives-and-negatives-of-cutting-tool.html
[Accessed 04 May 2015].

Yang, X. & Liu, R., 1999. Machining Titanium and its Alloys. *Machining Science and Technology: An International Journal*, pp. 107-139.

Yang, X. & Liu, R., 1999. MACHINING TITANIUM AND ITS ALLOYS. *Machining Science and Technology: An International Journal*, pp. 107-139.

Yue, L., Wang, Z. & Li, L., 2012. Material morphological characteristics in laser ablation of alpha case from titanium alloy. *Applied Surface Science*, p. 8065–8071.

Zhang, S., Li, J., Deng, J. & Li, Y., 2009. Investigation on diffusion wear during high-speed machiningTi-6Al-4V alloy with straight tungsten carbide tools. *International Journal of Advanced Manufacturing Technology*, Volume 44, pp. 17-25.

Appendix A: Regression Analysis

After the primary experiments have been completed, none of the cutting conditions fully met tool failure criteria set out by ISO for tool life testing. Further analysis was however needed and the projected total tool life for the cutting tools was an unknown factor which needed to be determined. Based on the tool wear data obtained in the primary machining experiments, regression analysis of tool wear was performed in an attempt to obtain total tool life. Some of the analyses which required the total tool life include statistical modelling, cost modelling and total amount of material removal. The regression analysis is performed on the available data is Figure 45.

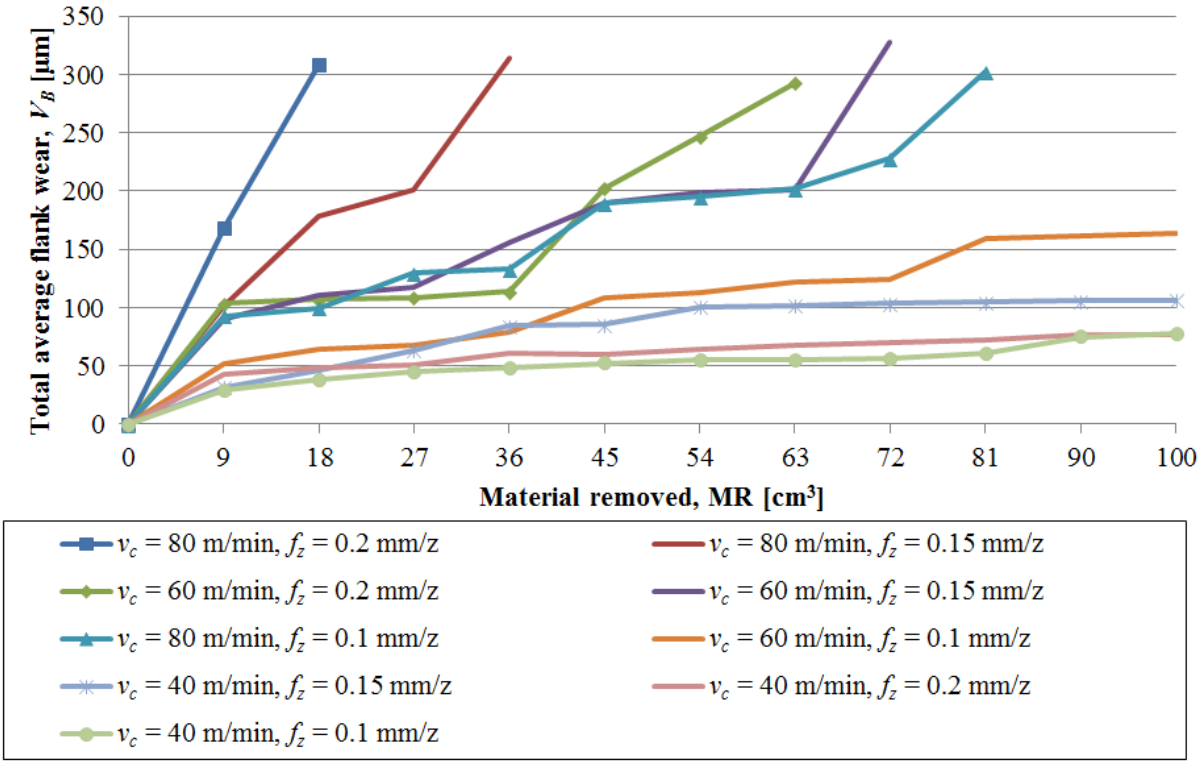

Figure A1: Wear curves for different feed and speed combinations used for regression analysis (based on Figure 45)

For the regression testing, all six individual insert wear measurement will be taken. This will increase the size of the sample pool and the regression analysis will be based on more accurate data.

To fit a regression line a simple equation needs to be developed first. This equation is:

$$y' = a + bx$$

The equation for a and b is as follows;

$$a = \bar{y} - b\bar{x}$$

$$b = \frac{\sum(x - \bar{x})(y - \bar{y})}{\sum(x - \bar{x})^2}$$

However, since tool wear for a new cutting tool starts at zero, a will be omitted and only a gradient will be used. Alternatively, Microsoft Excel provides a regression analysis tool in its analysis tool pack which fully calculates all relevant information. The results are listed below:

Regression analysis of tool life data for cutting condition v_c = 40 m/min, f_z = 0.1 mm/z

SUMMARY OUTPUT

Regression Statistics	
Multiple R	0.955
R Square	0.911
Adjusted R Square	0.896
Standard Error	18.342
Observations	66

ANOVA

	df	*SS*	*MS*	*F*	*Significance F*
Regression	1	224047.80	224047.80	665.95	1.54472E-35
Residual	65	21868.21	336.43		
Total	66	245916.00			

	Coefficients	*Standard Error*	*t Stat*	*P-value*	*Lower 95%*	*Upper 95%*
Intercept	0	#N/A	#N/A	#N/A	#N/A	#N/A
X Variable 1	1.0336	0.0401	25.8060	7.19055E-36	0.954	1.114

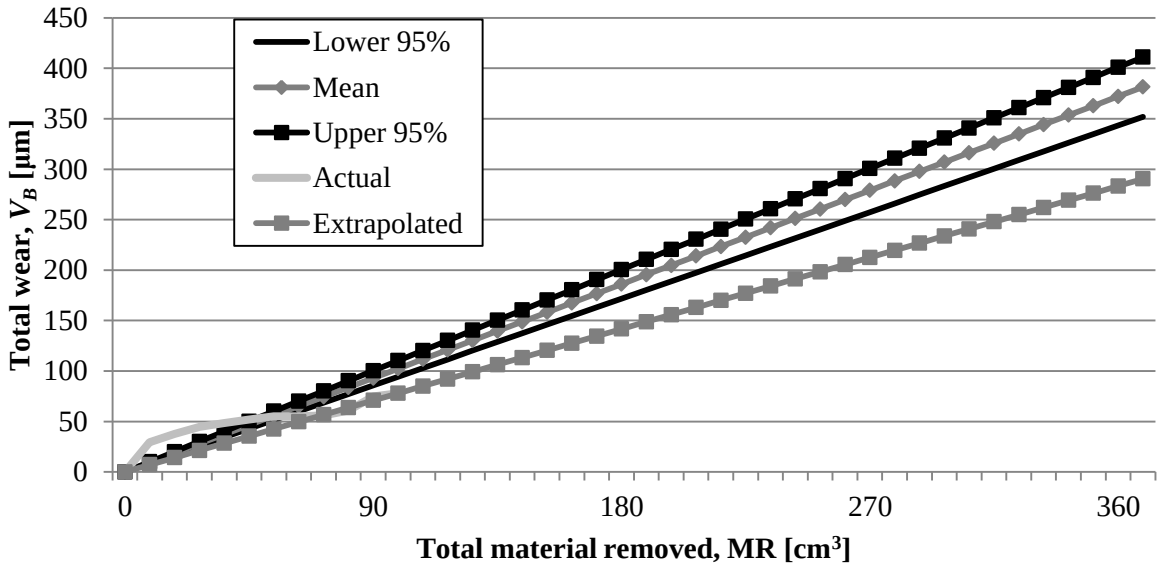

Figure A2: Tool life projection curve for machining at vc = 40 m/min, fz = 0.1 mm/z, exhibiting the upper 95%, lower 95% and mean of the regression analysis, as well as the actual and extrapolated curve

Regression analysis of tool life data for cutting condition vc = 60 m/min, fz = 0.1 mm/z

SUMMARY OUTPUT

Regression Statistics	
Multiple R	0.95
R Square	0.90
Adjusted R Square	0.89
Standard Error	38.55
Observations	66

ANOVA

	df	*SS*	*MS*	*F*	*Significance F*
Regression	1	878843.47	878843.47	591.37	4.88587E-34
Residual	65	96597.39	1486.11		
Total	66	975440.87			

	Coefficients	*Standard Error*	*t Stat*	*P-value*	*Lower 95%*	*Upper 95%*
Intercept	0	#N/A	#N/A	#N/A	#N/A	#N/A
X Variable 1	1.89	0.08	24.32	2.38832E-34	1.74	2.05

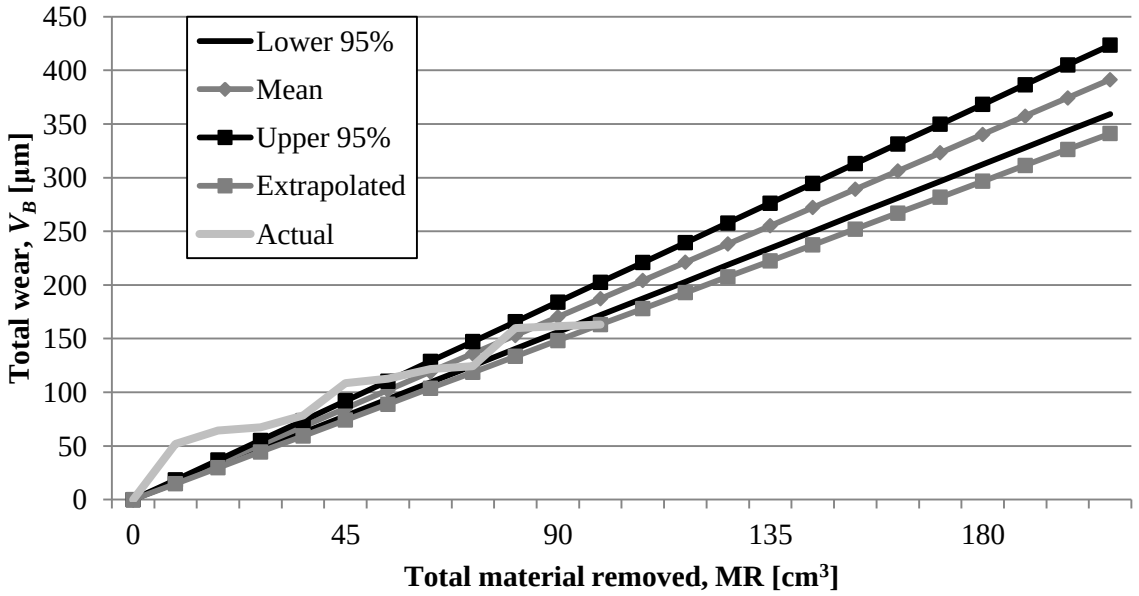

Figure A2: Tool life projection curve for machining at vc = 60 m/min, fz = 0.1 mm/z, exhibiting the upper 95%, lower 95% and mean of the regression analysis, as well as the actual and extrapolated curve

Regression analysis of tool life data for cutting condition vc = 80 m/min, fz = 0.1 mm/z

SUMMARY OUTPUT

Regression Statistics	
Multiple R	0.97
R Square	0.94
Adjusted R Square	0.93
Standard Error	44.9
Observations	54

ANOVA

	df	*SS*	*MS*	*F*	*Significance F*
Regression	1	1817528.25	1817528.25	900.97	1.63553E-34
Residual	53	106917.57	2017.31		
Total	54	1924445.82			

	Coefficients	*Standard Error*	*t Stat*	*P-value*	*Lower 95%*	*Upper 95%*
Intercept	0	#N/A	#N/A	#N/A	#N/A	#N/A
X Variable 1	3.62	0.12	30.02	6.10102E-35	3.38	3.86

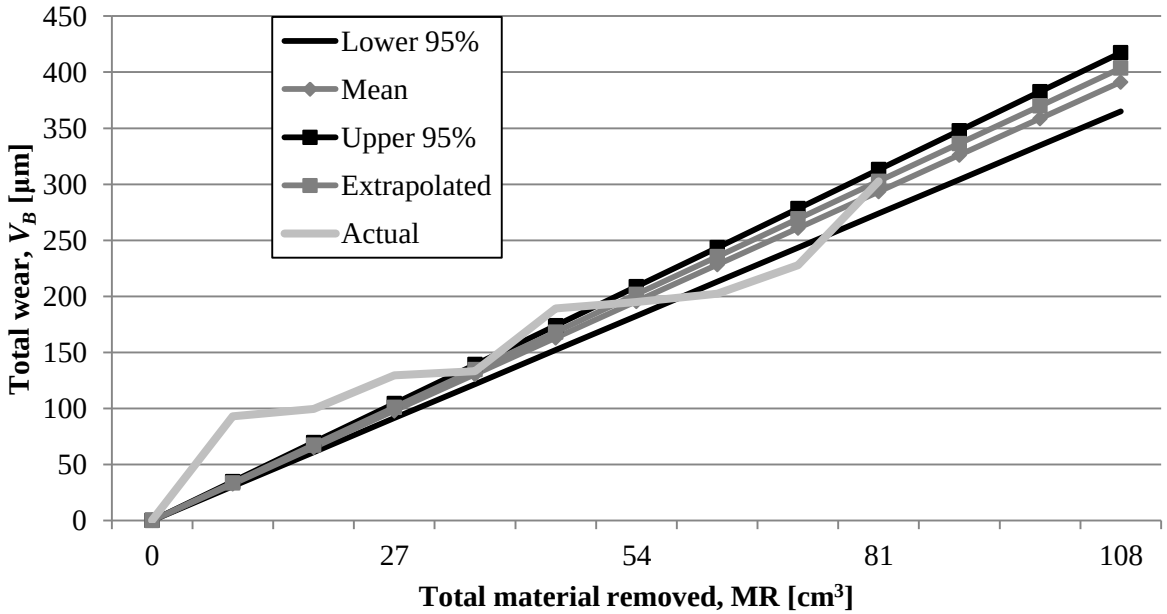

Figure A2: Tool life projection curve for machining at vc = 80 m/min, fz = 0.1 mm/z, exhibiting the upper 95%, lower 95% and mean of the regression analysis, as well as the actual and extrapolated curve

Regression analysis of tool life data for cutting condition vc = 40 m/min, fz = 0.15 mm/z

SUMMARY OUTPUT

Regression Statistics	
Multiple R	0.83
R Square	0.68
Adjusted R Square	0.67
Standard Error	58.1
Observations	66

ANOVA

	df	*SS*	*MS*	*F*	*Significance F*
Regression	1	470831.89	470831.89	139.59	9.85515E-18
Residual	65	219241.98	3372.95		
Total	66	690073.87			

	Coefficients	*Standard Error*	*t Stat*	*P-value*	*Lower 95%*	*Upper 95%*
Intercept	0	#N/A	#N/A	#N/A	#N/A	#N/A
X Variable 1	1.38	0.12	11.81	7.75841E-18	1.15	1.62

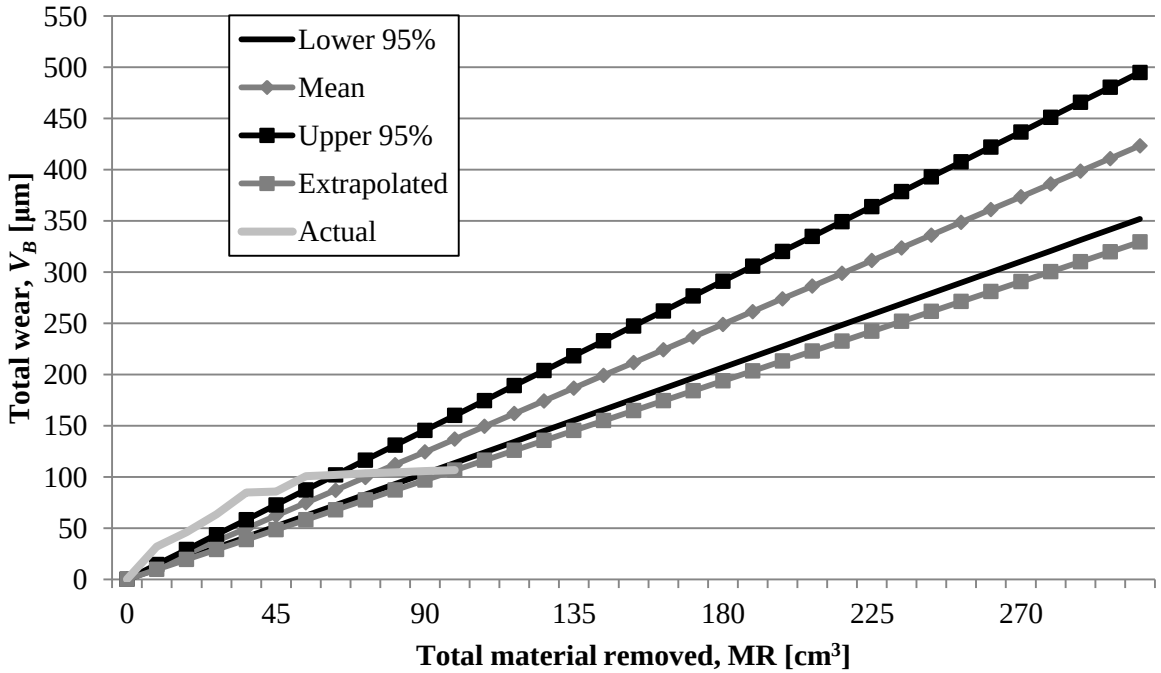

Figure A2: Tool life projection curve for machining at vc = 40 m/min, fz = 0.15 mm/z, exhibiting the upper 95%, lower 95% and mean of the regression analysis, as well as the actual and extrapolated curve

Regression analysis of tool life data for cutting condition vc = 60 m/min, fz = 0.15 mm/z

SUMMARY OUTPUT

Regression Statistics	
Multiple R	0.95
R Square	0.9
Adjusted R Square	0.88
Standard Error	63.5
Observations	48

ANOVA

	df	*SS*	*MS*	*F*	*Significance F*
Regression	1	1635154.89	1635154.89	406.13	1.83159E-24
Residual	47	189230.19	4026.17		
Total	48	1824385.08			

	Coefficients	*Standard Error*	*t Stat*	*P-value*	*Lower 95%*	*Upper 95%*
Intercept	0	#N/A	#N/A	#N/A	#N/A	#N/A
X Variable 1	4.06	0.20	20.15	9.10703E-25	3.66	4.47

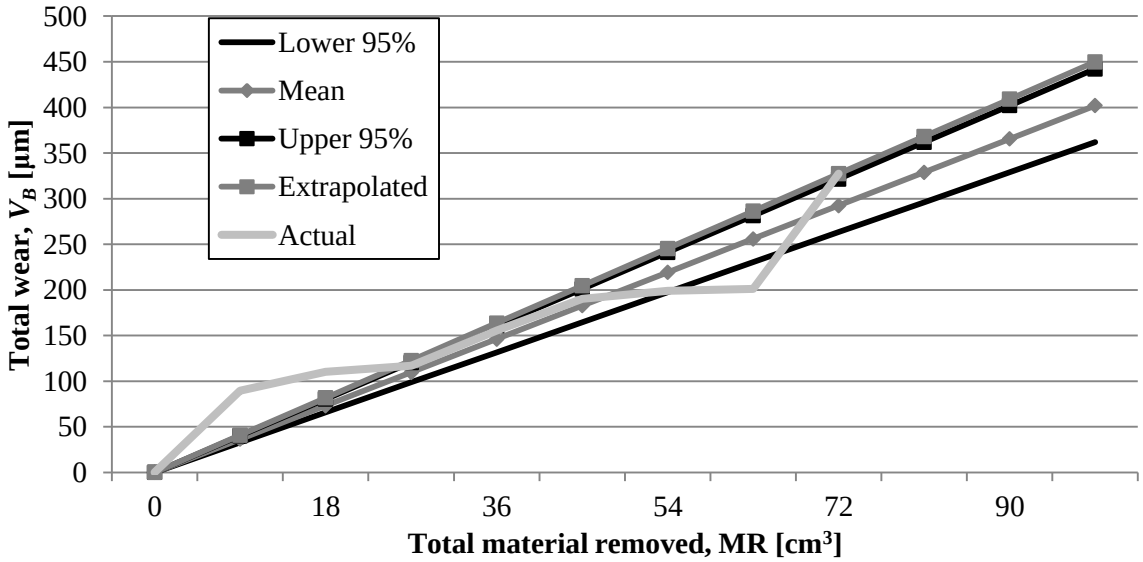

Figure A2: Tool life projection curve for machining at vc = 60 m/min, fz = 0.15 mm/z, exhibiting the upper 95%, lower 95% and mean of the regression analysis, as well as the actual and extrapolated curve

Regression analysis of tool life data for cutting condition vc = 80 m/min, fz = 0.15 mm/z

SUMMARY OUTPUT

Regression Statistics	
Multiple R	0.99
R Square	0.98
Adjusted R Square	0.93
Standard Error	33.6
Observations	24

ANOVA

	df	*SS*	*MS*	*F*	*Significance F*
Regression	1	1073100.10	1073100.10	949.78	1.36062E-19
Residual	23	25986.26	1129.84		
Total	24	1099086.36			

	Coefficients	*Standard Error*	*t Stat*	*P-value*	*Lower 95%*	*Upper 95%*
Intercept	0	#N/A	#N/A	#N/A	#N/A	#N/A
X Variable 1	8.58	0.28	30.82	3.30233E-20	8.00	9.15

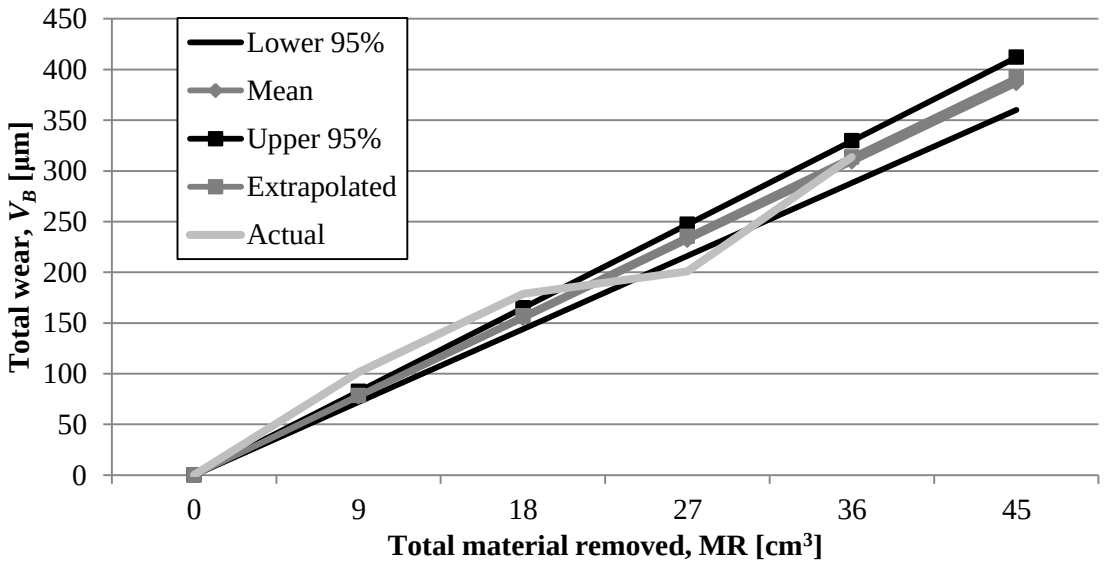

Figure A2: Tool life projection curve for machining at vc = 80 m/min, fz = 0.15 mm/z, exhibiting the upper 95%, lower 95% and mean of the regression analysis, as well as the actual and extrapolated curve

Regression analysis of tool life data for cutting condition vc = 40 m/min, fz = 0.2 mm/z

SUMMARY OUTPUT

Regression Statistics	
Multiple R	0.94
R Square	0.88
Adjusted R Square	0.86
Standard Error	22.8
Observations	66

ANOVA

	df	*SS*	*MS*	*F*	*Significance F*
Regression	1	243094.72	243094.72	468.94	3.69915E-31
Residual	65	33695.50	518.39		
Total	66	276790.22			

	Coefficients	*Standard Error*	*t Stat*	*P-value*	*Lower 95%*	*Upper 95%*
Intercept	0	#N/A	#N/A	#N/A	#N/A	#N/A
X Variable 1	0.99	0.05	21.66	1.98287E-31	0.90	1.09

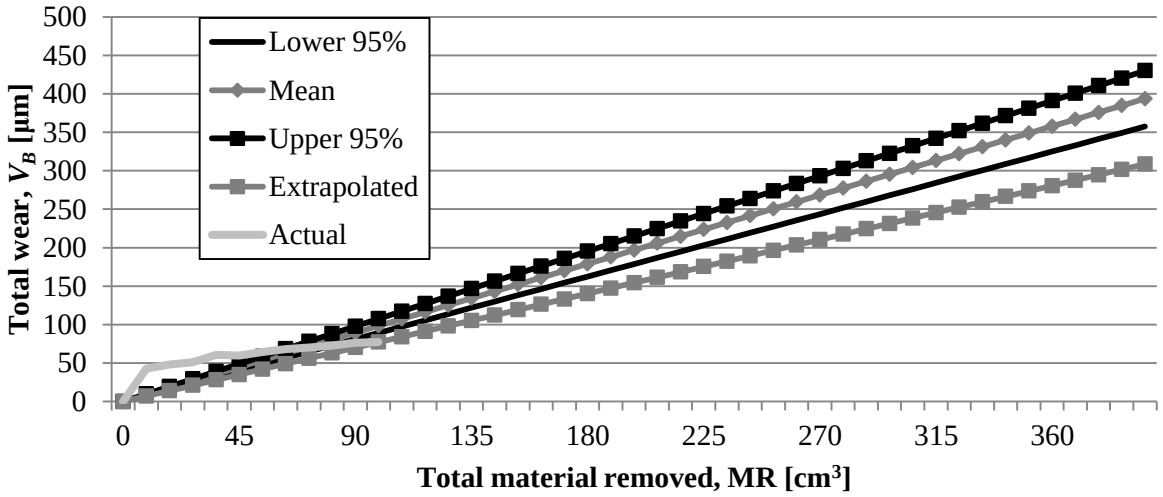

Figure A2: Tool life projection curve for machining at vc = 40 m/min, fz = 0.2 mm/z, exhibiting the upper 95%, lower 95% and mean of the regression analysis, as well as the actual and extrapolated curve

Regression analysis of tool life data for cutting condition vc = 60 m/min, fz = 0.2 mm/z

SUMMARY OUTPUT

Regression Statistics	
Multiple R	0.97
R Square	0.94
Adjusted R Square	0.92
Standard Error	44.4
Observations	42

ANOVA

	df	*SS*	*MS*	*F*	*Significance F*
Regression	1	1365348.11	1365348.11	693.64	6.93963E-27
Residual	41	80703.84	1968.39		
Total	42	1446051.95			

	Coefficients	*Standard Error*	*t Stat*	*P-value*	*Lower 95%*	*Upper 95%*
Intercept	0	#N/A	#N/A	#N/A	#N/A	#N/A
X Variable 1	4.48	0.17	26.34	2.58426E-27	4.14	4.82

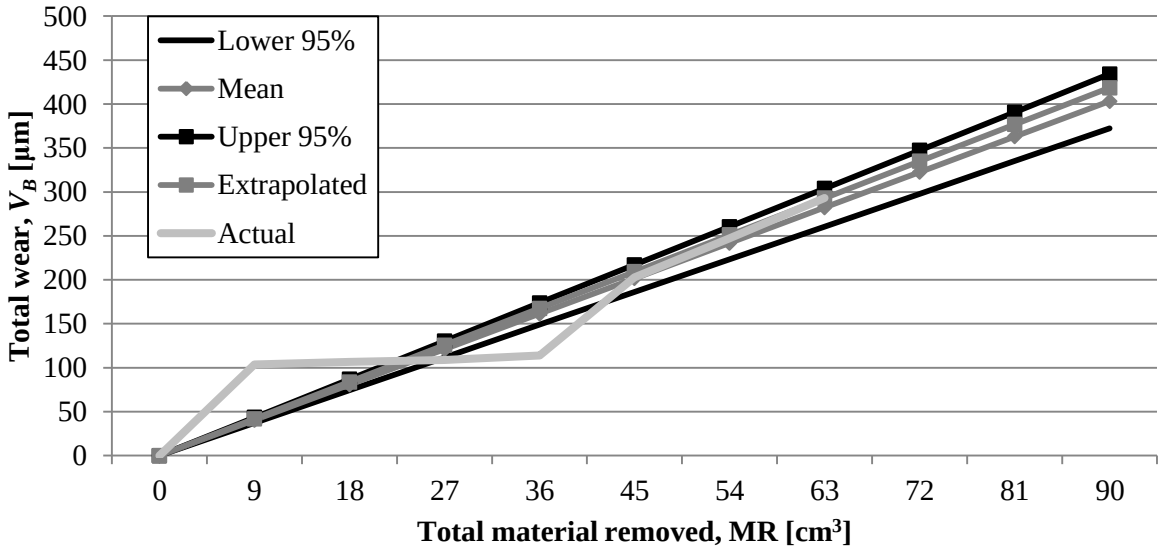

Figure A2: Tool life projection curve for machining at vc = 60 m/min, fz = 0.2 mm/z, exhibiting the upper 95%, lower 95% and mean of the regression analysis, as well as the actual and extrapolated curve

Regression analysis of tool life data for cutting condition vc = 80 m/min, fz = 0.2 mm/z

SUMMARY OUTPUT

Regression Statistics	
Multiple R	0.99
R Square	0.99
Adjusted R Square	0.9
Standard Error	30.7
Observations	12

ANOVA

	df	*SS*	*MS*	*F*	*Significance F*
Regression	1	737345.75	737345.75	780.01	8.03979E-11
Residual	11	10398.35	945.30		
Total	12	747744.10			

	Coefficients	*Standard Error*	*t Stat*	*P-value*	*Lower 95%*	*Upper 95%*
Intercept	0	#N/A	#N/A	#N/A	#N/A	#N/A
X Variable 1	17.42	0.62	27.93	1.45084E-11	16.05	18.79

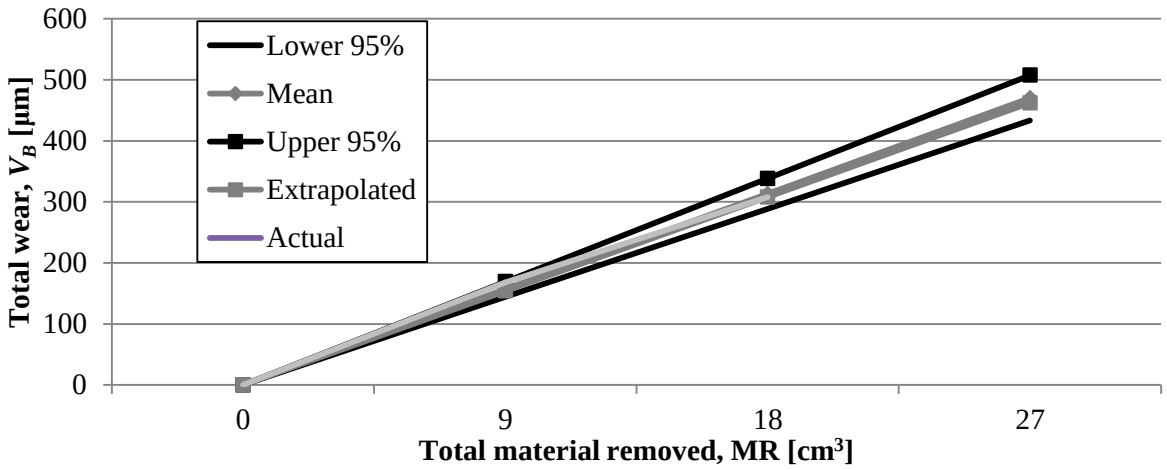

Figure A2: Tool life projection curve for machining at vc = 80 m/min, fz = 0.2 mm/z, exhibiting the upper 95%, lower 95% and mean of the regression analysis, as well as the actual and extrapolated curve

Conclusion of regression analysis

In each of the regression analyses the Significance F and the P-Value is tremendously small. These values indicate towards the effectiveness of the regression analysis. In all the cases above the decision should be made to reject the regression analysis as it does not adequately fit the data. Therefore the regression results cannot be used in this investigation. As a result an alternative must be sought. It was decided to simply use the average gradient that results from the limited amount of data available. This is not an accurate or sophisticated forecast, and it may underestimate the total lifespan of the tool as the most aggressive period of tool wear is at the beginning, but it will suffice for the purposes of this study.

Appendix B: Statistical Interpretation

The coefficient of determination (R^2) is the percent of the variation of the response explained or accounted for by the model. It is a measure of fit, i.e. how well the model fits the data. It is determined by measuring the variability of the data set through different sums of squares, such as the total sum of squares, the regression sum of squares and the sum of squares of residuals (Montgomery & Runger, 2010).

$$R^2 = \frac{SS_{reg}}{SS_{tot}} = 1 - \frac{SS_{res}}{SS_{tot}}$$

$$SS_{reg} = Regression\ sum\ of\ squares$$
$$SS_{res} = Residual\ sum\ of\ squares$$
$$SS_{tot} = Total\ sum\ of\ squares$$

The relationship between the Sum of Squares is:

$$SS_{res} + SS_{reg} = SS_{tot}$$

To calculate SS_{reg}, SS_{res} and SS_{tot} requires the following. A data set has n values marked $y_1...y_n$ (collectively known as y_i), each associated with a predicted (or modeled) value $f_1...f_n$ (known as f_i) The mean for the observed data $\bar{x}$ and $\bar{y}$ respectively is:

$$\bar{x} = \frac{1}{n}\sum_{i=1}^{n} x_i \qquad\qquad \bar{y} = \frac{1}{n}\sum_{i=1}^{n} y_i$$

To calculate the regression or predicted line requires the following equation:

$$f_i = a + bx$$

The value for a and b is calculated by using the following equations respectively

$$a = \bar{y} - b\bar{x} \qquad\qquad b = \frac{\sum(x - \bar{x})(y - \bar{y})}{\sum(x - \bar{x})^2}$$

The total sum of squares of the residual variance is:

$$SS_{res} = \sum_i (y_i - f_i)^2$$

The total sum of squares of the regression variance is:

$$SS_{reg} = \sum_i (f_i - \bar{y})^2$$

The total sum of squares of the total variance is:

$$SS_{tot} = \sum_i (y_i - \bar{y})^2$$

$$a = \bar{y} - b\bar{x}$$

The predictive squared correlation coefficient (Q^2) is the percent of variation of the response predicted by the model according to cross validation. Q^2 is related to how well the model predicts new data. A useful model should have a large Q^2, as Q^2 shows and estimates the future prediction precision. In a model with a good R^2, and moderate model validity with a design with many degrees of freedom, it is possible to have a poor Q^2 due to insignificant terms in the model. Q^2 should be greater than 0.1 for a significant model and greater than 0.5 for a good model.

The measures of model predictive ability are very similar to those defined for the goodness of fit and are based on the Predictive Error Sum of Squares (PRESS) which substitutes the Residual Sum of Squares (RSS)

The Predictive Error Sum of Squares (PRESS) is the sum of the squared differences between the experimental response y and the response predicted by the regression model, i.e. for an object that was not used for model estimation. It is defined as:

$$PRESS = \sum_{i=1}^{n} (y_i + f_{i/i})^2$$

The notation i/i indicates that the response is predicted by a model estimated when the i-th sample was left out from the training set.

Therefore, an equivalent parameter to R^2 can be defined, using in place of RSS the quantity PRESS. This parameter is called cross-validated R^2 and the accepted symbols are R^2_{CV} or Q^2 :

$$R^2_{CV} \equiv Q^2 = 1 - \frac{PRESS}{SS_{tot}} = 1 - \frac{\sum_i (y_i - f_{i/i})^2}{\sum_i (y_i - \bar{y})^2}$$

Appendix C: Cost Calculation

The total material removed (MR) for 10 inserts is calculated by using the projected tool life (ptl) of Figure 55, along with the cutting parameters in Table 5 to first calculate the theoretical material removal rate (MRR), and then to calculate the total material removed in the lifespan of the tool. The particular carbide inserts used in this investigation comes in packets of ten. There are 16 cutting edges on a carbide insert, giving a total of 160 cutting edges in a packet, and the face milling cutter can hold a maximum of six inserts at a time. Total material removal is therefore as per Equation 2;

$$Material\ removed\ (cm^3) = ptl \times MRR \times 160 \div 6 \quad [2]$$

Total machine cost is calculated by using the projected tool life, calculating total machine time for 160 cutting edges, multiplied to the hourly rate prescribed by the machine shop (R500/h). Machine cost per cubic centimetre is subsequently calculated by dividing the total machine cost by the total amount of material removed as per Equation 3;

$$Total\ machine\ cost\ (Rand) = ptl \times 160 \times 6 \div 60 \times 500.00 \quad [3]$$

Tooling cost for 10 inserts is fixed across all cutting parameters. It is the efficiency of the cutting tool at certain cutting conditions that defines cost affordability of the tool. A packet of 10 inserts cost roughly R2500.00, and the total cost per cubic centimetre is calculated as follows as per Equation 4;

$$Tooling\ cost\ per\ cubic\ centimetre = R2500.00 \div material\ removed\ (MR) \quad [4]$$

Finally, adding the tooling cost per cubic centimetre and machine cost per cubic centimetre yields the theoretical total cost per cubic centimetre for the removal of alpha case from Ti6Al4V hot rolled products by machining at various cutting parameters. The most economical cutting condition is at v_c = 40 m/min and f_z = 0.2 mm/z. This yields a projected tool life of t = 42.40 minutes, after which MR = 453.67 cm^3 of material has been removed. Total cost per cubic centimetre of material removal is calculated at R0.99/cm^3.